A COMPARATIVE STUDY OF THE EFFECT OF SURFACE DISCHARGE ON THE IMPULSE BREAKDOWN VOLTAGE OF OIL-IMPREGNATED PRESSBOARD INSULATION

Mulalo Mercy Tshivhilinge

A dissertation submitted to the Faculty of Engineering and the Built Environment, University of the Witwatersrand, Johannesburg in fulfillment of the requirements for the degree of Master of Science in Engineering.

Johannesburg, 2014

Declaration

I declare that this dissertation is my own unaided work. It is being submitted to the Degree of Master of Science in Engineering in the University of the Witwatersrand, Johannesburg. It has not been submitted before for any degree or examination in any other university.

Candidate Full Name: Mulalo Mercy Tshivhilinge

Candidate Signature: _____

Signed on the _____day of _____ 2014

Abstract

The increasing demand for electrical power energy comes with a challenge to design power transformers with optimised dimensions at the same time meeting the energy requirements. The dimension of a power transformer is influence by the insulation system. The use of composite insulation comprising of transformer oil and cellulose (paper and pressboard) is still currently the most economical insulation technology allowing for dimension reduction. Although over the years, there have been developments of alternative insulation systems; the conventional insulation type is still predominant due to various reasons. The main disadvantage with the conventional composite insulation system is relative permittivity mismatch of the different material, which leads to localised electrical stresses at their interface. The localised electrical stress causes surface discharge on solid insulation material at normal operating voltage thereby slowly developing into a permanent conduction path, which leads to dielectric failure. It is known that about 25% to 30% of major dielectric failures of power transformers are due to switching and lightning impulses associated with solid insulation ageing and contamination. The objective of this dissertation is to study the effect of surface discharge on the lightning impulse (LI) breakdown voltage of oil-impregnated pressboard used in power transformers. Needles placed at an acute angle on the surface of an oil-impregnated pressboard sample to plane electrode geometry were used to age 24 pressboard samples with surface discharge. The electrode gap distance was set at an optimised distance of 45 mm. The test samples were continuously aged by surface discharge at a constant supply voltage of 30 kV. The ageing experiment was performed in an array of 12 test samples set simultaneously aged for a period of 3 hours and another set for 7 hours. A set of 6 out of the 12 aged samples were tested for positive and another set for negative LI breakdown voltage. The experimental findings are that surface discharge reduces the LI breakdown voltage of oil-impregnated pressboard and this is a function of exposure period to surface discharge. Furthermore, although negative LI breakdown voltage of pressboard is higher than positive LI breakdown voltage, the former is affected relatively more by surface discharge ageing. The presence of any surface discharge in power transformers should therefore not be tolerated.

Acknowledgement

I would like to express my deepest gratitude to Dr Cuthbert Nyamupangedengu for his constructive feedback, insightful comments and consistent feedback to this dissertation as well as encouragement throughout the study period. Special thanks to Matshediso Phoshoko, Mpendulo Dlamini and Nomxolisi Makubalo for their constructive review feedback and comments. I received generous support from Matsepe Matjipa with 3D Solid Works simulation for the FEM models. I would also like to thank Mluleki Hlatshwayo whose opinions and information have helped throughout the production of this study, as well as his encouraging words.

I have had support and encouragement from these friends; Sandile Miya-Mokoena and Ellan Phaahla. Thank you so much guys.

I would also like to express my gratitude to my family for their moral support and warm encouragements, and understanding at times when I could not spend time with them. I really appreciate it. You are my rock.

Finally, I would like to express my gratitude to Powertech Transformers (Pty) Ltd for financial support and time resource, with special thanks to Powertech Transformers' Group Technology Manager, Nico Günter.

Thank you Lord for blessing me with this opportunity.

Table of Contents

List of Figures

List of Tables

Acronyms and Abbreviations

α	Alpha
β	Beta
ε_0	Permittivity of free space
ε_r	Relative permittivity of the insulation medium
µs	Micro seconds
χ	Electrical susceptibility
AC	Alternating Current
BIL	Basic Insulation Level
CH_4	Methane
CO	Carbon monoxide
CO_2	Carbon dioxide
C_a	Test object capacitance
C_k	Coupling capacitor
d	Insulation gap distance between the two electrodes
d_c	Creep distance
d_t	Thickness of pressboard material
D	Electric flux density
DC	Direct Current
DGA	Dissolved Gas Analysis
DP	Degree of Polymerisation
E	Electric field
E	Electric field intensity
E_b	Electric field breakdown strength
E_c	Occurring electric field stress along the surface of pressboard
E_{sd}	Surface discharge electric field strength
f	frequency
FEM	Finite Element Method
FRA	Frequency Response Analysis
H	Hydrogen
H_2O	Water
HV	High Voltage
IEC	International Electrotechnical Commission
kV	kilovolts

LI	Lightning Impulse
LV	Low Voltage
mm	millimeter
M_i	PD measuring instrument
M/DBT	Mono/Dibezyltoluene
P	Density of the electrical dipole moments
PB	Pressboard
pC	pico Coulomb
PD	Partial Discharge
PRPD	Phase Resolved Partial Discharge
PRPDA	Phase Resolved Partial Discharge Analysis
Reg	Regulating winding
STD Dev.	Standard Deviation
t	time
T_r	Test transformer
U_m	Highest equipment voltage
V	Voltage
Z_m	Measuring impedance for PD measurement
Z_n	Noise blocking filter

Chapter 1: Introduction

1.1 Background

Gas, solids and liquids are the common forms of insulation media used to insulate electrical conducting bodies (electrodes) from each other. A good insulating medium is defined by its ability to resist current flow through it. This depends on the medium's electrical properties such as relative permittivity, electrical breakdown strength, dielectric losses, and resistivity.

Cellulose based paper and pressboard materials continue to be the most economic solid insulation used in oil-immersed power transformers. With the knowledge accumulated over many years of research and experience, it is understood that ageing of the cellulosic material is the main life limiting factor of an oil-immersed transformer [1]. The life expectancy of an oil-immersed power transformer with cellulosic insulation material is about 40 years. The main factors that are known to accelerate the ageing rate of the cellulose insulation materials are; moisture, thermal stress, electrical stress and mechanical stress [1 - 3].

Degradation of cellulose based insulation material has been the main concern since the early years of its application in power transformers [1]. There are many power transformers that have been in service for years, and the challenge facing the utilities with regards to these transformers is accurately determining their expected end of life. For this reason, there has been on-going research to understand the ageing factors and their mechanisms, with the aim of developing and improving the current insulation condition monitoring techniques for transformers in service [1, 4 - 6]. The common methods of assessing the condition of the transformer insulation systems are; dissolved gas analysis (DGA), frequency response analysis (FRA), tan-delta and partial discharge (PD) measurements. The limitation of the present diagnostic methods is the incapability to reasonably and accurately determine the condition of the solid insulation (pressboard and paper); especially determining the remaining life for transformers onsite [7].

Surface discharge is one of the ageing factors of solid insulation. It is caused by localised electrical stress at an interface of two different types of insulation media, either a solid with a liquid medium or a solid with a gas medium or interface between metal and insulation material. Surface discharge is known to reduce the dielectric strength of the insulation system. Once it is initiated on the surface of a solid material, it develops over time under normal operating conditions of a transformer, creating carbon traces. These carbon traces (shaped like tree branches) form a permanent conduction path (current path) which eventually leads to catastrophic failure/breakdown of the insulation material.

There is on-going research work worldwide investigating various aspects of surface discharge phenomenon on the pressboard material and its diagnostic methods [8 - 13].

The research work of this dissertation focuses on the study of the effect of surface discharges on the lightning impulse (LI) breakdown voltage of oil-impregnated pressboard. The results from this research contribute towards the knowledge of condition monitoring and diagnosis of the pressboard insulation.

1.2 Problem statement

The carbon conduction path due to surface discharge on pressboard creates a weak link in the insulation system. It is a challenge to assess the level of weakness of the pressboard with surface discharge activity. An obvious method to determine the severity of surface discharge on the oil-impregnated pressboard is through physical observation. However, the challenge is to assess the condition of the material through the transformer's tank inspection covers, where one cannot see the condition of the pressboard between the windings. It is almost impossible to visually inspect or replace an aged/degraded oil-impregnated pressboard in a transformer while it is in operation. The challenge faced in assessing the development of surface discharge on the pressboard while a transformer is in-service is to reliably determine its severity using transformer diagnostic methods, such as PD measurements, DGA, tan-delta and FRA. In most cases, to replace degraded pressboard materials requires that the transformer be taken out of service and dismantled in the factory environment for repairs; which is a lengthy and costly process procedure to undertake.

Literature shows that about 25% to 30% of major causes of dielectric failures in power transformers are attributed to switching and lightning impulses, in association with oil contamination and insulation ageing [14 - 17]. Oil contamination is one of the factors which contribute to the initiation of surface discharge on the oil-impregnated pressboard that reduces its dielectric strength. The worst case is when the surface discharge is not detected and an impulse voltage stresses the transformer, causing a complete insulation breakdown due to the weakened area of the pressboard by surface discharge. It is therefore, critical for utilities and transformer manufacturers to understand the surface discharge failure mechanisms, the effect on the dielectric impulse breakdown voltage. Such knowledge is useful in making necessary design, operation and maintenance decisions.

1.3 Research objectives

The aim of this research is to study the effect of surface discharges on the LI breakdown voltage of the oil-impregnated pressboard. This research study seeks to answer the following questions:

If surface discharge decreases the dielectric strength of an oil-impregnated pressboard:

- How does it affect its LI dielectric breakdown voltage?
- How does the duration of exposure to surface discharge affect the LI breakdown voltage?

1.4 Experimental approach

Surface discharge is induced on the oil-impregnated pressboard using a needle at an angle to plane electrode geometry in a laboratory environment. The LI breakdown voltage of the test samples aged by surface discharge are then determined, and compared to un-aged test samples. Figure 1-1 depicts the experimental procedure followed in this dissertation. The details of each component of the experiment are discussed in Chapter 4 to Chapter 6. The measurements and experiments are conducted based partly and fully on some of the international standards as follows:

- Pre-conditioning of the test samples based on international electrotechnical commission (IEC) 60554 - 2 [18].
- PD measurements based on IEC 60270 [19].
- Standard LI simulation using Marx generator IEC 60060-1 [20].
- LI breakdown voltage experiment based on IEC 60243-1[21] and IEC 60243-3 [22].
- Statistical analysis of the results partly based on the guidelines of IEEE 930 [23].

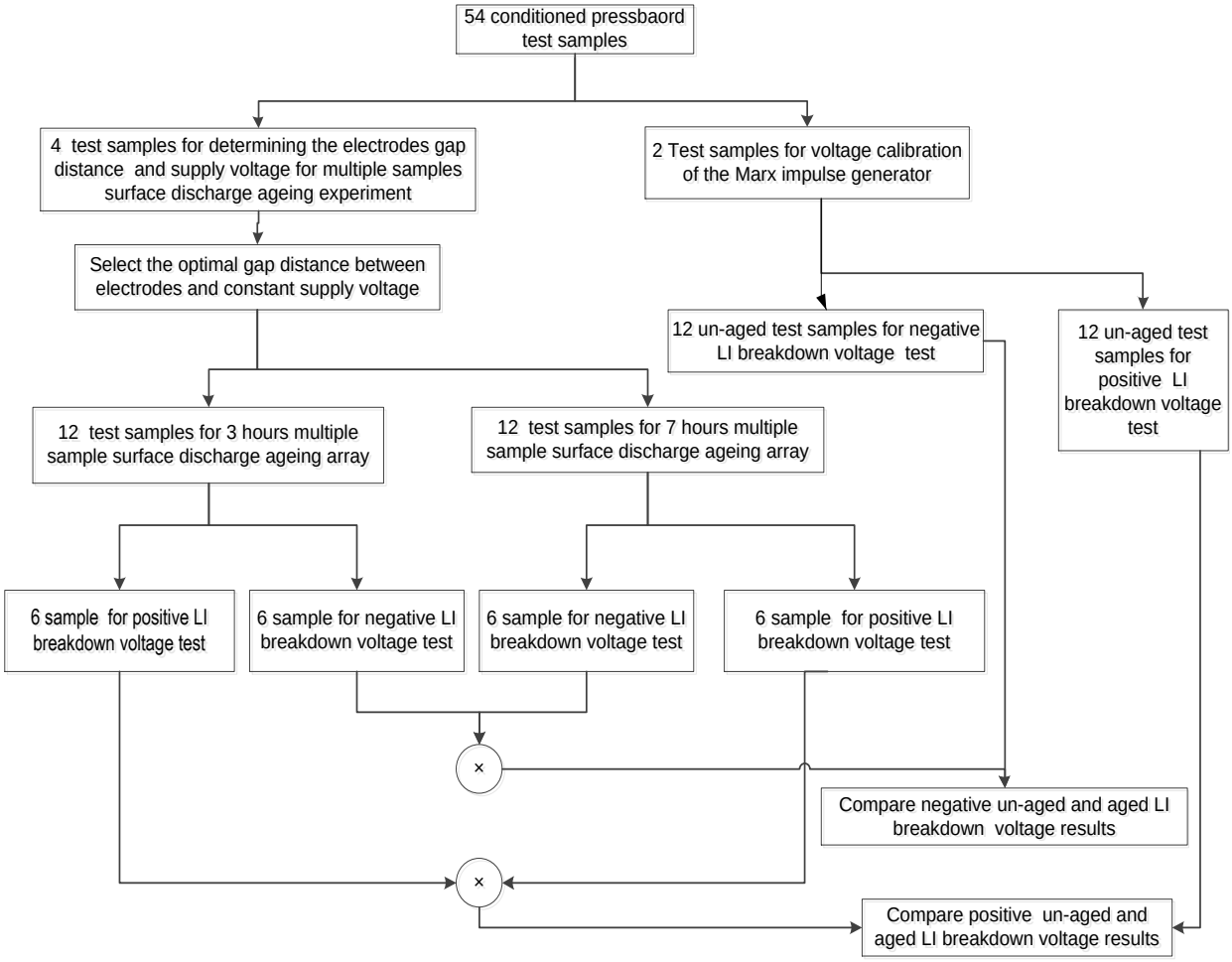

Figure 1-1: Experimental procedure overview

1.5 Dissertation structure

The chapters in this dissertation are laid out as follows:

Chapter 2 – Covers the background on the key factors that influence the dielectric strength of oil-impregnated pressboard material. It concludes with a section focusing on the surface discharge literature review.

Chapter 3 – This chapter discusses different methods of creating surface discharge on an oil-impregnated pressboard test sample in a laboratory environment, from which the best electrode arrangement for the purpose of this study is selected. A brief discussion on PD measurement methods is also presented.

Chapter 4 – Presented in this chapter are the details on determining the optimal electrode gap distance between the electrodes for the multiple test samples surface discharge ageing array

experiment. Also discussed in the chapter is the surface discharge failure mechanism based on experimental observations and PD measurement results.

Chapter 5 – The multiple sample surface discharge ageing array experiment details and the results are presented in this chapter.

Chapter 6 – This chapter presents the experimental setup and procedure for the positive and negative LI breakdown voltage tests. Conclusions from the experimental results are drawn and compared with other data from literature.

Chapter 7 – Presented in this chapter is the results discussion of the experimental LI breakdown voltage and statistical analysis of the breakdown voltages using the Weibull distribution function.

Chapter 8 – This chapter concludes the research, highlighting the key findings. Possible further research ideas are suggested.

Appendix A.1 – A detailed drawing of the cellulose structure showing the inter-polymer chain bonds is presented.

Appendix A.2 – The details of the materials and components that were used in the laboratory experiments are summarised.

Appendix A.3 – Presented in this appendix are the measured PD results and the recorded phase resolved partial discharge (PRPD) patterns for the electrodes gap distance experiment.

Appendix A.5 – The Matlab® code used in analysing the LI breakdown voltages with Weibull distribution function is presented in this Appendix. The codes' input data and the statistical output data not discussed in detail in Chapter 7 are presented as well as additional information from the Weibull analysis results.

1.6 Conclusion

The background on transformer insulation, research hypothesis and objective are presented in this chapter. The dissertation structure is also outlined.

Chapter 2: Literature Review – Oil-impregnated pressboard as insulation material in power transformers

2.1 Introduction

The fundamentals of a transformer's operating principles were discovered by Michael Faraday in 1831 [24]. He demonstrated the law of induction using two independent wires wound around a closed iron ring. He showed that when current is flowing in one wire, the change in magnetic flux induces a voltage on the other wire. His discovery led to more experiments with transformers, electrical energy generation and their applications. The first transformer was designed and built in the early 1880s by three Hungarian engineers [24]. Since then, transformer technology has continued to develop to this day, and research to improve the technology and transformer performance is on-going.

Power transformers are a key part of an electrical power system, from generating stations to the distribution of power right up to the end user. Reliability of a power transformer in the network and its safe operation is vital. Its failure can lead to a power outage, loss of revenue and loss of production. In the case of a transformer explosion, injury or even death of personnel in its vicinity may occur, and contamination of the environment in cases of oil spillage and other related problems. The safe operation of a power transformer depends on its design pillars namely; thermal performance, short circuit durability, cooling system and dielectric stability.

Over the years, the increasing demand of electrical energy has led to an increase in the electrical equipment's dimensions. As a result, power transformer designers are faced with a challenge to reduce these ever-increasing dimensions while meeting the power demand. One of the ways to minimise the power transformer's dimensions is to reduce the electrical insulation volumes by choosing a reliable insulation medium with high electrical, mechanical and thermal strength. Reduction of insulation volume can be achieved by using composite insulation technology. Oil-impregnated cellulose material is a common composite insulating material found in the high voltage equipment. It is mostly used in power cables, bushings and power transformers.

Transformer oil as an insulating and cooling medium was introduced around 1892 [25]. In the late 1920s, Weidmann developed a cellulose based transformerboard® (also known as pressboard) as a solid insulation for power transformer applications [25]. It was during this time that composite insulation of oil and cellulose was introduced as a dielectric insulation system in oil-immersed transformers. Research work into dielectric performance of oil-impregnated pressboard under electrical, thermal and mechanical stresses during this period increased [26 – 27].

With accumulated knowledge and information since the early 19th century on oil-cellulose composite insulation systems, the cellulose based insulation materials still remain a popular choice of solid insulation for application in power transformers and bushings. It is comparatively cheaper when compared to other available synthetic insulation materials like aramid (also known as Nomex®) and is produced from the slow growing soft wood (natural renewable raw material). When compared to wood, which is also used in transformer as laminated boards, its mechanical and electrical strength for application in power transformers out performs the wood.

Cellulose based insulation material on its own has some weakness as a dielectric material, however, when impregnated with oil its composite dielectric strength increases. This composite insulation system has added advantages of such as improving the thermal, mechanical and electrical properties of cellulose material [28].

Considering cellulose material's chemical structure (details in Figure A1-1 in Appendix A.1), the matrix has a polar oxygen–hydrogen group also referred to as hydroxyl (-OH) which extends laterally from the cellulose molecule chain. These hydroxyl groups make it possible for hydrogen bonds to form between the cellulose molecules in the same chains and neighboring chains, making cross-links to create a crystalline region. These cross-links result in micro voids between individual cellulose molecule chains, forming a long capillary of a diameter of about 10 nm to a few micrometers within the fibre [3]. The cavities can trap air that leads to internal PD when an external voltage source is applied across the material. Oil impregnation is the process of filling up the air cavities with oil to avoid this internal PD. Therefore, the dielectric strength of cellulose material is improved by proper impregnation with oil. This is an example of a way of changing one type of composite insulation material to the other, i.e. from a gas-solid composite insulation system to a liquid-solid composite insulation system.

Another advantage of oil impregnating the pressboard material is the improvement of its relative permittivity. When dry, the relative permittivity of cellulose pressboard is 5.6 [29] which reduces to 4.4 when oil impregnated. Considering that the gas in dry cellulose is air with permittivity of 1.006 and transformer oil relative permittivity of 2.2, there is a significant relative permittivity mismatch between air-filled pressboard compared to oil-impregnated pressboard. Therefore, by extracting air from the cellulose capillaries and filling them with oil, the relative permittivity mismatch is improved resulting in better electrical stress distribution. A detailed discussion on relative permittivity mismatch is presented in section 2.4.5.

In this chapter, the key factors that influence the dielectric strength of the oil-cellulose composite insulation system in transformers are presented. The literature review on the knowledge of the oil-pressboard/paper composite insulation system is discussed. The chapter concludes with a section on the review of surface discharge phenomena.

2.2 Composite insulation technology in power transformers

There has been continuously developing research work for exploring alternative composite insulation materials to cellulose and mineral oil composite insulation for application in power transformers [30]. These alternative composite insulation materials include cellulose impregnated with synthetic/natural ester oil, aramid impregnated with mineral oil or with synthetic/natural ester oil. There are two types of ester oils; natural ester (also known as vegetable oil) and synthetic ester. Unless otherwise stated in this document; ester oil will refer to both natural and synthetic ester. There is limited information on the dielectric performance compatibility of these alternative composites insulation, especially in power transformer application and design [31 - 34]. The evidence from the literature, [3] and [30], substantiated that aramid and wood are the preferred alternative solid insulation for power transformer application. However, wood has lower dielectric and mechanical strength than cellulose, as a result it can only be used for certain insulation components. Because of its rigid structure, wood cannot be used to produce mouldable insulation components and flexible cylinders for partitioning the oil gaps. In Figure 2-1, examples of different mouldable and non-mouldable cellulose insulation components in transformer application are shown. In contrast, aramid has higher mechanical and thermal strength than cellulose. This is an advantage for overload and high short circuit applications. Aramid also has a relative permittivity of 2.9 [30] when impregnated with mineral oil resulting in reduced permittivity mismatch between mineral oil and aramid material, hence the electrical stress distribution is improved.

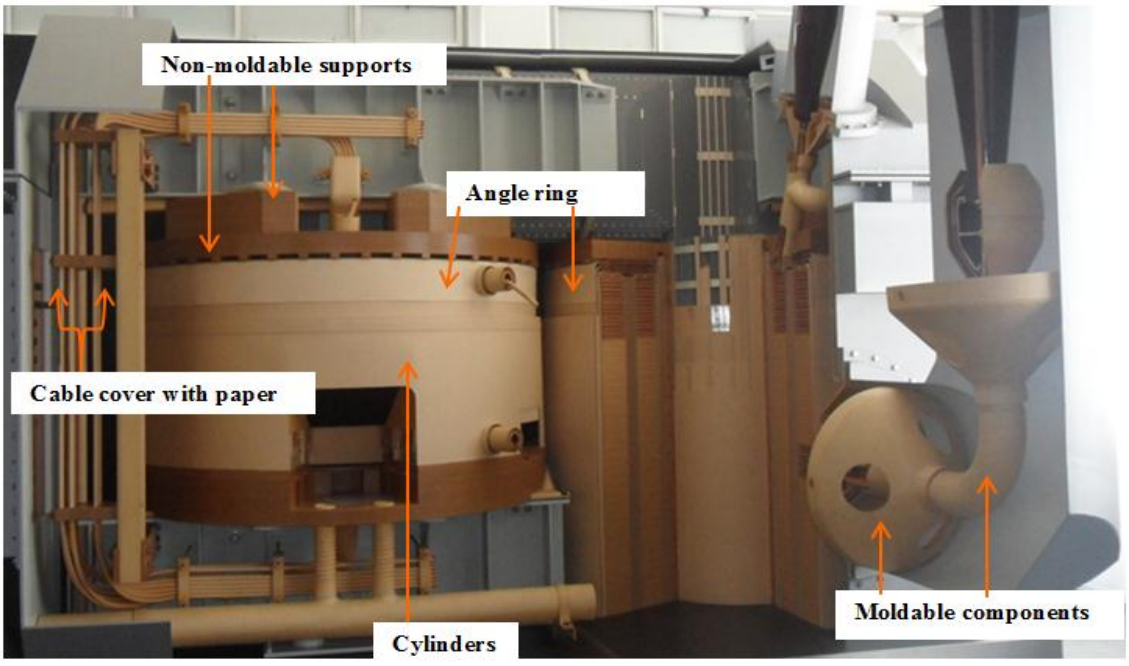

Figure 2-1: Mouldable and non-mouldable cellulose insulation components in a transformer application (courtesy of Weidmann Technology AG, 8640 Rapperswil, Switzerland)

The benefits of this alternative insulation material come at a price, making it economically unjustifiable for use in power transformers. The cost of alternative materials is mainly justified by the long term benefits such as the increase in the transformer loading capacity and the life cycle, as well as the opportunities of "going green" for retro-filling and retro-fitting transformers. Most of the research work for alternative composite systems is geared towards renewable and environmentally friendly insulation systems, as well as the thermal performance of the transformer [33 - 38].

The thermal performance of transformer insulation system defines its loading capability. IEC 60076-14 gives guidance on using hybrid insulation systems, to increase the thermal performance of a transformer [39]. This standard concentrates on the thermal performance of the insulation system. There is little literature available for the dielectric performance of these alternative composite insulation mediums for power transformer application.

There is information available indicating that dielectric performance of the ester oil and mineral oil is similar. The difference is in the areas of non-uniform fields where the streamers in ester oil are observed to propagate faster than in mineral oil at lower voltages of AC and lightning impulse [33, 40 - 42]. The probability of PD initiation is increased in insulation system with ester oil; hence the transformer designer must increase safety margins in such a design. The latter entails increasing the dimensions of the insulation system, which translates to increasing the dimensions of the transformer as a whole. Another disadvantage of using ester oil is its high viscosity, which slows down the oil circulation to the cooling system resulting in hot spots in transformers' active parts and metal structure such as tank walls [43].

Another alternative insulating liquid besides synthetic ester is silicone oil for application in transformer [44 - 45]. The disadvantage of silicone oil is that it is not biodegradable, has a high viscosity at high temperatures, forming jelly bridges of silicone-oxide during an arc and is incompatible with on-load tap changers [33, 38]. However, it offers a fire safety advantage and can be used in transformers that do not require voltage regulation.

Mono/dibezyltoluene (M/DBT) is another alternative liquid insulation material that is commonly used in capacitive voltage transformers, high voltage capacitors and bushings. It is still in the research stage for application in transformers. Currently it is used to reduce the gassing tendency of mineral oil by adding a percentage of M/DBT to the oil [46].

It can be concluded that, although there are alternative insulation systems, the costs and dielectric performance limit their application in power transformers. Furthermore, the experience that transformer manufacturers and power utilities have with the unconventional insulation as well as limited existing knowledge on these materials is hindering their application. Nevertheless, there seems to be a growing interest in understanding the behavior of these alternative materials since the

beginning of the 20th century and the research and development results are promising for application in medium power transformers [31].

Most of the alternative insulation systems have gained popularity in industrial transformer applications such as traction and mobile transformers where weight and size matter, as well as in furnace transformers and wind farm applications [44].

In the following sub-sections, the background on the application of mineral oil with cellulose based material as a composite insulation system in power transformers is presented.

2.2.1 Electrical insulating oil

Mineral oil is an insulating liquid used in electrical equipment such as power cables, circuit breakers, transformers and condensers. It is organic oil distilled from natural petroleum oil consisting mainly of saturated and unsaturated hydrocarbons (compound of hydrogen and carbon atoms). Transformer oil is a type of mineral oil with molecular structure consisting of varying percentage compositions of hydrocarbons of saturated paraffin (C_nH_{2n+2}), saturated naphthenic, and unsaturated aromatic structure [28, 38], as shown in Figure 2-2. Transformer oil is referred to as *naphthenic oil* if the composite percentage of the naphthenic compound in the whole molecular structure of the oil is higher than that of the paraffinic compound, and vice versa. When the amount of paraffinic compound is the same as naphthenic compound the oil is referred to as *mixed o*il. Transformer oil is mostly used in electrical equipment as an insulating liquid and a heat transfer medium. Viscosity and electrical breakdown strength are the important parameters for heat transfer and electrical insulation in the transformer applications, respectively [47]. Oil increases the dielectric strength of pressboard as discussed in above. The following subsection gives a background of the pressboard material and its base raw material.

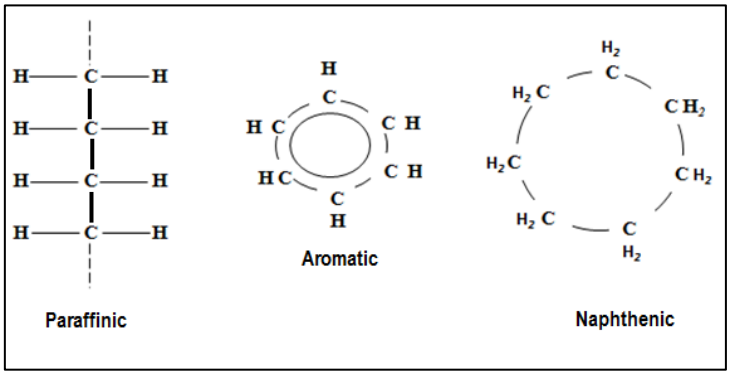

Figure 2-2: Hydrocarbon compound of mineral oil [28]

2.2.2 Electrical insulating pressboard

Pressboard insulation is made from layers of laminated cellulose paper. The paper used for electrical insulation purposes is produced from unbleached cellulose mainly obtained from softwood using the Kraft process. Kraft process (also referred to as the sulfate process) is a process of converting wood logs into pulp wood consisting mainly of cellulose fibres by removing substances such as lignin, resin and unwanted minerals from the wood. Cellulose fibre is a long chain polymer made of repeating units (rings) of ß-D-glucose, a simple sugar bonded together via an oxygen bond/bridge. The oxygen bridge is between the 1^{st} carbon atom of the glucose ring and 4^{th} carbon atom of the next glucose ring; shown Figure A1-1 in Appendix A.1. The number of links per chain is called the *degree of polymerisation* (DP) [49]. The chemical formula is $[C_5H_{10}O_5]_n$, where *n* is the DP, ranging from 1100 to 1200 for new cellulose [25]. The number of links per chain indicates the mechanical strength of cellulose fibre. Cellulose gives the structural support to the cell walls of leaves and plants. Depicted in Figure 2-3 are different stages of cellulose from the tree logs to the last chain of the cellulose molecules linked by the oxygen atom.

The hydroxyl attached to the 1^{st} carbon is opposite to the 4^{th} carbon with oxygen atom, which results in the chain of cellulose extending in a straight line. This means that the fibre can be long. The hydroxyls protruding laterally along the extension of the chain are readily available for hydrogen bonding. This hydrogen bond results in a stable crystalline region called a micelles (a ball of molecules as in Figure 2-3). This crystalline region gives the fibre strength and insolubility. The individual cellulose molecule groups between the micelles forming micro void structures of capillaries with diameters of about 10 nm to a few microns within the fibre. This makes cellulose very hydroscopic, meaning that cellulose can absorb water.

The next section provides a brief application of mineral oil and pressboard in transformers.

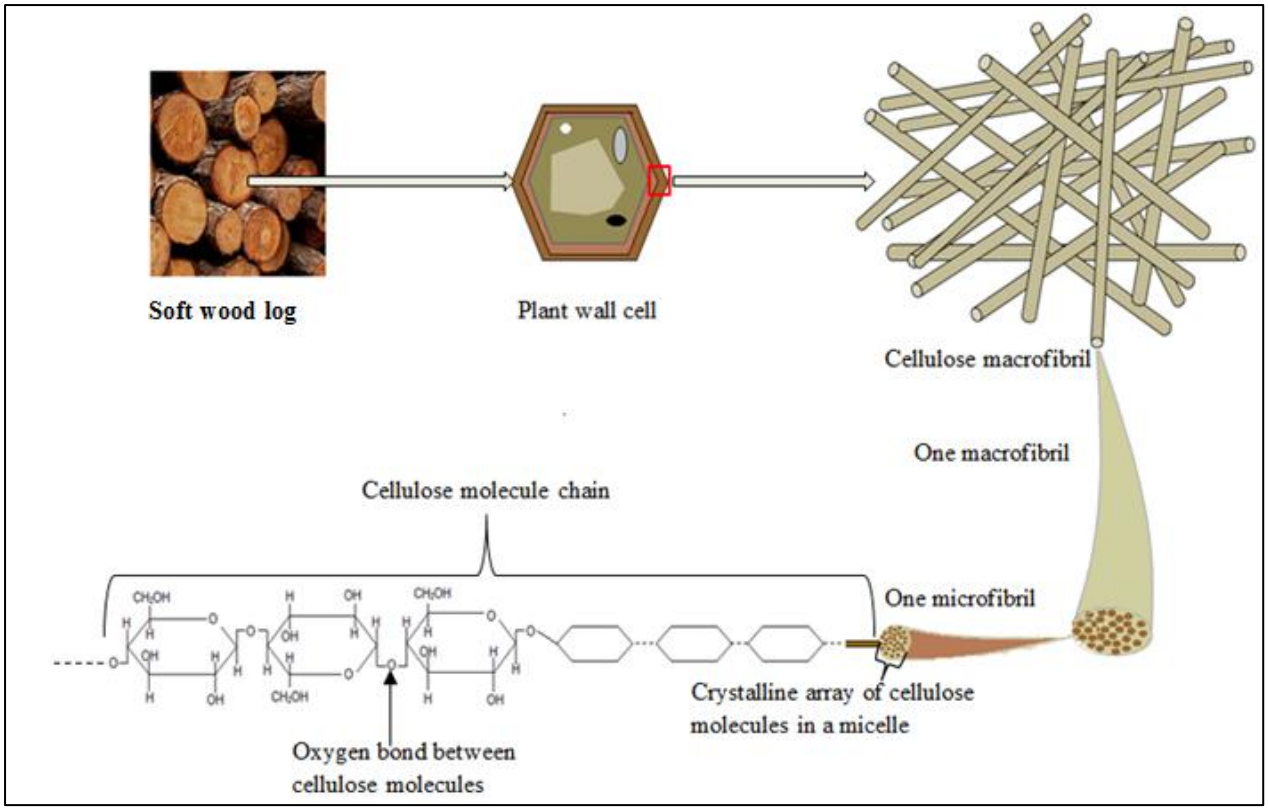

Figure 2-3: Macro to micro structure of cellulose fibre [48].

2.3 The function of mineral oil and pressboard in a transformer

The main function of a pressboard in a transformer is to subdivide the insulation gap between the low voltage (LV) and the high voltage (HV) windings into smaller gaps to increase the dielectric strength of the gap. It is also used to insulate the two windings from electrical streamer propagation, like a barrier layer. In addition, it provides the mechanical support to the winding coils. Figure 2-4 shows illustration pictures of the application of pressboard in a transformer.

Heat is continuously generated in the windings, core and structural metal parts due to material intrinsic loss and circulating currents when the transformer is in service. This heat is transferred to the surrounding insulation medium. Transformer oil continuously circulates between the transformer's active parts and the external cooling system such as radiators. The hot oil circulates to the top of the transformer's active part to the external cooling system, and the cooled oil returns into the transformer at the bottom via cooling pipes as illustrated in Figure 2-5.

Mineral oil has two main functions in the transformer; to cool the active part of the transformer and to improve the dielectric strength of cellulose materials through the impregnation.

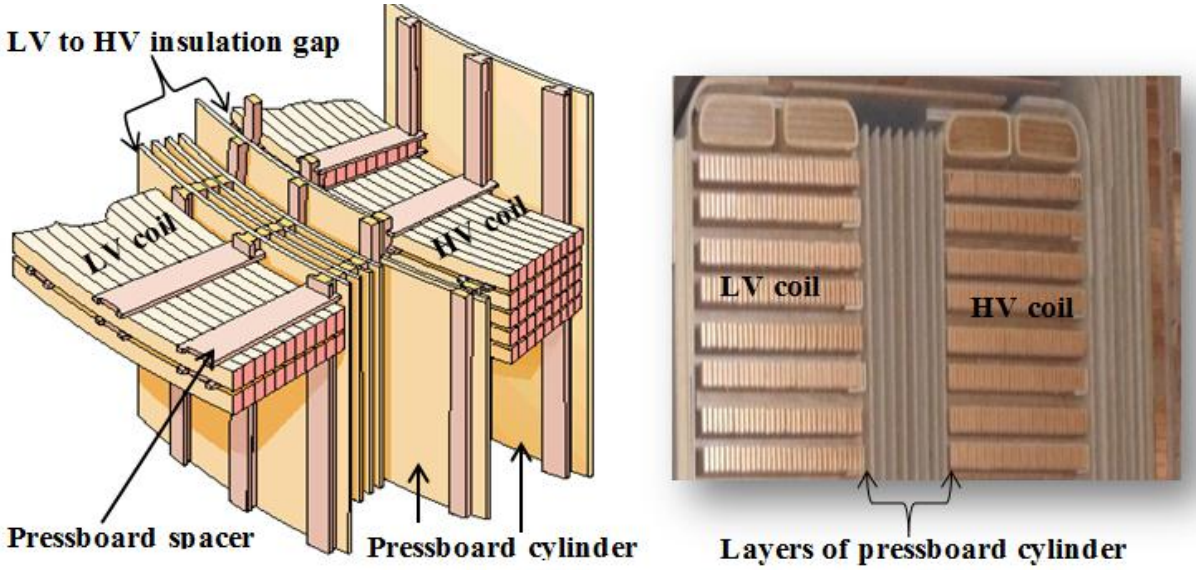

Figure 2-4: Application of pressboard as insulation in a transformer

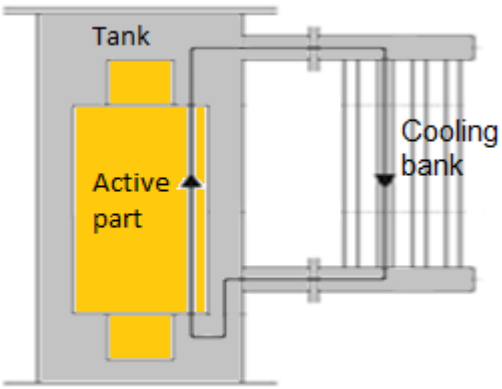

Figure 2-5: Circulation of oil in a transformer [32]

2.4 Factors that influence the electrical strength of oil-impregnated pressboard

The electrical strength of oil-impregnated pressboard depends on its physical and chemical properties. It is affected by mechanical, thermal and electrical stresses. It is also affected by the environmental conditions; impurities and contaminations have effects on its electrical and mechanical strength. The damage caused by the breakdown due to electrical, thermal or mechanical stresses on the oil-impregnated pressboard has an irreversible effect. Furthermore, when the cellulose pressboard degrades, it releases degradation by-products which pollute the surrounding oil; ultimately decreasing the dielectric strength of the whole composite insulation system.

The following subsections discuss some of the key factors that have effects on the electrical strength of oil-impregnated pressboard; moisture, temperature, contaminations, supply voltage frequency and surface discharge.

2.4.1 Effect of moisture on oil-impregnated pressboard

Moisture can enter a transformer's insulation system during the manufacturing process through inadequately dried insulation systems and inadequately sealed gaskets. While in service, moisture can find its way into the transformer's insulation through open breathing systems and improperly sealed turrets. Therefore, it is practically impossible to manufacture a transformer that is 100% moisture proof. Moisture has an effect on both electrical and mechanical properties of the composite oil-pressboard insulation.

The cellulose pressboard is hygroscopic in nature; it absorbs moisture from its surrounding environment. This is due to the –OH groups in the chemical structure (depicted in Appendix A.1) which attract the water molecules. The attachment of water molecules to the cellulose material happens until an equilibrium state is reached between the ambient moisture and the moisture in the cellulose material. Figure 2-6 shows the chemical reaction of cellulose molecule with water, which results in breakdown of the oxygen bond between the molecules. This process reduces the mechanical strength of the material and accelerates the ageing progression. Moisture in cellulose material also decreases the electrical breakdown strength of the material, lowers the PD inception voltage and also increases the dielectric losses. The knowledge of the effect of moisture on the dielectric strength of the composite oil-impregnated pressboard insulation system used in transformers has been established over the years [2, 15, 50 - 52]. According to the study done by Ding et al, moisture levels of less than 4% in the oil-impregnated pressboard has shown no significant change in the AC dielectric strength [11]. In another paper published on the study of the effect of ageing on the LI breakdown strength, the effect of moisture less than 4% was also found to be insignificant [53].

One of the shortfalls of cellulose based insulation system is hygroscopicity. In the manufacturing environment, various techniques are used to seal the pressboards exposed to ambient moisture. These techniques include drying the pressboard under heat and impregnating it with oil, cover with plastics, and controlling the factory's ambient conditions. This is a process important to manufacturers in ensuring that the transformer's insulation system moisture content is less than 1% [54] .

Besides factories' efforts of dealing with moisture, in early 1990s an attempt was made by Oommen et al to reduce the hygroscopicity of cellulose by a thorough process called *graft polymerisation* [54].

Graft polymerisation is a process of attaching the synthetic polymer chains to the back end of the cellulose polymer. The moisture absorption on a grafted paper is lowered when compared to normal cellulose paper. However, the modification on the cellulose material results in a brittle, increased thickness with high dissipation factors which makes it undesirable for transformer application. Moisture control in the factory is a major concern, if not controlled it leads to undersized or oversized pressboard insulation dimensions. This becomes a problem in the manufacturing process, when assembling the insulation components. The unpredictable dimensions due to moisture ingress in the cellulose insulation material lead to uncontrolled design and manufacturing process.

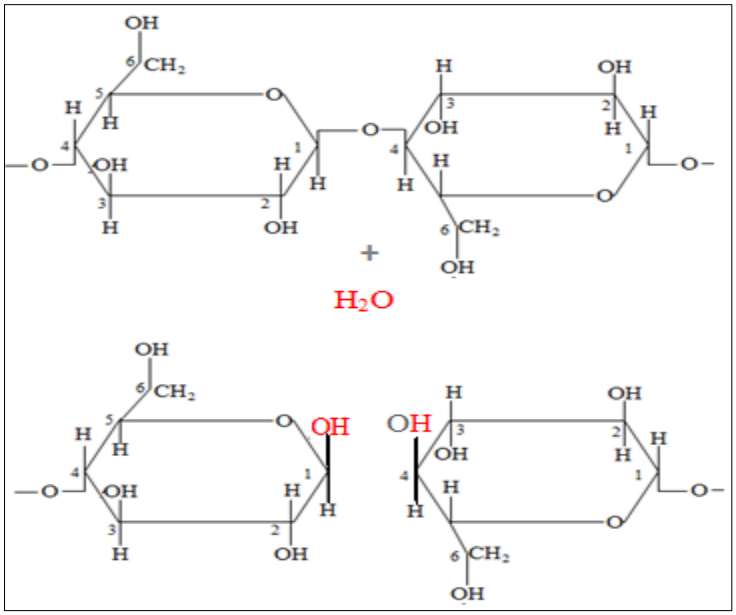

Figure 2-6: Illustration of water molecule attachment to the cellulose molecule [48]

2.4.2 Temperature effects on the oil-impregnated pressboard

In the previous section the effect of moisture on the electrical strength of oil-impregnated cellulose material was discussed. This section explores the influence of temperature on the dielectric strength of oil-impregnated pressboard material.

The distribution of moisture in the oil and cellulose material is temperature dependent. The increase in temperature has an opposite effect on oil as compared to cellulose material. When temperature increases, moisture migrates from the cellulose material into oil and when it decreases it migrates from oil back to the cellulose material. Hence, temperature plays a role in distributing moisture in the insulation system, in turn influencing the dielectric strength of the composite insulation system.

Under electrical stresses, conduction currents start to flow through the insulation system. This current flow causes temperature rise in the pressboard material, which in turn increases the conductivity of the material. Thermal runaway may be reached when the generated heat exceeds the rate of cooling or heat dissipation resulting in thermal breakdown and this is a dielectric breakdown due to increased temperature [52, 56 - 57].

Although high temperature has a negative influence on the insulation system, it has been shown that an increase in temperature increases the dielectric strength of oil. This is explained by the rate at which the gas bubbles present in the oil dissolve quicker at increased temperature [52]. Temperature is also known for accelerating the ageing of cellulose material, by decreasing the DP value, through chemical reaction that breaks the polymer chain.

Most solutions to temperature problems are based on using synthetic materials that have high temperature tolerance than cellulose and mineral oil; such as aramid, ester oil and other synthetic alternative insulation material. Unfortunately, the applications of these alternative insulation materials are limited in power transformer technology due to other shortfalls.

2.4.3 Contamination in oil-impregnated pressboard

In a transformer insulation system, it is possible to find loose cellulose fibres and small copper particles floating in the oil. Stringent housekeeping rules are emphasised by transformer manufacturers to maintain a clean manufacturing floor, free from foreign particles. Floating particles in oil get polarised in the presence of an applied electrical field resulting in a development of conduction path between electrodes. This results in PD, or in the worst case, total breakdown of the insulation system. Floating particles in oil are known to initiate surface discharge on solid insulation systems. Surface discharge, the subject of this dissertation is covered in more detail later in Section 2.4.6.

Other ways of contamination forming in a transformer include degradation by-products. Increased temperature in the insulation system results in thermo-kinetic degradation of the cellulose macromolecules. The thermal energy supplies the kinetic energy to individual atoms of the molecules. These atoms vibrate and break the bond between the chains of cellulose molecules. This process results in by-products like carbon dioxide (CO_2), carbon monoxide (CO), water (H_2O), hydrogen (H) and methane (CH_4). The thermo-ageing process also results in the formation of other substances such as sludge and acids which interact with transformer oil [3]. All these by-products form part of contaminants of the insulation system, which cannot be avoided during the lifetime of a transformer.

Chemical degradation by-products are also produced during electrical discharge in the gas filled voids of the pressboard material, resulting in carbon traces. Voids are one of the insulation contaminants known to initiate discharges on the surface of the solid insulation material [13].

2.4.4 Supply voltage frequency effect on oil-impregnated pressboard

The effect of frequency on the insulation system was an interesting topic in the early 1920's when induced voltage tests for windings with solidly earthed neutrals were introduced. The induced voltage test is performed at more than twice the normal operating frequency to avoid saturating the core and to reduce the amount of power required for excitation. This raised questions about the effects that this higher frequency has on the dielectric strength of the insulation system in power transformers. Vogel and Montsinger were among the pioneers in the research to study the effects of time and frequency of the supply voltage on the power transformer's insulation system in the laboratory environment [58 - 59]. Their research work showed that the increase in the frequency results in the decrease of the electrical strength of the insulation system. To get the same degree of severity during induced voltage tests, it was concluded that the time of voltage application must be reduced for an increase in frequency.

Equation (2.1) shows the relationship between the electrical breakdown strength (E), the supply voltage frequency (*f*), the time of voltage application (t), and the thickness of pressboard (d_t) [59]. It is noticeable from Equation (2.1) that the electrical strength varies exponentially as a function of frequency.

$$E = \frac{25.7}{{d_t}^{0.33}}\left(\frac{1.75}{f^{0.137}}\right)\left(0.5 + \frac{0.5}{t^{1/4}}\right) \tag{2.1}$$

The increase in frequency has a less significant effect on the transformer oil as compared to the solid insulation system [52, 58 - 59].

The dipoles of the insulating material vibrate when an alternating voltage is applied resulting in heat being generated in the insulating material. The heat is initially stored in the insulation, as it increases; it is dissipated to the surrounding environment which is at a lower temperature. This process continues until a state of equilibrium is reached, wherein the heat dissipated is equal to the heat generated. With the increase in temperature, the resistance of the pressboard insulation decreases due

to the negative temperature coefficient of resistance resulting in current flow in the material [52]. This increases the dielectric loss, leading to thermal instability and eventually; breakdown. Dielectric loss is the measure of the energy that is absorbed by an insulation material when alternating current is applied [28]. Equation (2.2) shows the relationship between the dielectric loss power (P_d) and frequency of the applied voltage (*f*), the magnitude of the applied voltage (V), capacitance (C) of the insulation material and tan delta (dissipation factor) [28, 56]. Frequency has a direct influence on the dielectrics power loss of the material. The equation (2.2) shows that the frequency has a direct influence on the dielectric power loss of the material.

$$P_d = 2\pi V^2 f C \tan\delta \tag{2.2}$$

Supply voltage frequency has also been used in research work as an ageing accelerator agent as done by Vogel and Montsinger in their research as discussed in the beginning of this subsection. The impact of varying supply voltage frequency on the PD spectral content is a research field of interest in cables for the purposes of PD diagnostics [61] . Frequencies other than power frequency are used to reduce the testing power rating for PD measurement in cables. Lower frequencies are desired for testing capacitive equipment and higher frequencies for testing inductive equipment. Lately, there has been a developing interest for understanding the effect of high frequency range on the properties of transformer oil insulation. Nagel et al studied the effect of high frequency ranging from 135 kHz to 170 kHz and high voltage on the dielectric strength of mineral transformer oil [62]. Ariastina et al studied the effect of voltage supply frequency variation in accelerating the deterioration of oil impregnated pressboard [63]. Their experimental findings agreed with the study done by Vogel and Montsinger that the ageing of pressboard increases with increase in voltage supply frequency [58 - 59].

2.4.5 Relative permittivity mismatch effect on oil-impregnated pressboard

The electrical characteristics of a composite insulation system depend on the relative permittivity of the bulk medium and the electrical breakdown at the interface of the two mediums. When an insulating material is exposed to an external electric field, the charge distribution gets modified; resulting in the polarisation of the material, acquiring a dipole moment. This means that the positive charges align in the direction of the applied field and the negative charges in the opposite direction.

Figure 2-7 and 2-8 show a sketch of a polarised and non-polarised of insulation material between parallel electrodes, respectively.

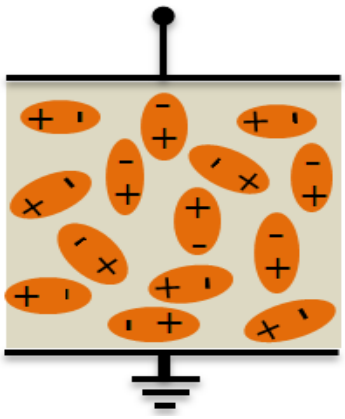

Figure 2-7: Non–polarised insulation material

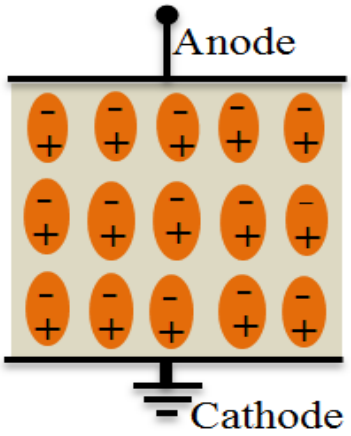

Figure 2-8: Polarised insulation material

The ability of the insulation medium to get polarised is described by the electrical susceptibility, which is represented by equation (2.3) [64].

$$\mathbf{P} = \varepsilon_0 \chi \mathbf{E} \tag{2.3}$$

Where:

P is the density of the electrical dipole moments

ε_0 is the permittivity of free space (F/m)

χ is the electrical susceptibility

E is the applied electric field intensity (V/m)

The electric flux density **D** is related to the polarisation vector **P** and electric field intensity **E** by equation (2.4).

$$\mathbf{D} = \varepsilon_0 \mathbf{E} + \mathbf{P} = \varepsilon_0 (1 + \chi)\mathbf{E} = \varepsilon_0 \varepsilon_r \mathbf{E} \tag{2.4}$$

Where:

ε_r is the relative permittivity of the insulation medium calculated by equation (2.5).

$$\varepsilon_r = 1 + \chi \tag{2.5}$$

It is understood that the difference in relative permittivity of the insulation materials plays a significant role in determining the breakdown mechanisms at the oil-pressboard interface [13, 65]. Figure 2-9 shows a sketch of a parallel plate electrode that is insulated by a composite insulation system; material 1 and material 2. In the case of two dielectric materials with different relative permittivity values in a uniform field, the electric flux density of the field is the same in each material i.e. $\mathbf{D_1 = D_2}$.

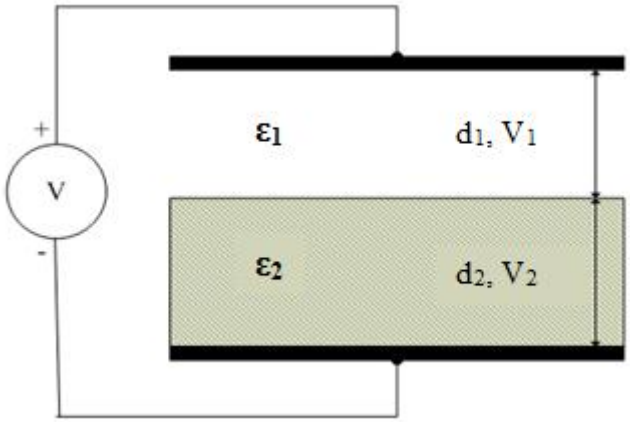

Figure 2-9: Parallel plate electrodes insulated by two dielectric materials

The ratio of the electric field stress in each dielectric material is related to the ratio of their relative permittivity values, given by equation (2.6).

$$\frac{E_1}{E_2} = \frac{\varepsilon_2}{\varepsilon_1} \tag{2.6}$$

Where:

E_1 is the electric field stress in material 1

E_2 is electric field stress in material 2

ε_1 is relative permittivity of material 1

ε_2 is relative permittivity of material 2

It is evident from equation (2.6) that the electric stress is higher in the material with a lower relative permittivity. If material 1 is oil which has a relative permittivity of 2.2 and material 2 is oil-impregnated pressboard which has a relative permittivity of 4.4 [30], oil is electrically stressed than pressboard.

When pressboard material is inadequately impregnated with oil, the capillaries of cellulose fibres are filled with air. Air has a low relative permittivity than the surrounding pressboard fibres. When voltage is applied across the pressboard, electrical stress is concentrated at the interface of air voids and pressboard fibres, initiating PD. The pressboard surfaces adjacent to the air void become the anode and cathode electrodes. The electrons bump against the anode with sufficient energy, breaking the chemical bonds of the cellulose structure. Positive ions bombarding the cathode increase the surface temperature of pressboard producing local thermal instability. Similarly, chemical degradation also occurs from the electrical discharge by-products. The net effect of all these processes is a slow erosion of the pressboard material and a consequent reduction in its thickness, leading to electrochemical breakdown [56 - 57]. This is a simple example of the effect that the difference in the relative permittivity values of the insulation media has on the electrical strength of the insulation system.

Relative permittivity mismatch in the composite insulation system of mineral oil and cellulose solid materials is an obvious disadvantage. Depending on the design of the insulation system, areas of high electrical stresses in the insulation system are formed. Attempts have been made to resolve the relative permittivity mismatch challenge. Ester oil has a permittivity of 3.2 compared to transformer oil of 2.2, bringing the permittivity mismatch ratio from approximately 2 to 1.4, when considering a relative permittivity of 4.4 for oil-impregnated pressboard [30]. However, due to faster streamer propagation in ester oil compared to transformer oil, it is an undesired solution for power transformer application. Further research is required to determine the effects of faster streamer propagation on the design electrical stress curves of the ester oil gaps. Design electrical stress curves are empirical plots of electrical stress in oil versus insulation gap, representing 1% probability of PD [3].

There is blooming research work on the electrical properties of biodegradable oils as these are being investigated as possible alternative liquid insulation for power transformer application and as a way of moving towards “green” transformers [66 - 67].

2.4.6 Surface discharge effect on the oil-impregnated pressboard

A surface discharge is characterised by tree-like patterns of carbon, deposited on the solid surface as a result of pyrolysis. Pyrolysis is a process of thermo-chemical decomposition of the hydrocarbon molecules of the material due to localised enhancement of electrical and thermal stresses. These treeing patterns are irreversible and the carbon deposits gradually create a permanent conductive path [56 - 68]. Surface discharge is sometimes referred to as creepage discharge or tracking discharge. This type of discharge results in catastrophic failures under normal operating conditions, making it a

dangerous failure mode of the insulation system [11, 13 - 15]. Surface discharge occurs at the interface of two different insulation mediums when the composite insulation system is subjected to voltage levels exceeding the interface voltage withstand capability. It can also result from sharp points of conducting materials that are in contact with the insulation material under high electrical stresses.

In power transformers the point-plane geometry electrode setup is often in the form of a conducting particle, either stuck on a solid insulation material or freely moving in the bulk oil. These particles do not have to be in direct contact with an electrode to cause breakdown [69]. Hence, the needle-plane electrode is the most used method to artificially create surface discharge in solid insulating materials in the laboratory setups. Other methods are discussed in Chapter 3.

To reduce the chance of surface discharge at the interface of the oil-pressboard system, the transformer insulation structure is designed such that the pressboard surface is parallel to the equipotential lines. This is achieved by using cylindrical pressboard barriers between windings and using shield rings, shielding conductors and yoke collars (angle rings) of different radii; towards the end of the windings. The placement of these insulation components is such that the equipotential lines are approximately parallel to the pressboard insulation surface. A finite Element Method (FEM) package for an electrostatic problem (which solves partial differential equation) is used to estimate and simulate the distribution of the equipotential lines and the electrical stresses at different areas in the transformer. The calculated electrical stresses are compared to the empirically developed stress criteria curves and a certain safety margin must be achieved to meet the design requirements for dielectric failure proof insulation system. Therefore, a certain arrangement of the insulation components depends on these empirical curves and the manufacturing tolerances.

Figure 2-10 illustrates an example of a 2-D FEM simulation of the equipotential line distribution of a single phase transformer winding arrangement. Also shown in the plot is the arrangement of the insulation structure between the LV and the HV winding and towards the winding ends. Figure 2-11, shows the corresponding FEM electric field stress plot. The red circles in the figure highlight the areas of localised electrical stresses. This is due to the non-uniform field distribution towards the winding ends as compared to approximately uniform distribution at the mid winding height.

In a power transformer, optimisation of insulation arrangement is not always feasible due to the complicated winding structure. It is not economically possible to bend the pressboard material to any desired radius or shape. Consequently, areas of localised electrical stresses might result and cause surface discharges on the pressboard material. The discharges in turn may result in a destructive effect that in the long run causes the deterioration of the dielectric strength of the transformer [12, 56, 70]. Figure 2-12 is a picture of an oil-impregnated pressboard material that failed during switching impulse dielectric tests of a transformer in the factory. Traces of surface discharge were found on the

pressboard during the failure investigation. Fine copper particles were found on the surface of the pressboard, which were suspected to have formed a conduction path when voltage was applied. These conduction paths lead to total dielectric failure, between the HV and LV windings. It is apparent from the figure that a conduction path of carbon tracks were formed on the pressboard that eventually led to a total flashover and puncturing of the pressboard material. Surface discharge can occur at any stage during a transformer's life. It can initiate during factory dielectric tests and continue to develop when the transformer is in-service. Depending on the severity of surface discharge, dielectric failure may occur during the factory test or during service in the field.

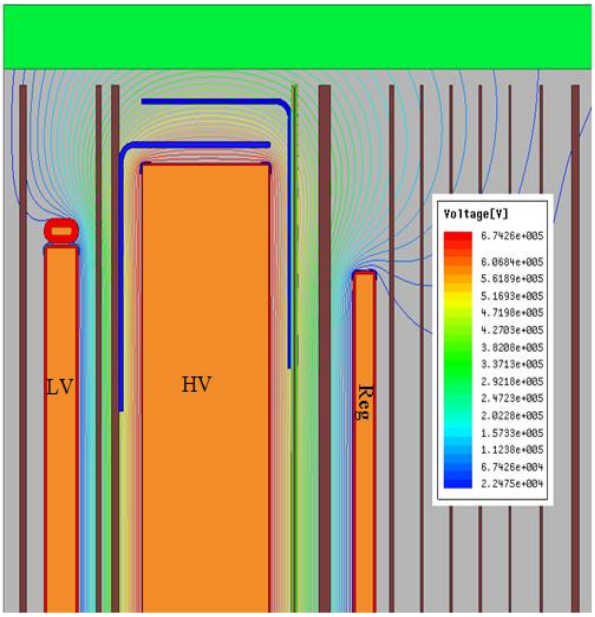

Figure 2-10: Axisymmetric 2D view of equipotential plot

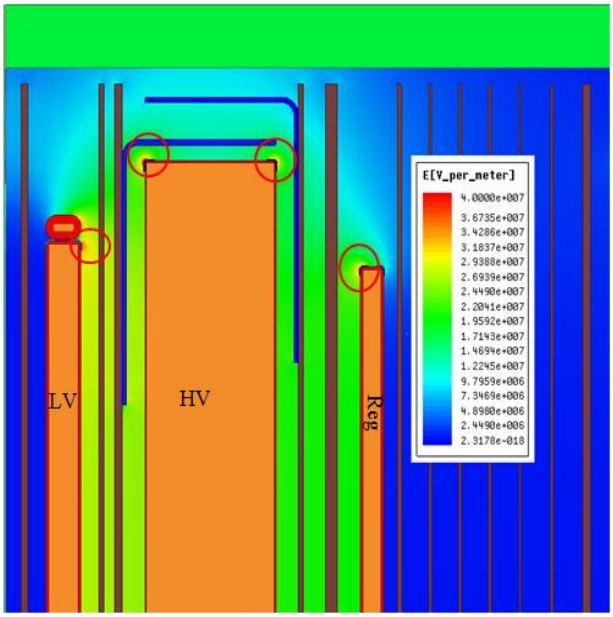

Figure 2-11: Axisymmetric 2D view of electric field stress plot

There is therefore a need to understand the consequences of surface discharge on the insulation system's dielectric withstand strength and how to improve its diagnosis methods. There are scarce studies about the effect of surface discharge on the LI breakdown strength [12]. This research work therefore aims at contributing to this knowledge gap.

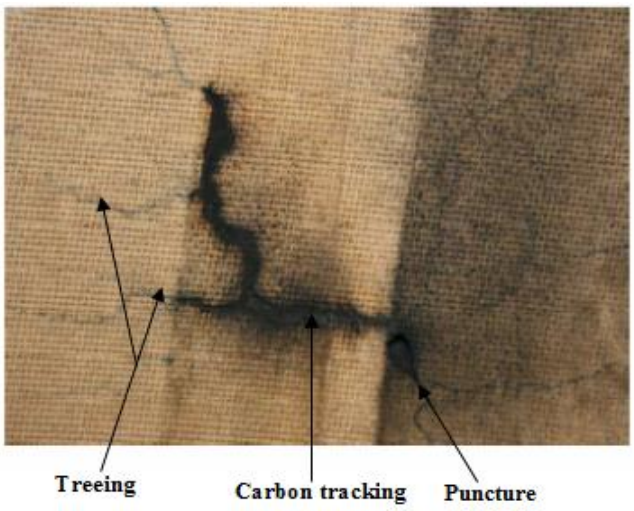

Figure 2-12: An example of treeing, carbon tracking and a puncture on a pressboard material of an HV winding (courtesy of Powertech Transformers (Pty) Ltd, Pretoria West)

2.5 Conclusion

In this chapter, the background of the composite insulation system used in oil immersed transformers has been presented. Advantages and short coming of alternative insulation materials in an attempt to replace mineral oil and cellulose material were discussed. The key factors that influence the dielectric strength of the oil-pressboard composite insulation system were covered. Efforts have been made to explain the chemical structures of both mineral oil and cellulose, to assist with explaining how some of these key factors affect the molecular bonds and accelerate the degradation rate of the composite insulation.

Surface discharge is noted as one of the main causes of dielectric failures. It is referred to as a "slow killer" of the insulation system, as it can take minutes, hours to years for it to cause total failure of the insulation system under normal operating conditions. This means that there is a need to understand the effect it has on the insulating systems' dielectric strength and how it can be monitored using diagnostic methods like PD measurements. Discussed in the next chapter are the different methodologies of simulating the surface discharge on oil impregnated pressboard in the laboratory environment.

Chapter 3: The techniques of creating surface discharge on oil-impregnated pressboard in the laboratory environment

3.1 Introduction

In the previous chapter, discussions on the factors that influence the dielectric strength of oil-impregnated pressboard insulation were conducted. Surface discharges due to localised electrical stress were identified as one of the key factors that affect the dielectric strength of oil-impregnated pressboard. In designing the insulation structure of a power transformer, it is important to use finite element modeling (FEM) tools and empirical formulas to calculate electrical stresses. Surface discharge initiation stress (also referred to as creep stress) along the surface of pressboard material is one of the electrical stresses that is analysed in detail for insulation structure design to minimise probability of surface discharge formation. The calculated surface discharge stresses must be within the acceptable values according to the electrical stress design curve criteria and with certain tolerance margin. These design curves are developed from laboratory data, considering different electrodes arrangement. Weidmann design curves are an example of such design curves [72], though different transformer manufacturers might have different curves specific to their factory, in general they follow a similar basic design methodology. Although, transformer designs are based on these design methods and attempts to minimise the formation of surface discharge are done, the formation of contamination due to insulation degradation cannot be completely avoided. Hence, the chance of surface discharge forming during the transformer life cycle cannot in reality be dismissed.

A literature review on laboratory studies focusing on surface discharges and the effect they have on the dielectric strength of oil-impregnated pressboard is discussed in this chapter. Different methods of simulating surface discharge on the pressboard in the laboratory environment are also presented. The experimental test setup used to simultaneously age 12 test samples by surface discharge is presented.

3.2 Background

The study of the pressboard insulation life expectancy by accelerated ageing has been in practice since the 1930s [1]. The life expectancy of pressboard is determined by its DP value and tensile strength. A DP value of 200 or tensile strength of pressboard of 50% of its initial value is regarded as the end of life [73]. The commonly used method of accelerating the ageing process of pressboard is thermal ageing [3, 66, 71, 73]. This is a time consuming process, where the ageing can take days, weeks,

months and even years depending on the temperature and the purpose of the study. The pressboard test samples are kept in the ageing tubes under increased temperature. After a certain period, physio-chemical tests are performed on the samples to determine the degradation severity. An electrical withstand strength is also performed on these aged samples to study the effect of ageing. There is no evidence in literature regarding this method being used to study surface discharges on aged pressboard.

Another method of accelerated ageing of pressboard insulation is by applying voltage at high frequency. As discussed earlier in Section 2.4.4, high supply frequency is an ageing agent itself and therefore undesirable.

Surface discharge accelerated ageing methods on wet pressboard with a moisture content of more than 0.5% is a common ageing technique [13, 68, 74]. When the electrical stress is applied on the wet pressboard, moisture evaporates from the board leaving a trace of white marks shaped like tree branches. These marks continue to grow until a conduction path is formed between the high voltage and earth electrode. The traces of white marks are followed by a trace of carbon. In this method, the voltage is either applied in step increments at selected intervals or a constant voltage magnitude above PD inception is applied until breakdown occurs while taking PD measurements. These experiments are performed in a controlled environment, free from insulation contamination and the oil is usually changed after every breakdown. This experimental setup ageing technique can take hours to days, since the discharge development will depend on the arrangement, type, shape of the electrodes and the gap distance between the electrodes as well as the condition of the pressboard test samples. Raja et al used this approach to study the PD behavior of an oil-impregnated pressboard insulation model which took 3 to 6 hours before insulation breakdown [75]. In another study done by Mitchinson et al, it took up to 12 hours for surface flashover to occur [68].

Limited information is available in the literature on the lightning impulse (LI) breakdown voltage of pressboard pre-exposed to surface discharges. The questions to be answered are: What happens to the pressboard insulation when lightning strikes on the pressboard that has been pre-exposed to surface discharges? How is the ability of the pressboard to withstand LI affected? This research follows the method of accelerated ageing of oil-pressboard insulation material through application of constant voltage above the discharge inception voltage across a selected gap between the HV and earth electrodes. Section 3.3 gives a summary of some of the popular methods used to create artificial surface discharges.

3.3 Simulation of surface discharge in a laboratory environment

There are many methods of simulating surface discharge in a laboratory environment some of which are reported in research studies such as [13, 51, 68 - 71]. This section discusses some of the electrode arrangements in the literature used to simulate surface discharge on the pressboard surface. These methods can be summarised as follows:

1. **Rod-plane electrode arrangement** - A rod is connected to a high voltage source and placed on or near the surface of the pressboard. This result in an intense electric field stress around the rod tip, causing electrical discharges to occur around the needle tip, leaving radial carbon tracking patterns on the surface of the pressboard insulation. However, narrow rod produces a directional and intense electrical field stress, which can lead to a rapid electrical failure or puncture through the pressboard insulation material. Figure 3-1 shows the intensity profile of the electric field stress at rod tip directed towards the pressboard material. This method cannot reliably produce surface discharge as there is a high possibility of premature puncture of the pressboard.

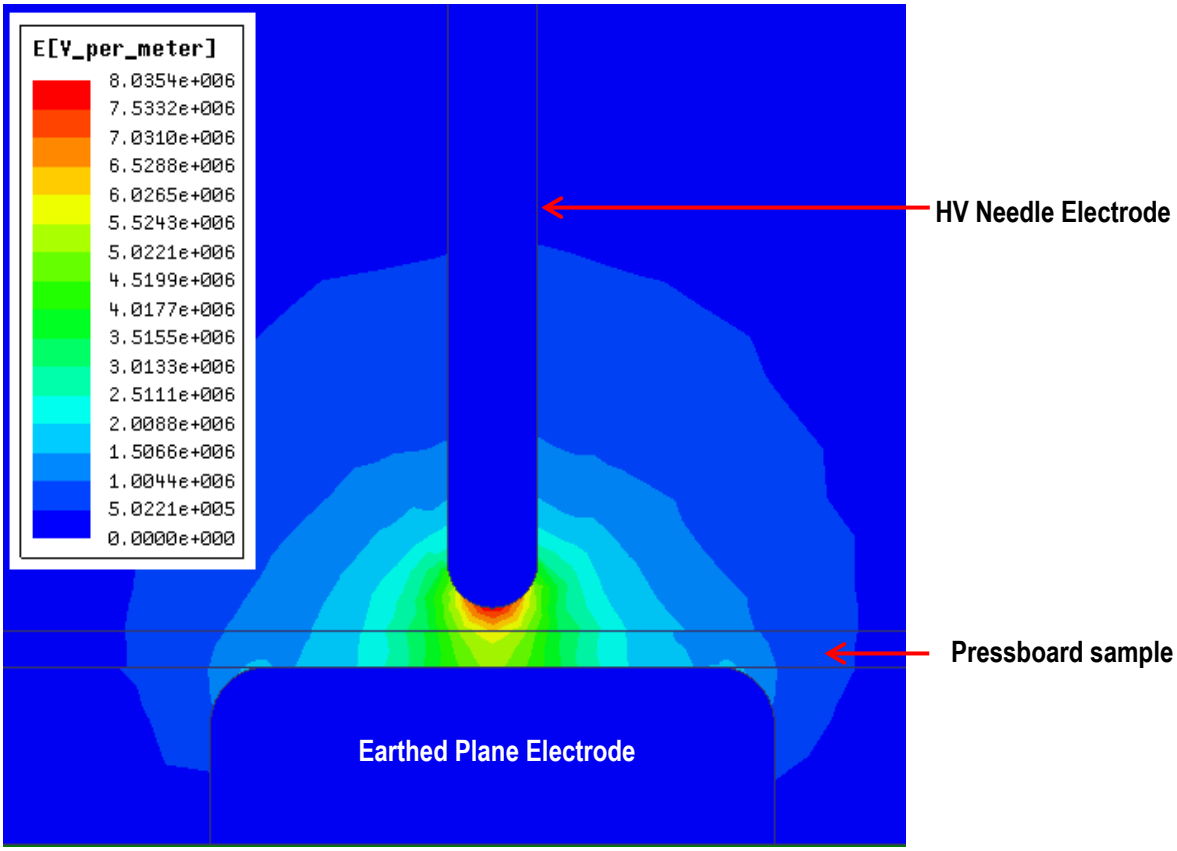

Figure 3-1: Illustration of the electric field stress for needle to plane electrodes arrangement

2. **Parallel plane–plane electrode arrangement** – Pressboard material is sandwiched between two plane electrodes. High electric stress is concentrated on the oil wedge and is where the surface discharge initiates. The challenge with this method is to avoid puncture of the pressboard before sufficient surface discharge is created. The possibility of puncture makes this method unreliable for creating surface discharge in an ageing experiment. Figure 3-2 shows an electrical field plot for this electrode arrangement.

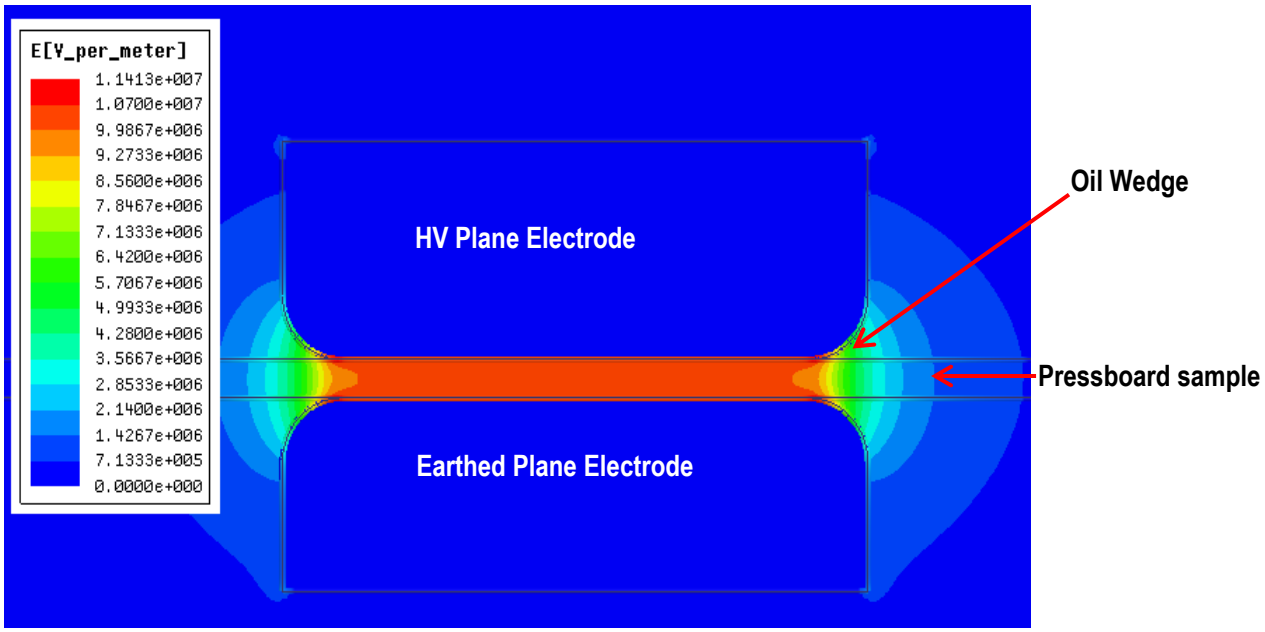

Figure 3-2: Illustration of the electric field stress for plane to plane electrodes arrangement

3. **Needle at an acute angle to plane electrode arrangement** –A needle is placed at an acute angle to the pressboard at some gap distance from an adjacent earthed electrode, as shown in Figure 3-3. The acute angle ensures that charge arising at the needle tip is directed along the surface of the pressboard rather than through the bulk of the pressboard material. This method has been found to reliably produce surface discharge and sustain the discharges for sufficiently long time before breakdown [13]. The onset of PD is a result of the local field conditions around the discharge source, the needle tip.

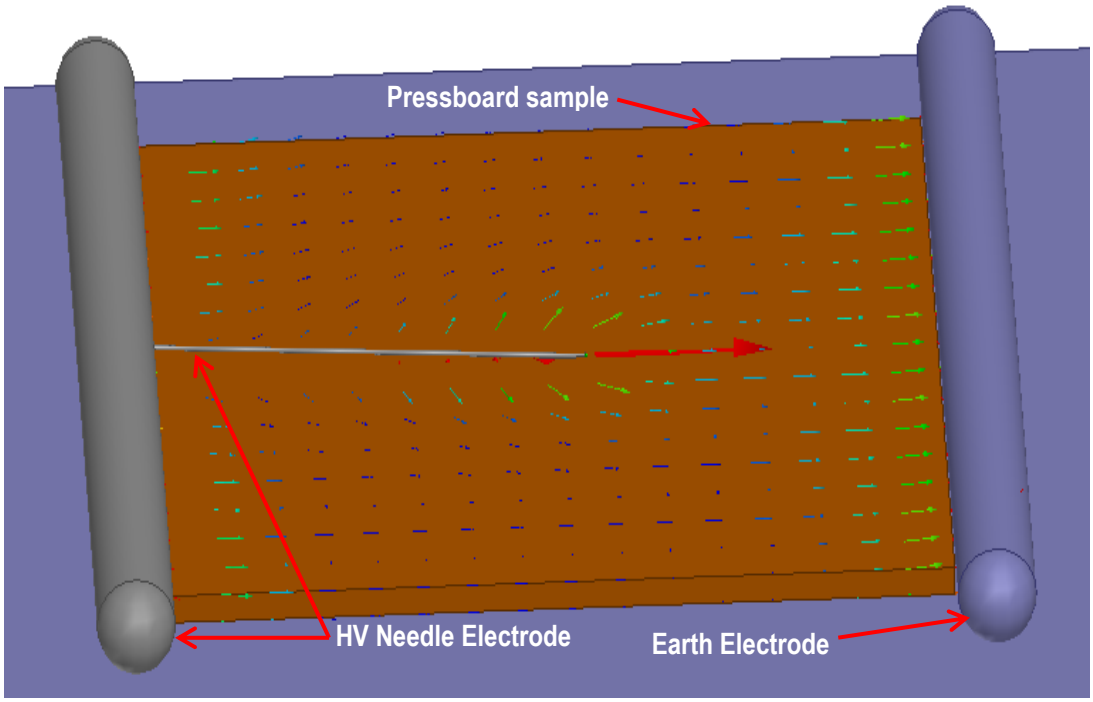

Figure 3-3: Illustration of electric field vector for needle at an acute angle to plane electrode arrangement

The needle at an acute angle to plane electrode setup for simulating surface discharge on the pressboard test sample is used in this dissertation research work.

3.4 Measurement of surface discharge

Surface discharge is a type of PD. Different types of on-line and offline PD diagnostic methods are used to assess the condition of the insulation system. Transformer manufacturers assess the quality of the insulation system by conducting routine delivery AC induced voltage test together with PD measurements. This test is performed on all transformers with highest equipment voltage (U_m) greater than 72.5 kV as a routine test and for $U_m \leq 72.5$ kV as a special test [76]. Utilities assess the insulation condition of the transformer connected to the network using on-line and off-line PD measurement systems. The obtained information is used to schedule the transformer maintenance. In the academic research field, PD measurements are done to study the failure mechanisms of different insulation media and to develop knowledge on interpretation of the different discharge phenomena.

3.4.1 What is PD?

PD is a localised electrical discharge or the dielectric breakdown of a small portion of solid or liquid electrical insulation system, under high electrical stress. It is a consequence of local electrical stress concentration in the insulation or on the surface of the insulation [56]. PD is characterised as a current pulse with durations in order of nanoseconds [56].

In a composite insulation system, differences in relative permittivity play a key role in creating uneven distribution of the electrical stress. The electrical stress is concentrated more in the insulation material with smaller relative permittivity. To illustrate how this phenomenon can result in PD, depicted in Figure 3-4 is a solid insulation such as pressboard materials with an air-filled void. The pressboard has a higher relative permittivity than the air in the void. This means that a higher electric field will be created in the air void according to equation (2.6). As the applied voltage is increased, it reaches the electrical breakdown voltage of air in the void. The PD current flows in the void and voltage in the void drops. Once the discharge current is extinguished, the voltage across the air void increases again until a threshold voltage is reached above the air breakdown voltage, and another PD current flow. This process continues as long the applied voltage exceeds the breakdown voltage of air in the void. The discharge voltage appears superimposed on the negative and the positive sine waveform of the applied voltage across the insulation system. This process can be visualised with the aid of Figure 3-5. V_a represents the applied voltage across the insulation system, V_c is the voltage across the air void. U^- and U^+ are the negative and positive breakdown voltage of air, respectively. V^+ and V^- are the voltage values to which the voltage drops during the PD current flow in the void. The resultant PD current pulses are shown below the voltage waveforms in Figure 3-5.

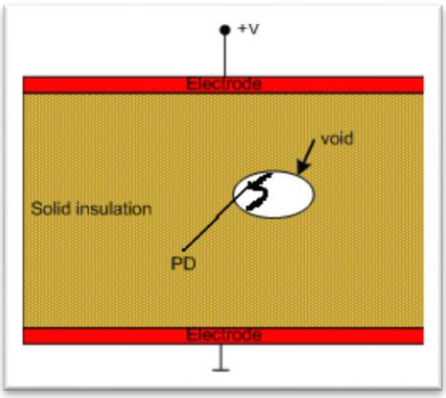

Figure 3-4: Illustration of air void in a solid insulation material initiating PD

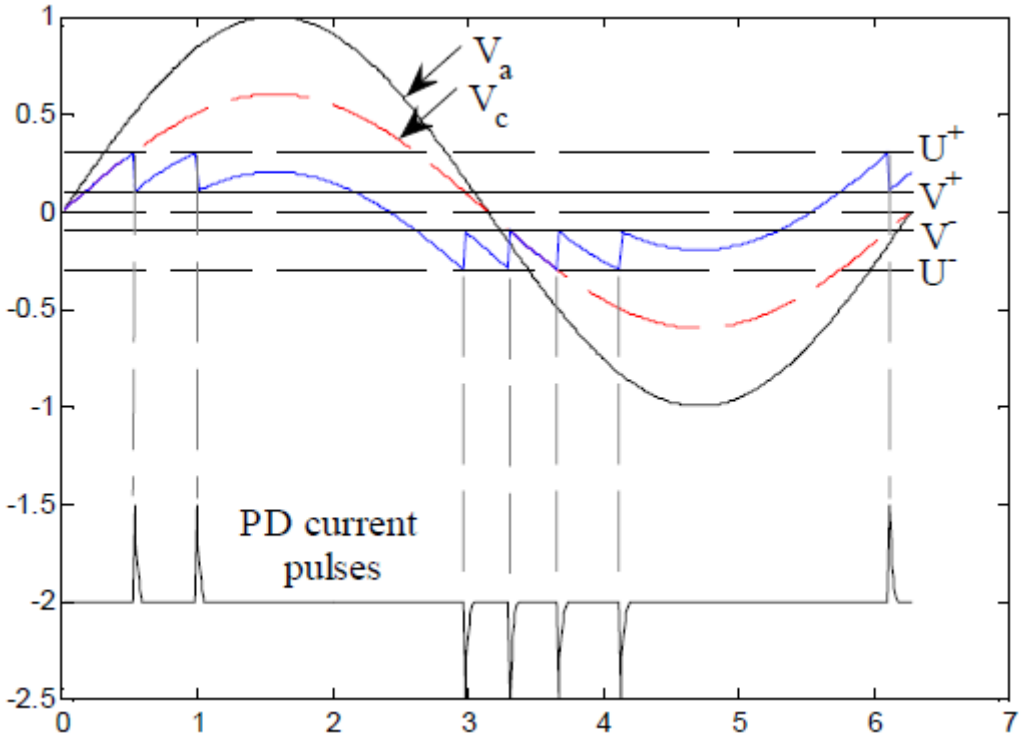

Figure 3-5: Representation of the repetition of PD pulse in a void [77]

As the PD activity continues in the void, the pressboard surface adjacent to the void gradually erodes. Carbon conduction path is created along the cavity surfaces thus, slowly bridging the insulation system and this eventually results in a complete insulation breakdown.

3.4.2 Methods of measuring PD

Different forms of energy are released during the PD activities such as; electrical, acoustic, optical, and chemical. These forms of energy are detected by PD measuring equipment and the measured data is analysed to locate and characterise the PD source. Detection of electrical current pulses of PD is a well-developed technique that has been used for many years.

PD measurement methods are classified in two groups; conventional and non-conventional methods. The conventional method is based on the electrical measurement of PD current pulse and chemical elements analysis using dissolved gas analysis (DGA). The non-conventional method is based on the detection of electromagnetic waves, acoustic energy and optical energy [6]. The IEC 62478 standard under review gives a guideline for PD measurement using non-conventional; electromagnetic and acoustic PD detection methods [78] whereas the conventional method is performed in accordance to the IEC 60270 [19]. Combining the two methods increases the chance of accurately locating the PD

source and more information can be gathered to perform a comprehensive assessment of the insulation defects.

In the transformer industry, a general procedure is followed for PD diagnosis, which can be summarised as follows [7]:

- Detect the PD activities indicating the insulation defects using suitable PD measurement systems.
- Identify the type of the insulation defect through interpretation of the measured PD data.
- Locate the PD source using combination of the conventional and non-conventional methods.
- Assess the risk for insulation failure based on the PD source investigation.

The next section discusses the conventional PD measurement, as it is the diagnostic method used in this study.

3.4.3 Conventional method

3.4.3.1 Electrical detection

The circuit in Figure 3-6 is commonly used for PD current pulse detection [78]. The connection of the coupling capacitor parallel to the test object protects the measuring system from the damage in case of short circuit in the test object. IEC 60270 recommends other circuit arrangements for the PD detection as well as the measuring equipment requirements [19].

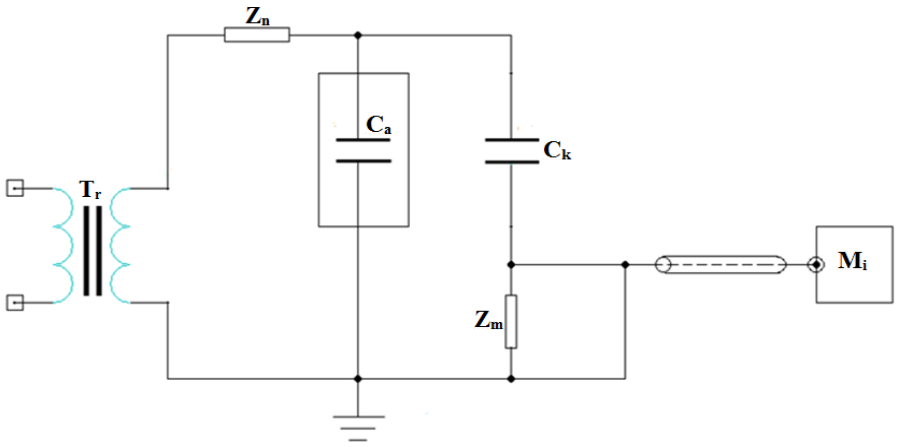

Figure 3-6: PD measuring electrical circuit [78].

Where:

C_a is the test object capacitance

C_k is the coupling capacitor

M_i is PD measuring instrument

T_r is the PD free test transformer

Z_m is the measuring impedance as part of the coupling device

Z_n is a noise blocking filter from the power supply

Locating the PD source in a transformer using this method is possible but complicated; experience with interpreting the phase-resolved-partial discharge patterns (PRPDP) is essential. Typical PRPD patterns for typical insulation defects in oil-immersed transformer are presented in [7, 77]. These PRPD characteristics can facilitate interpretation of the PD measurement results and to locate the source in a complex insulation structure. It can be a challenge to identify a PD defect when there are more than one PD sources, as the signals appear superimposed on the same PDRD pattern. Depicted in Figure 3-7 is an example of a PRPD for surface discharge produced on an oil-impregnated pressboard in an electrode setup as shown in Figure 3-8.

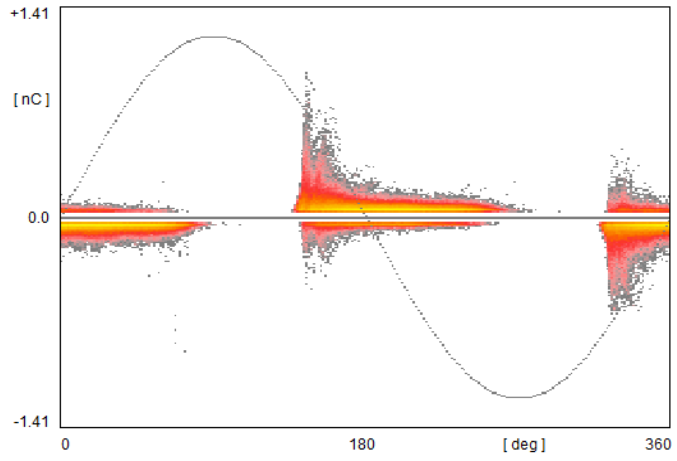

Figure 3-7: Typical PRPD pattern for surface discharge [77]

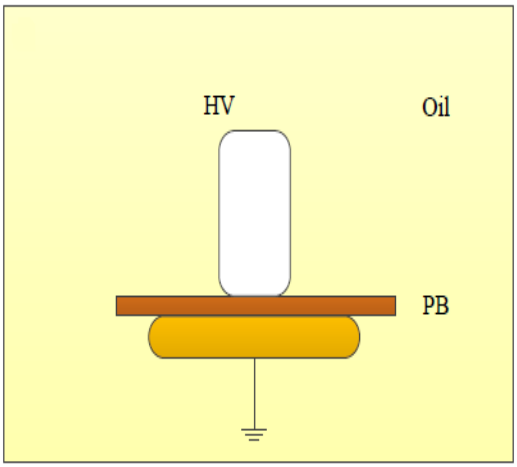

Figure 3-8: Electrode arrangement for surface discharge measurement [77]

3.5 Conclusion

Presented in this chapter are different methods of creating surface discharge in a laboratory environment, from which a needle at an acute angle to plane electrode arrangement was selected for this research work. Methods of surface discharge measurements were briefly discussed. The next

chapter presents the experiments for studying surface discharge on oil-impregnated pressboard. The results from the experimental work are analysed to explain the surface discharge effects on the pressboard.

Chapter 4: Determining optimal electrode gap distance for creating surface discharge on the pressboard test samples

4.1 Introduction

In the previous chapters, the research hypothesis was established; literature review on surface discharge and different methods of creating surface discharge in a laboratory were presented. In this chapter, the actual ageing experimental work by creating surface discharges on the pressboard test samples and a discussion of surface discharge failure mechanisms are presented.

The experiment in this chapter is aimed at determining the optimal gap distance between the HV needle tip and the earth electrode as well as the choice of test supply voltage value above the PD inception voltage. The gap distance and supply voltage must allow for a sustained surface discharge for hours without flashover in oil or through the pressboard test sample. The distance and the supply voltage are then used to set up the multiple test samples surface discharges ageing array experiment for 24 pressboard test samples, discussed in Chapter 5. The aged samples are then tested for LI breakdown voltage, discussed in Chapter 6.

Four test samples from the conditioned 54 pressboard test samples were used in the investigation to determine the discharge gap. Four electrode gap distances were selected in increment of 10 mm. PD inception voltage and supply voltage at which flashover in oil occurred at each gap distance were noted. In addition, the surface discharge activity was monitored. For every gap distance tried in this experiment, PD magnitudes were measured and PRPD patterns recorded to identify typical discharge patterns that correlated to similar observations in the literature [77, 79].

4.2 The electrode gap distance setting experimental procedure

Figure 4-1 depicts the test sample setup, showing the pressboard test sample, needle electrode, the earth electrode and the gap distance, *d*, between the electrodes. Appendix A.2 , Table A 2-1 lists the materials used in the experiment and their dimensions. This setup was immersed in new transformer oil from ENGEN Petroleum Ltd. This is an uninhibited transformer oil known as POWEROIL TO 1020 (60 UX) ™. Figure 4-2 depicts the circuit schematic used in the setup experiment to measure PD as part of the gap size determination procedure.

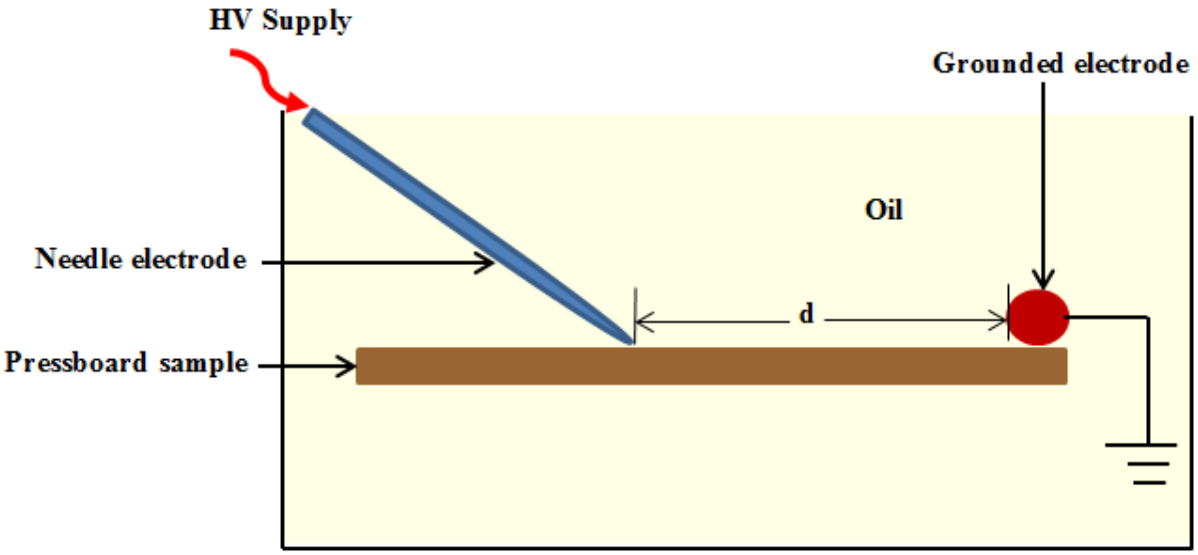

Figure 4-1: Test sample placed between electrodes

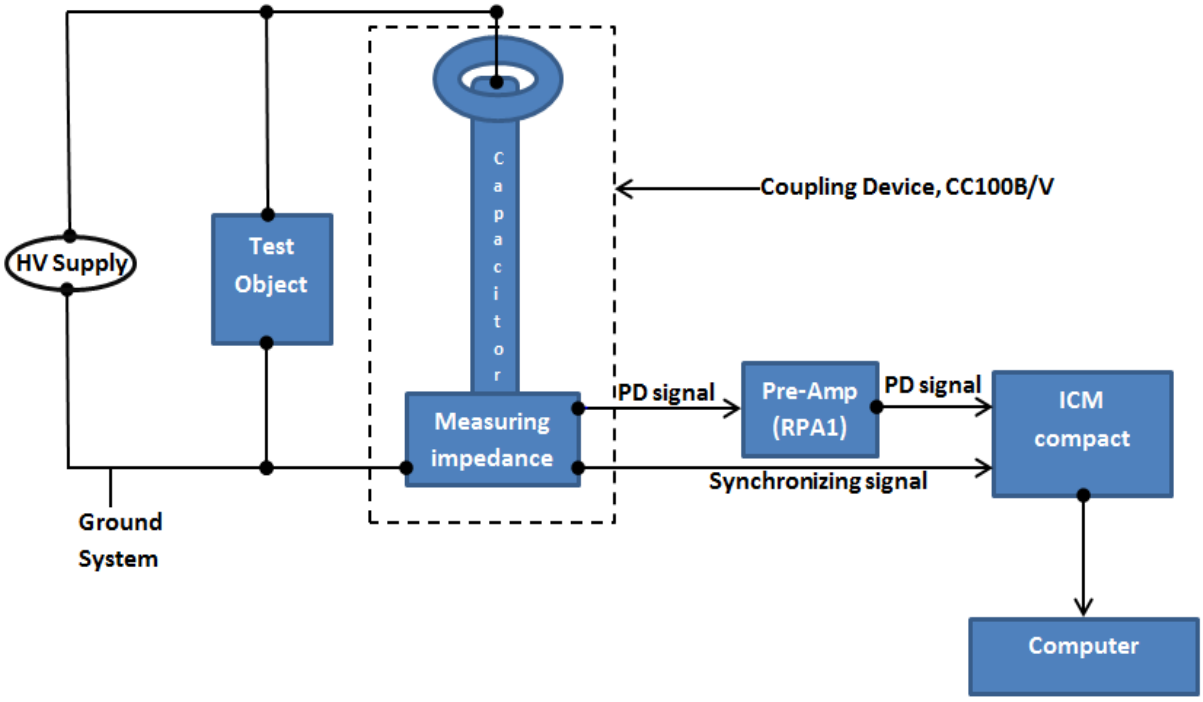

Figure 4-2: The schematic for the PD measuring system

4.3 Measurement method

The PD measurement system was calibrated in accordance with IEC 60270. After every insulation gap distance setup change, the calibration was repeated before starting the next test setup.

A 20 minute period was allowed between each gap distance test in order to allow the oil to settle and tiny bubbles to dissolve. The oil was changed after two sets of tests to avoid influence of contamination on the results. The voltage was increased in steps of 5 kV up to 20 kV; and then in steps of 3 kV from 20 kV to 50 kV. Each voltage level was held for 5 minutes to allow the discharge to stabilise. The highest measured background noise during the experiments was about 1.8 pC and the lowest was 0.60 pC. The PD parameters (PRPDP, PDIV and PDEV) were recorded using the Power Diagnostix^{TM} ICMcompact system.

The needle tip to earth electrode gap distances investigated in this experiment were; 55 mm, 45 mm, 35 mm and 25 mm. These distances were limited by the size of the pressboard test sample and the possible achievable distance from the needle tip to the earth electrode. The selected distances were sufficient for this study as it has been established by Dai et al through a laboratory experiment that for any gap distance of less than 30 mm, direct breakdown through oil occurs and stable surface discharge was found to be at gap distance more than 30 mm [51].

4.4 Experimental results and observations

A plot of the PD magnitude as a function of gap distance in a given voltage range is shown in Figure 4-3. Presented in Appendix A.3 , Table A 3-1 are the peak measured PD magnitudes per distance setup, for supply voltage ranging from 5 kV to 50 kV. Table A 3-2 to A 3-5 give a plot the PRPD patterns captured at supply voltage level from 20 kV to 50 kV, for gap distance of 55 mm, 45 mm, 35 mm and 25 mm, respectively. Supply voltages for 5 kV to 15 kV are not presented as the PD magnitudes were low (at background noise level) and no PRPD patterns were visible on the measuring scope. During the experiment, a video recording was setup near the test sample tank to monitor and record the physical PD activities on the test sample through a transparent Perspex oil tank housing the test samples. The oil color was transparent, allowing for visual observation. The recorded information from the video was later analysed and the physical and audible sound observations were correlated to the measured PD magnitudes and PRPD patterns to explain the surface discharge failure mechanisms.

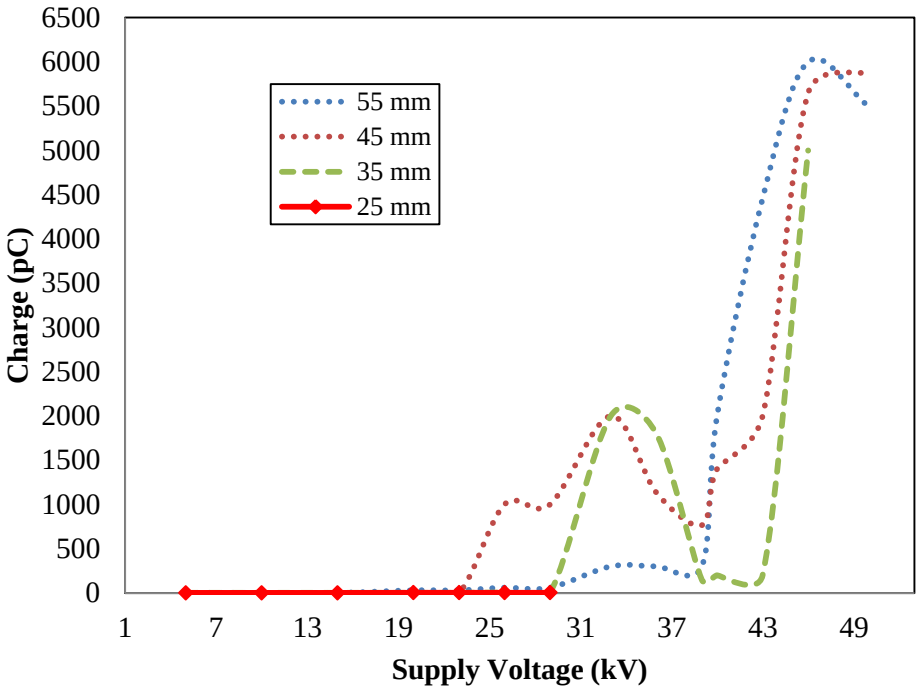

Figure 4-3: The peak charge magnitude vs. supply voltage

The following sub-sections present the main observations during the experiment per gap distance setup.

4.4.1 Discharges at 25 mm gap distance

The gap distance of 25 mm could not withstand 50 kV supply voltage, and relatively low PD peak charge values were measured throughout the experiment. The background noise was measured to be 0.7 pC. The measured PD inception voltage above the background noise was 20 kV. After a few minutes at 23 kV applied voltage level, flashovers in oil were observed with low charge magnitude (as in Figure 4-3). When the supply voltage was raised to 29 kV, the rate of flashovers in oil increased. The highest reached supply voltage was 29 kV. No further increase in supply voltage was possible due to the consistent oil flashovers. Physical observation of the test sample pressboard showed no marks of discharge traces (such as white marks or carbon traces). The result of the 25 mm is in agreement with the study done by Dai et al [51]; that no surface discharge can be recorded at gap distance less than 30 mm.

4.4.2 Discharges at 35 mm gap distance

As the 25 mm gap, 50 kV supply voltage could not be withstood. The recorded background noise was 1.6 pC. The PD inception voltage was 23 kV. No surface discharges were detected at voltages less than 36 kV. At 36 kV, audible corona discharges in oil were heard, and a few repetitive sparks in oil were observed. After 2 minutes at this voltage level, the surface discharge PRPD pattern similar to that observed by Niasar [77] and Cheng et al [79] were observed on the PD measuring instrument. Similar patterns were recorded by Wang et al [10] using an ultra-high frequency (UHF) PD diagnostic system. Appendix A.3, Table A 3-4 shows the recorded PRPD pattern at this voltage level. The phase angle of PD activities is in agreement with Niasar's records, which was approximately between 150 to 270 degrees and 330 to 90 degrees.

After about 3 minutes at 36 kV, the discharge magnitude started to decrease. This decrease in PD magnitude was also observed by Zainuddin et al [80]. The decrease in the discharge reveals vital PD diagnosis analysis information. The philosophy that is used in the industry where the decreasing PD magnitude is associated with a sign of PD disappearing is suggested to be invalid based on these results. The sudden decrease in PD magnitude was a sign of initiation of white marks on the surface of pressboard. The white marks are as a result of moisture drying from the pressboard due to the heat generated in the discharge process; these marks are also referred to as dry-bands. Furthermore, this sudden decrease does not change the PRPD pattern.

Distinct white marks were noticed on the pressboard at 39 kV supply voltage. This is a sign that the PD activity is causing a localised thermal heating on the pressboard. This heat initiates chemical reactions in the cellulose molecules, breaking the chain bond and producing gases into the surrounding oil (as discussed in Chapter 2). Wang et al recorded surface discharge temperature on the oil-impregnated board of about 800 ^{o}C to 1200 ^{o}C. Figure 4-4 is a picture of the test sample used in the 35 mm gap distance experiment [10].

The white marks initiated at the tip of the needle developed towards the earth electrode. The rate of development of the white marks corresponds to the voltage magnitude and duration. As the white marks reached the earth electrode, a repetitive surface flashover was observed at about 46 kV. After which the flashovers were intermittent and continually released smoke which quickly dissolved in oil. As the frequency of surface discharge flashovers increased, the corresponding PD also increased.

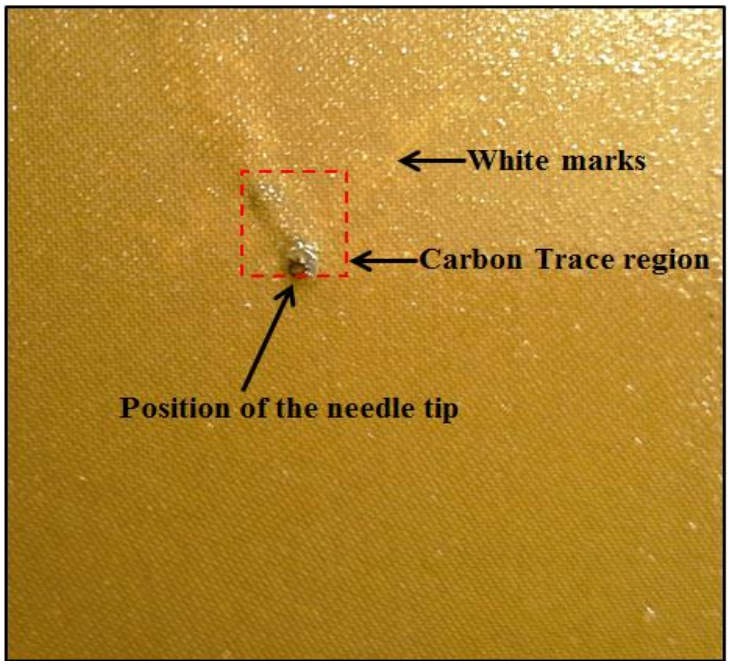

Figure 4-4: Carbon marks following white marks for 35 mm gap distance

Whenever there was a flashover, the subsequent PD signals were relatively much bigger. This is attributable to PD in resultant gas bubbles. There would then be more than one source of PD. This is evident in the PRPD pattern recorded at 46 kV (see Appendix A.3, Table A 3-4). This is expected as PD activities in free bubbles in oil are characterised by high magnitudes [7]. The sudden increase in the PD magnitude is clearly noticed in Figure 4-3. The repeating surface flashovers were followed by a glowing spark, as shown in Figure 4-5. The observed spark immediately extinguished as soon as the voltage was switched off, and the smoke dissolved in the oil. A similar glowing spark was observed by Mitchinson et al when 45 kV supply voltage was applied to an oil-impregnated pressboard for 35 mm gap distance [12]. A physical examination of the test sample after switching off the power supply revealed that the last breakdown released sufficient energy to force the upper layer of the pressboard to swell with more bulging evident near the needle tip as well as a sign of puncture or "electron ejection hole" from the needle tip as shown in Figure 4-4. Therefore at 35 mm gap, the supply voltage could not be increased beyond 46 kV as it would result in immediate flashover.

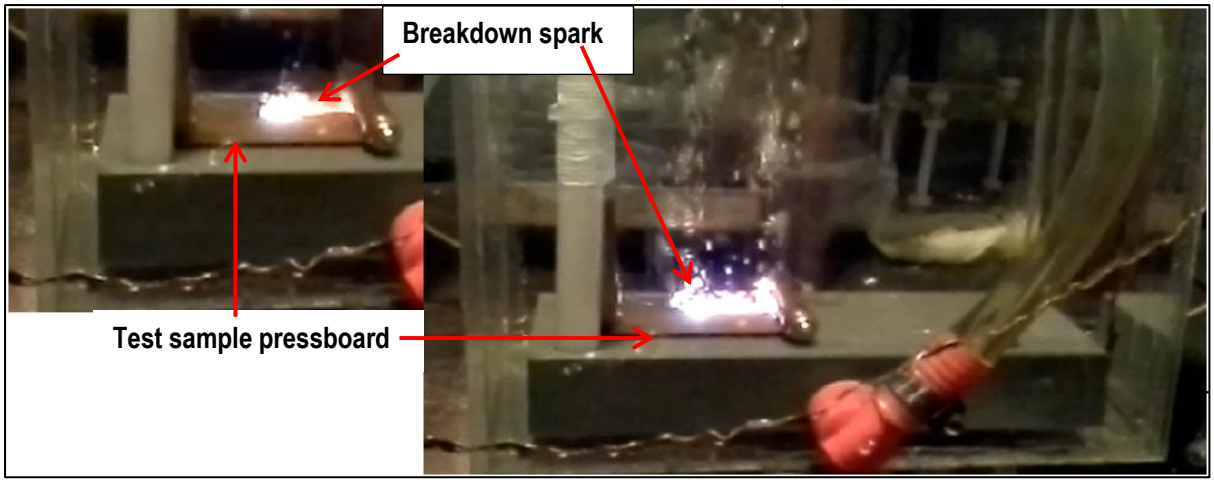

Figure 4-5: Full surface breakdown for 35 mm gap distance

4.4.3 Discharge at 45 mm gap distance

The background noise was 0.6 pC and the measured PD inception voltage was 23 kV. At 29 kV a small glowing light of corona at the tip of the needle was observed. However, no visible white marks were observed on the test sample.

The discharge pattern was consistent with the typical phase angle of PD activities approximately between 150 to 270 degrees and 330 to 90 degrees, similar to the pattern observed at 35 mm gap distance. At 36 kV, the PD started to decrease (see in Figure 4-3) as visible white marks developed from the needle tip towards the earth electrode. The PD magnitude continued to decrease until 39 kV, when intermittent flashovers initiated in oil. At 40 kV, the PD magnitude started to increase again, without changes in the PRPD pattern. Further voltage increase, increased the flashover instances. The flashover repetition rate, however, was far less than the flashovers observed at a 35 mm distance. At 46 kV, the discharge pattern was consistent, with increasing PD magnitude without surface discharge flashovers.

At 50 kV, the white marks continued to increase with increasing PD magnitude. Increased repetition rates of flashovers in oil were noted after 5 minutes at this voltage level. Audible sounds of flashover in oil were heard. A visible corona glow at the earth electrode was also observed. Figure 4-6 is an image showing corona glow on the earth electrode. The glow on the earth electrode is a sign of streamers developing (cloud of electrons) between earth electrode and the pressboard sample; forming a breakdown path for the electrons. The glow on the earth electrode initiated as soon as the white tracks bridged the distance setup. Consistent flashovers in the oil, repeating at a faster rate started within seconds. The flashovers in oil were followed by smoke (see Figure 4-7) in the oil near the earth

electrode where the visible corona glow was observed. The resulting discharge behavior observed in this experiment is similar to that observed by Zainuddin et al [80].

Physical examination of the pressboard test sample showed a small dot of carbon trace near the needle tip and the white marks across the distance gap between the electrodes, as shown in Figure 4-8.

4.4.4 Observations for 55 mm gap distance

The 55 mm gap distance was the last setup that was considered for the surface discharge creation experiment. The background noise was at 1.8 pC and the PD inception was 20 kV. At 20 kV, the PRPD pattern did not resemble the expected pattern of surface discharge, as it was noted at the 35 mm and 45 mm distances. The PRPD for this gap distance are summarised in appendix A.3, Table A 3-2. Visible glowing corona at 33 kV and 36 kV voltage level were observed. Figure 4-9 shows the observed corona glow at the needle tip. This observation was similar to the discharge characteristics of a corona in oil described by Niasar [77]. Figure 4-10 and 4-11 shows the comparison of the PRPD pattern recorded at 29 kV voltage level and the typical signature PRPD pattern in transformer insulation, respectively. At 39 kV, the discharge magnitude decreased slightly, as can be observed in Figure 4-3. At 40 kV, the PD magnitude started to increase but the PRPD pattern did not change. The observed PRPD patterns from 20 kV to 43 kV were consistent with typical corona in oil with a tip electrode in direct contact with the surface of the insulation [7]. The phase position of the PD pulses was from 0-90 degrees and 180 degrees to approximately 270 degrees. The PRPD pattern was symmetrical with higher PD magnitudes on the negative cycle of the sinusoidal signal than to the positive cycle.

At 46 kV, the expected PRPD patterns for surface discharge appeared. After 5 minutes at supply voltage of 50 kV, only two flashovers occurred. There was neither surface discharge flashover nor complete bridge of the gap either. The white marks did not bridge the gap. It was decided to stop the experiment at this voltage level. It is noticeable that the white marks manifested dryness of pressboard due to discharge heat effect. Reabsorption of moisture would clear the trace of the marks and this was observed in the experiment.

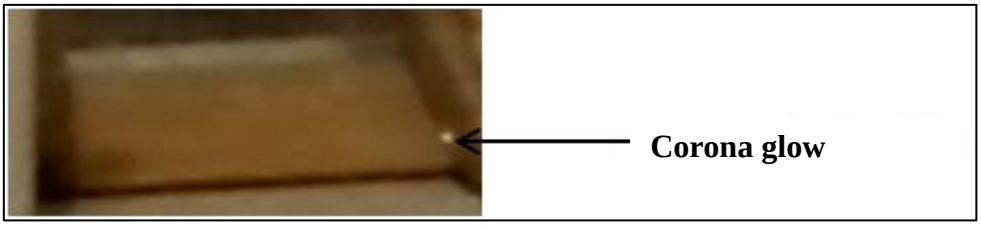

Figure 4-6: A distinct glow on the earth electrode

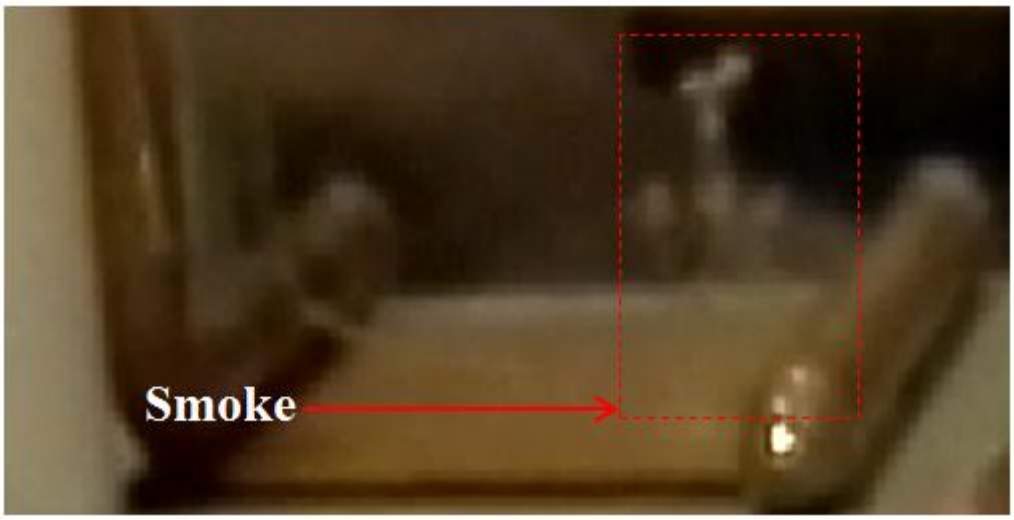

Figure 4-7: Smoke after flashover in oil

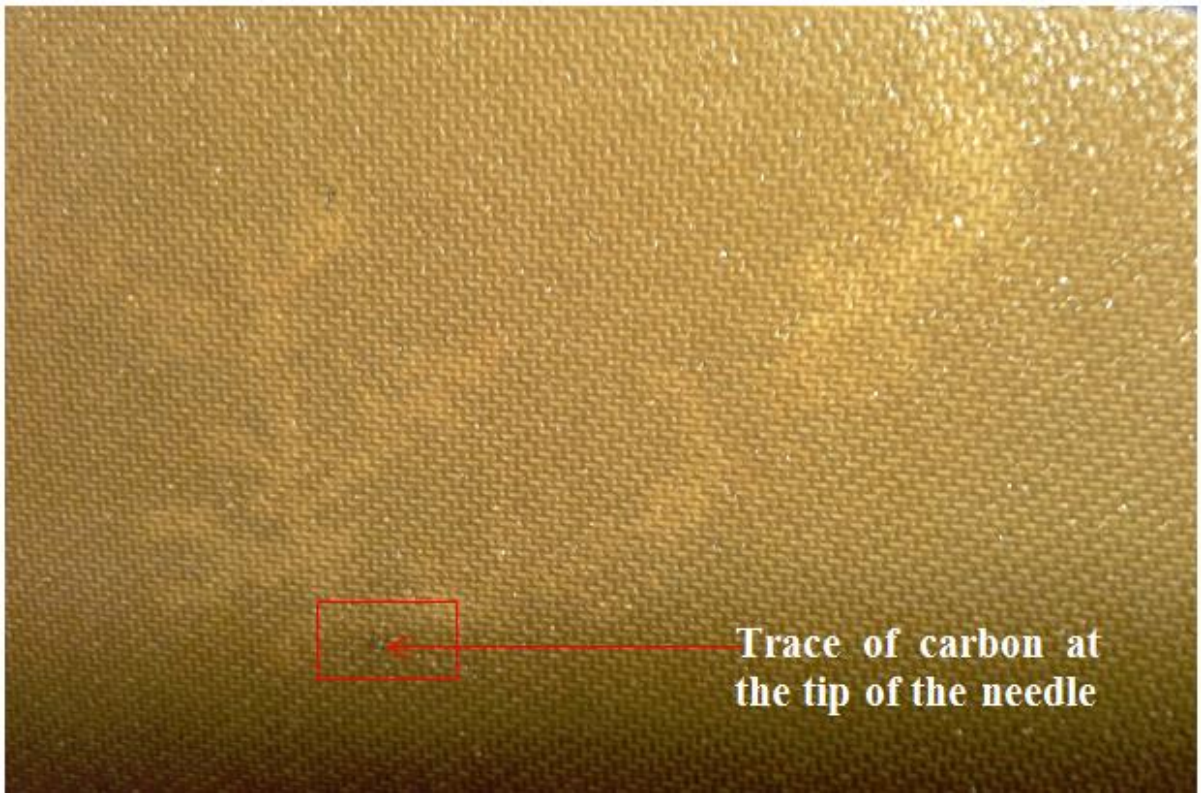

Figure 4-8: Observation on the test sample of 45 mm distance setup

Figure 4-9: Corona glow at the needle tip at 55 mm setup distance

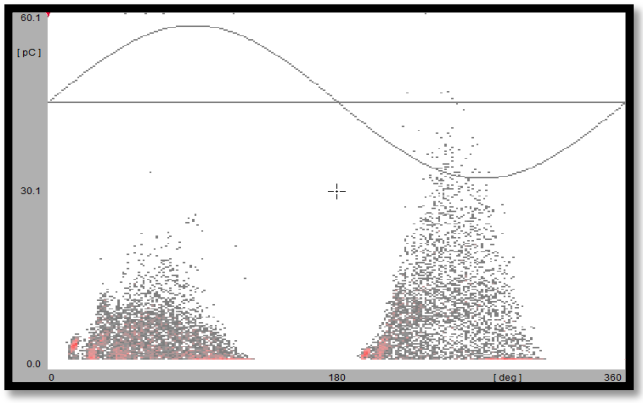

Figure 4-10: Recorded PRPD pattern of corona in oil

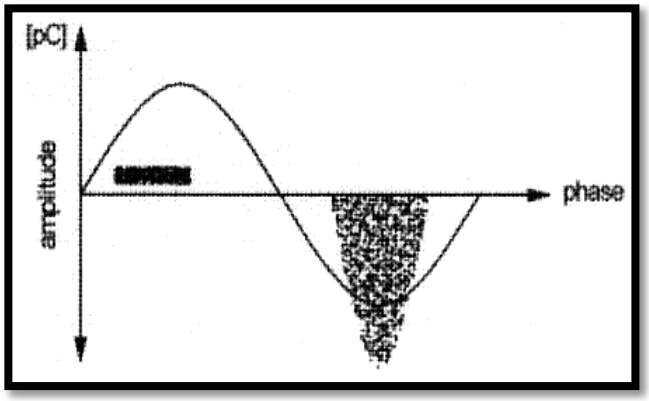

Figure 4-11: Typical PRPD pattern for corona in oil [7]

4.4.5 Combined discussion on all gap distances

The key findings from the four gap distance setups investigated are summarised in this section. A selection of the gap distance setup that will be used for the multiple surface discharges ageing experiment on test sample is based on these results.

The plot in Figure 4-12 is the PD inception and oil flashover voltage as a function of the gap distance plotted using the data presented in Appendix A.3, Table A 3-6. It can be concluded from the PD inception of the four gap distance setups that the discharge onset is independent of the distance between the needle tip and the earth electrode. It is as a result of the local electrical field. However, the oil flashover voltage and the surface breakdown voltage are dependent on the gap distance. As the gap distance increases, the oil flashover and surface discharge also increase.

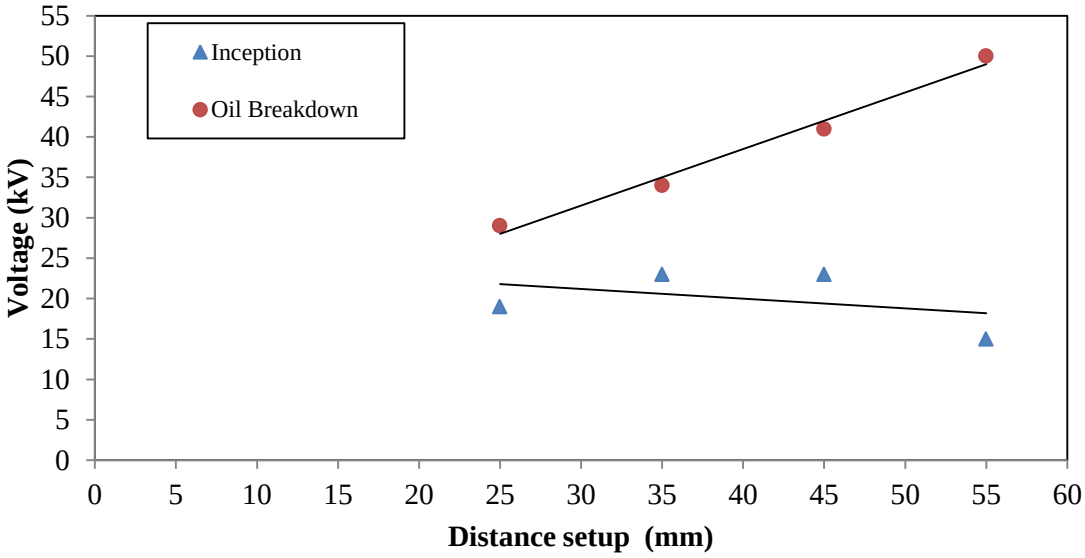

Figure 4-12: PD inception voltage and oil flashover voltages vs. gap distance

The 45 mm electrode gap size was regarded as optimal for surface discharge ageing experimentation for the following reasons:

- The shorter gap of 25 mm flashed over at relatively low voltage of 29 kV. No significant surface discharges were detected prior. It would be therefore difficult to create sufficient surface discharge to age the pressboard.
- The 35 mm gap produced surface discharge. However, it flashed over at a relatively lower voltage of 46 kV. This gap size was not sufficient to sustain the surface discharge for hours without flashover. For these reasons, it was not selected for the multiple surface discharges ageing experiment.
- The gap of 55 mm gave both surface discharge and corona in oil. After applying the highest possible voltage of 50 kV, the discharge extended halfway into the gap. Meaning longer time would be required for surface discharge to fully develop.
- The gap of 45 mm gave typical discharge similar to those reported elsewhere in the literature.

The following section presents simulation and calculation of the electric field on the needle tip in the point to plane electrode setup at the gap size and voltage of respectively 45 mm and 30 kV. Figure 4-13 and 4-14 show the recorded PD current pulse superimposed on the supply voltage and the corresponding PRPD pattern, respectively, for this setup.

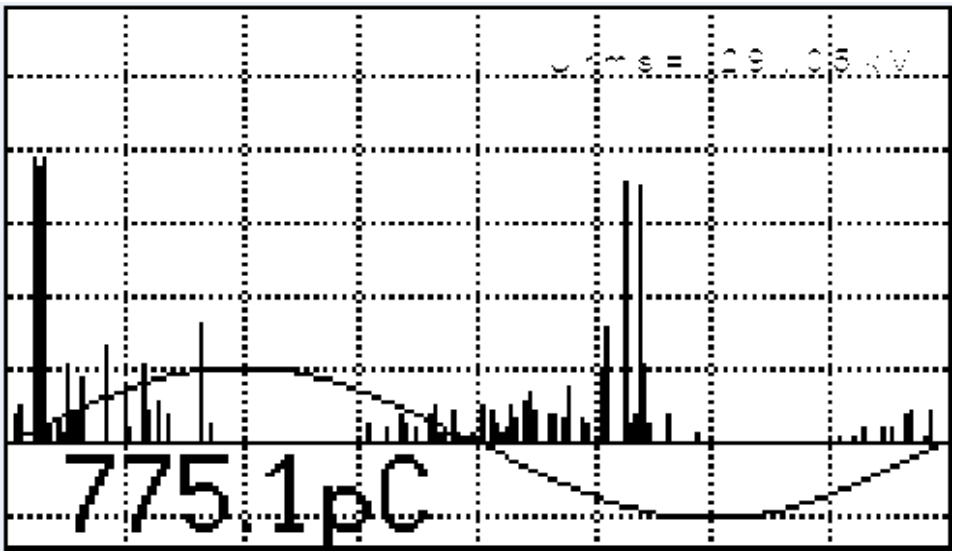

Figure 4-13: PD current pulses superimposed on the supply sine wave for 45 mm distance

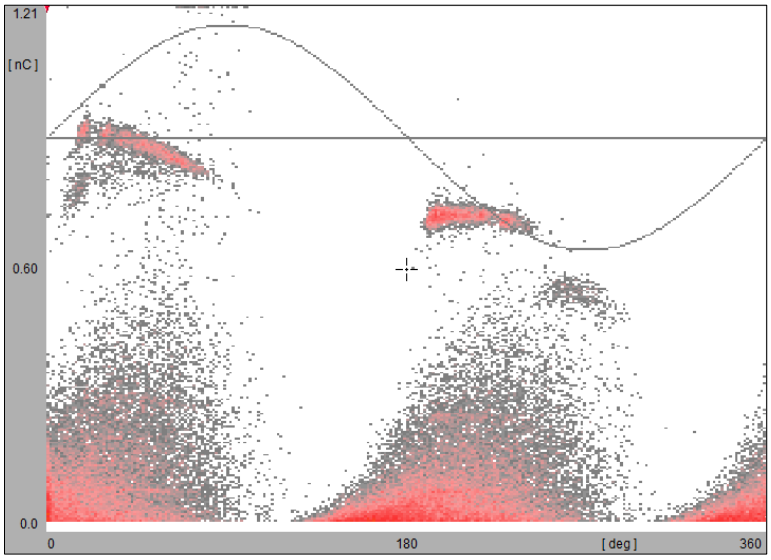

Figure 4-14: PRPD pattern for 45 mm distance at supply voltage

4.5 Determination of the electric field stress for the selected gap distance by FEM simulation and empirical formulas

In the previous section, the gap distance experiment results were presented. Four gap distance arrangements, 25 mm, 35 mm, 45 mm and 55 mm between the needle tip and the earth electrode were studied. The aim of the experiment was to determine the optimal distance between the electrodes and the voltage that would be used to create surface discharge on pressboard test samples in one setup. In

this section, the selection of 45 mm distance setup is further verified using FEM simulation and analytical formulas for the electric fields.

4.5.1 Analytical calculations of the electric field in the 45 mm gap distance

Equation (4.1) is used to calculate the limiting electric field stress, E_{sd} (kV/mm) along the surface of an oil-impregnated pressboard at power frequency [60]. The equation shows that E_{sd} reduces with surface discharge gap distance d_c (that is creep distance between the needle tip and the earth electrode). The electric field stress, E_c on the pressboard surface should therefore not exceed E_{sd}. In practice however, in designing transformer insulation a safety margin should be provided between E_c and E_{sd}. Equation (4.2) is used to calculate the safety factor. The aim is to get the safety factor higher than one.

$$E_{sd} = 16.6{d_c}^{-0.46} \text{ [60]} \tag{4.1}$$

$$Safety\ factor = \frac{E_{sd}}{E_c} \tag{4.2}$$

Where, d_c is the creepage distance (mm) between the electrodes, in this case it is 45 mm. Using equation (4.1) the limiting electric field stress along the surface of pressboard for the 45 mm creep distance is 2.88 kV/mm.

The maximum electric field stress at the needle tip is calculated by equation (4.3). Where V is the supply voltage (kV), r is the needle tip radius (mm) and d is the gap distance between the needle tip and the earth electrode (mm). For 45 mm gap, with the needle tip radius of 0.117 mm (radius of the needle used in this study) and the supply voltage of 30 kV, the maximum electric stress is therefore 69.8 kV/mm. The electrical breakdown voltage of transformer oil (POWEROIL TO 1020 (60 UX ™)) is 70 kV [82], measured according to IEC 60296 [83] and IEC 60156 for an electrode gap distance of 2.5 mm [84], which corresponds to electric field strength of 28 kV/mm. The electrical breakdown strength of oil-impregnated pressboard at power frequency is 40 kV/mm [3]. Therefore, the maximum electric field stress of 69.8 kV/mm at the needle tip much higher than the breakdown strength of both oil and pressboard which proves that the requirements for initiation of surface discharge are met for the gap distance of 45 mm.

$$E_{max} = \frac{2V}{r \ln\left(1+\frac{4d}{r}\right)} \text{ [81]} \tag{4.3}$$

4.5.2 FEM simulation

FEM simulation model was implemented to calculate the expected resultant surface discharge simulating the stress in the test sample, to determine and confirm whether a supply voltage of 30 kV is sufficient to cause surface discharge. Furthermore, the occurring maximum stress at the needle tip is confirmed.

The needle-plane electrode setup was simulated in Ansoft Maxwell® using 3D model shown in Figure 4-15. The material properties are listed in Table 4-1 while the HV electrode was assigned a voltage boundary of 30 kV; earth electrode was assigned a zero potential boundary. A total of 10 solution iterations were used with a total energy error percentage between each iteration calculation set to 0.5%. Depicted in Figure 4-16 is a plot of the occurring maximum electrical field stress at the needle tip of 68 kV/mm, which is close to the analytically calculated value.

Table 4-1: Material properties defined for FEM simulation

Component Name	**Material Type**	**Relative permittivity**
HV electrode	Perfect conductor	1
Earth electrode	Perfect conductor	1
Test sample	Oil-impregnated pressboard	4.4
Oil tank	Oil	2.2
Support board	No material assigned	Represented as a non-model. This means that the solver does not include it in the solution.

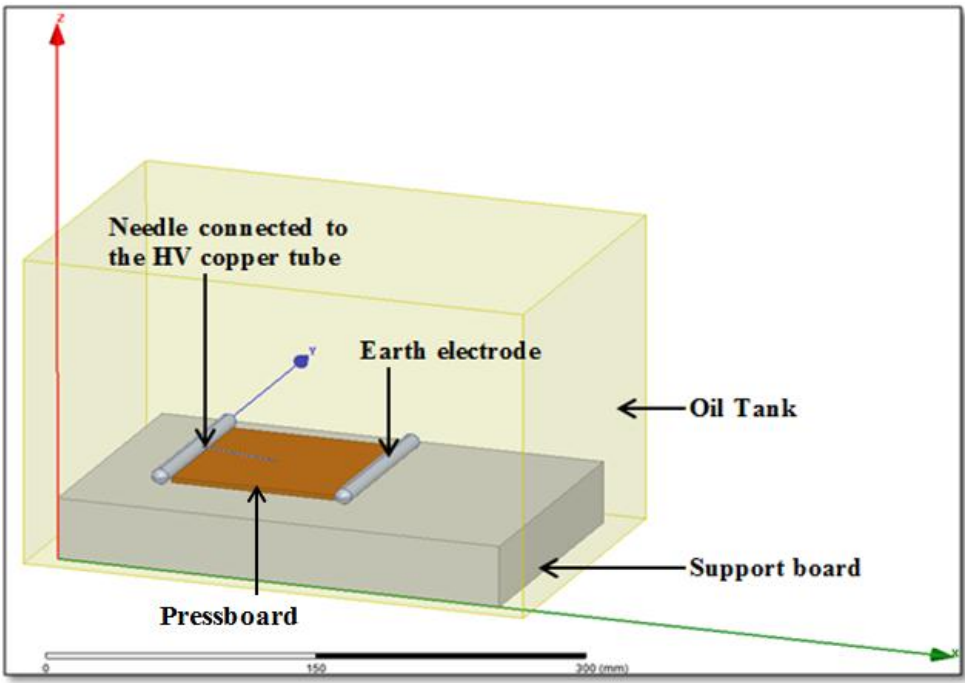

Figure 4-15: 3D FEM simulation model

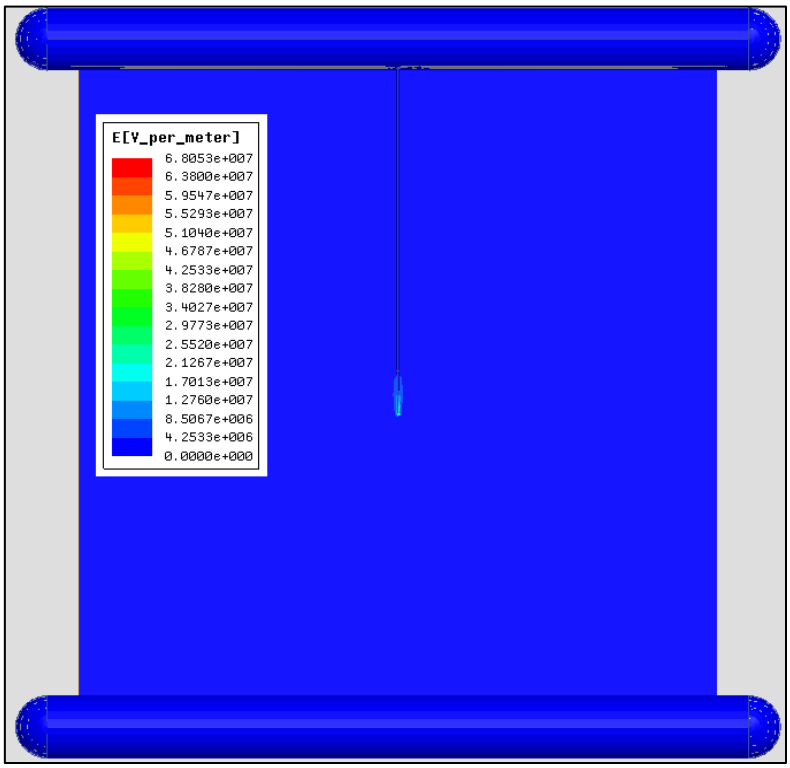

Figure 4-16: Electric field, E, plot for 45 mm setup distance at 30 kV supply voltage

The simulated electric field along the surface of pressboard was 0.82 kV/mm. Comparing this value to the limiting electric field stress calculated by equation (4.1) of 2.88 kV/mm, the resulting safety factor according to equation (4.2) is 3.51 pu. This means that for a creep distance of 45 mm at 30 kV,

surface discharge will not occur on the test sample. Therefore the development of surface discharge will solely depend on the local stress at the needle tip and the application duration of the supply voltage.

4.6 Conclusion

The optimal gap size between the needle tip and the grounded electrode was experimentally determined to be 45 mm. Furthermore, 30 kV test voltage was also deemed optimal for creating the required surface discharges to sufficiently age the pressboard test samples.

Chapter 5: The multiple test samples surface discharge ageing experiment

5.1 Introduction

An overview of the experimental work for this dissertation is presented in this chapter, followed by a discussion of the experimental setup and results for the multiple surface discharges ageing experiment.

5.2 An overview of the experimental methodology

The experimental work was divided into; determination of the optimal electrode gap distance and test voltage value (as presented in the previous chapter), multiple test sample ageing and then the lightning impulse voltage breakdown tests. Table 5-1 summaries the number of samples in each stage of the experimental investigation.

Table 5-1: A summary of the number of test samples per experiment

Experiment	**Number of samples**
Determination of the optimal electrode gap distance and test voltage value for creating surface discharge	4
Multiple tests samples surface discharge ageing experiment	24
Negative LI breakdown voltage test on un-aged and surface discharge aged test samples	12
Positive LI breakdown voltage test on un-aged and surface discharge aged test samples	12

5.2.1 Pre-conditioning of the pressboard test samples

Conditioning of the test samples was done at Powertech Transformers (Pty) Ltd and Powertech Insulation (Pty) Ltd; both factories are based in Pretoria West. Powertech Insulation (Pty) Ltd donated 54 pressboard test samples. The samples were cut to dimensions of 100 mm × 100 mm × 3 mm and pre-dried (surface drying) in hot air for about 18 hours and bathed in oil for 3 hours, after which they

were wrapped in plastic to avoid moisture absorption. This is a standard method followed to prevent bulk moisture absorption from the atmosphere.

A full vacuum dry cycle which includes evacuation, heating, pressure reduction, fine vacuum cycles and oil impregnation of the samples was done at Powertech Transformers (Pty) Ltd. Evacuation is a process where the autoclave (a chamber used for the drying and oil-impregnation processes) walls are activated, to extract the air from the autoclave. The evacuation process is performed at 5 to 7 mbar pressure. The heating cycle begins when the autoclave wall temperature is at 130 °C and the insulation temperature is at 120 °C. Once these temperatures are reached, pressure reduction process is initiated to remove water vapour from the autoclave. During fine vacuum, the kerosene (water based glue used for cellulose material) and moisture are evaporated from the cellulose insulation material. This process continues for 10 hours until the vacuum pressure in the autoclave is less than 1mbar.

The samples were placed in an autoclave for the full vacuum cycle; moisture was extracted from the samples during the heating cycle under a vacuum pressure of 0.24 mbar with an autoclave wall temperature of 126 ^{o}C. The samples were then fully immersed in oil for 3 hours. The conditioning period lasted for 50 hours. The average moisture level of the dried pressboard sample was determined to be less than 0.5%. The samples were wrapped with an aluminum foil and then covered with plastic to avoid moisture ingress whilst awaiting to be tested at the Wits' HV laboratory. Figure 5-1 shows a picture of the samples after conditioning, wrapped in foil and plastic. The samples were removed from the packaging material and placed in an air tight container with oil, for at least 24 hours before the surface discharge and LI experiments were conducted.

5.3 The multiple sample surface discharge ageing experimental setup

Presented in this section is the multiple test sample surface discharge ageing experiment. Depicted in Figure 5-2 is the electrical circuit used for this experiment. A constant voltage of 30 kV was applied to the test object through an AC 0-220 V / 0-50 kV transformer. The current in the circuit was limited to 0.15 A using a resistor of 200 kΩ. The voltage supplied to the test object was measured using a digital oscilloscope (Rigol DS1064B) using a 1000: 1 voltage divider.

Figure 5-1: Conditioned test samples wrapped in foil and plastic

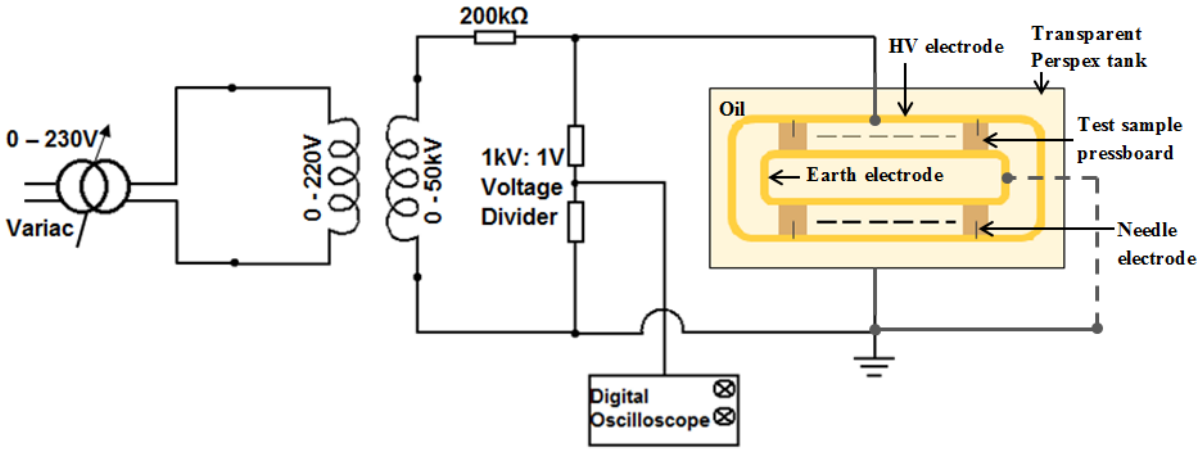

Figure 5-2: Electrical circuit for multiple surface discharges ageing experiment

The array of pressboard test samples were assembled in an air filled plastic tank covered with a transparent Perspex lid to allow for visual observation. The setup in the tank allowed for 12 pressboard test samples to be connected in parallel and simultaneously aged by surface discharge. The HV electrode was a copper tube on which 12 needles were attached. Figure 5-3 is a picture of the assembly.

In order to assess whether the duration of PD exposure had an influence on the LI breakdown voltage of the surface discharge aged pressboard samples, one set of 12 test samples was aged for 3 hours and the other for 7 hours.

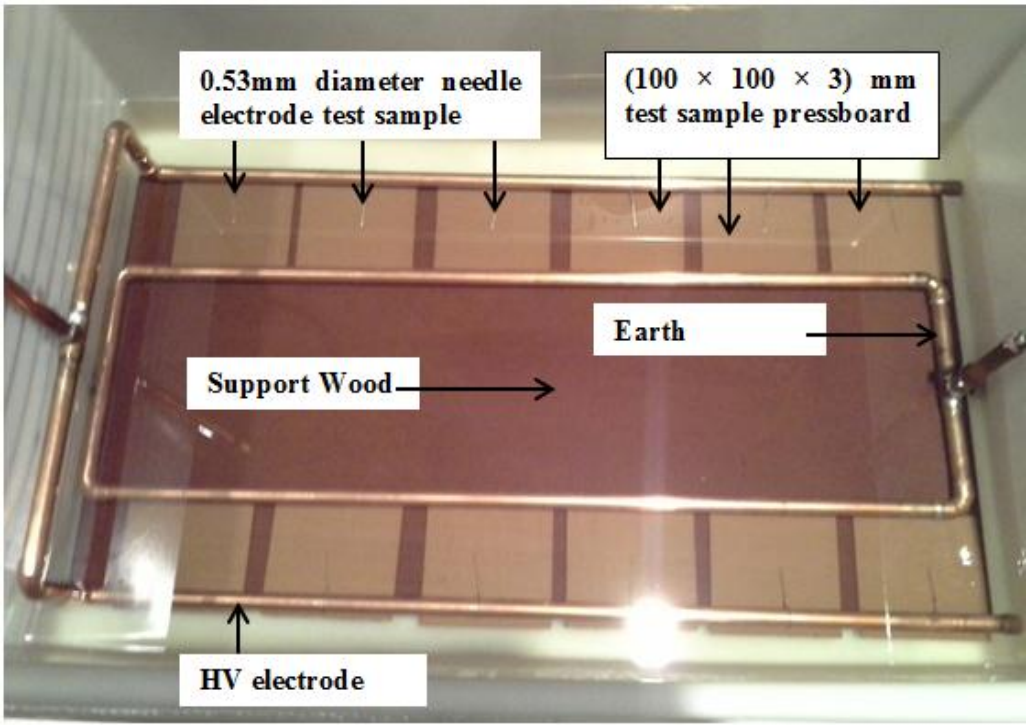

Figure 5-3: The arrangement of the test sample pressboards in a plastic tank covered with Perspex lid

5.4 Some notable observations during the ageing period

During the ageing period, the experimental setup was monitored and the observations are summarised as follows:

- **The 3 hours ageing experiment** - White marks started to appear in three test samples 30 minutes into voltage application. After an hour, a black carbon spot at the needle tip in 9 out of 12 test samples was observed. Subsequently, white marks developed. The developments of these white tracks were consistent with earlier observations in the gap distance setup experiment and subsequent observed processes. At the end of the 3 hours, two samples had white marks that bridged the gap (see Figure 5-4).
- **The 7 hour ageing experiment** - After 7 hours of ageing, 5 out of 12 samples had white marks that bridged the electrode gap. The rest of the samples had an area around the needle tip covered by carbon. Figure 5-5 shows a picture of the 12 test samples after 7 hours of ageing. A close up look on Figure 5-6 shows that surface discharge occurred underneath the first layer of the pressboard. The carbon traces followed a distinct path of the white marks. Furthermore, traces of carbon were also noticed to develop from the earth electrode.

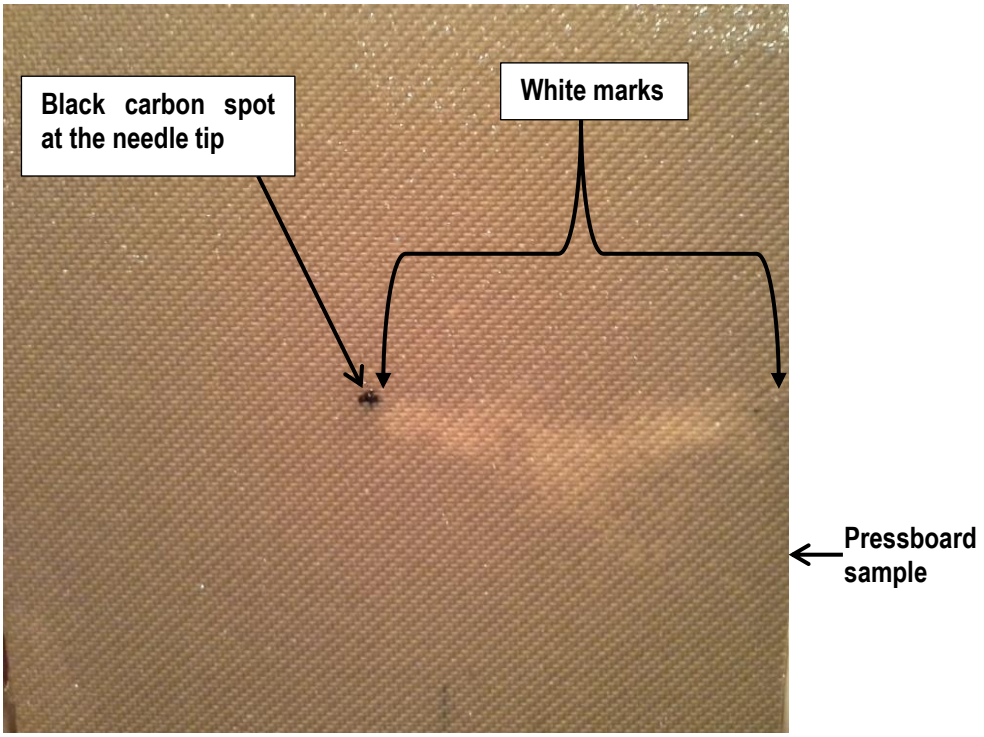

Figure 5-4: The 3 hours test sample pressboard with white marks that had bridged the gap

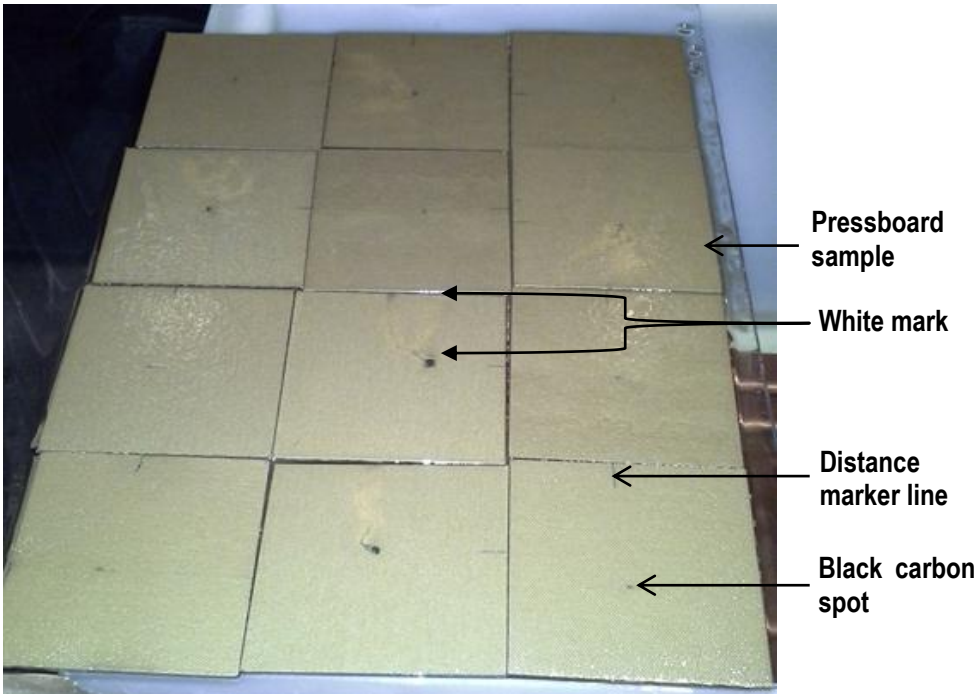

Figure 5-5: The 12 test sample pressboards after 7 hours of surface discharge ageing

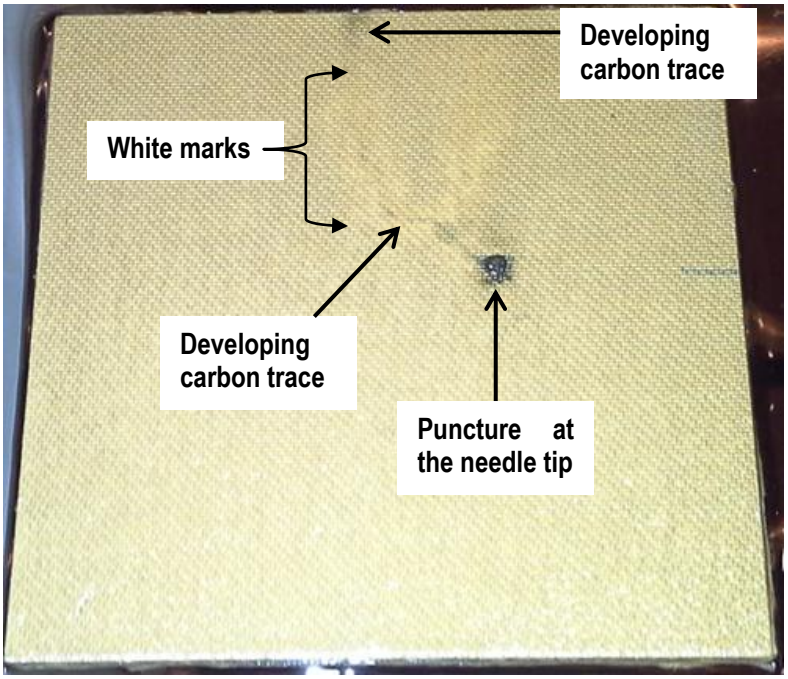

Figure 5-6: The 7 hours test sample pressboard, illustrating a puncture mark

5.5 Conclusion

A total of 24 test samples were simultaneously aged by surface discharge using a needle plane electrode setup with a gap of 45 mm. A set of 12 samples was aged for 3 hours and the other 12 for 7 hours. No complete surface breakdown in both the 3 and 7 hour ageing experiments was observed. The aged samples were then exposed to positive and negative LI breakdown voltage tests, presented in the next chapter.

Chapter 6: The lightning impulse breakdown tests of surface discharge aged and un-aged pressboard samples

6.1 Introduction

Chapter 5 presented surface discharge ageing of the pressboard test samples. In this chapter the experimental methods and results of the lightning impulse (LI) breakdown voltage tests are presented. This is the key element of this study, as the results will reveal whether the surface discharge has an impact on the breakdown voltage of oil-impregnated pressboard material. The results of the un-aged samples and 3 hour as well as 7 hour aged samples exposed to positive and negative LI breakdown voltage are compared and discussed in this chapter.

6.2 Background on lightning impulse voltages

Electrical equipment are exposed to different types of transients; natural and unnatural overvoltage. Lightning impulses are a natural overvoltage event that may disturb the functioning of electrical equipment. Switching impulses are an example of an unnatural transient event that occurs in the electrical network system. These transients create overvoltage and travelling waveforms which vary in shapes and frequency. IEC 60060-1 defines standard lightning impulse voltages [20], as an impulse with a front time of 1.2 μs and a time to half value of 50 μs. Presented in Figure 6-1 is a full LI voltage waveform.

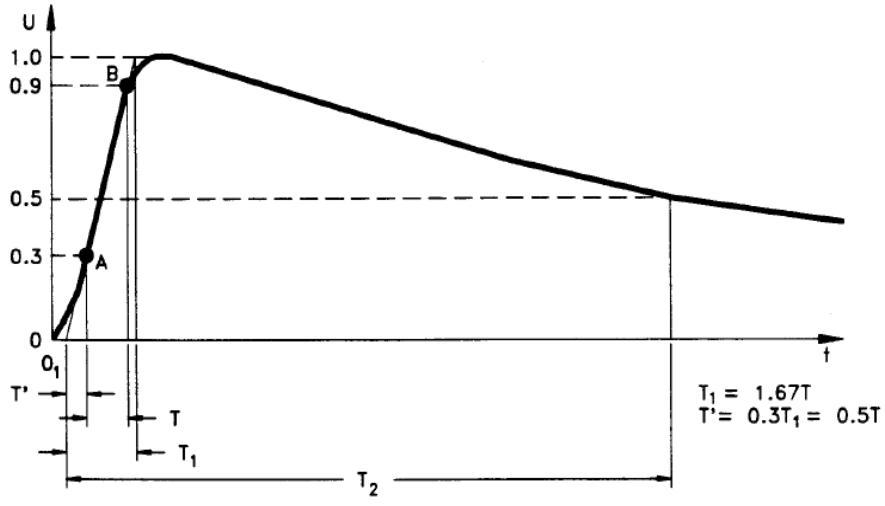

Figure 6-1: The full LI voltage waveform [20]

Where: *T1*, is the standard front time of 1.2 µs which is 1.67 times the interval *T* between the instants when the impulse is 30% and 90% of its peak value. *T2* is the standard time to half-value of 50 µs, defined as time between the virtual zero, *T'* and time when the LI peak has fallen to 50%. *T1* has a tolerance of ±30% and *T2* has tolerance of ±20% [20].

A full LI waveform is generated in the laboratory environment using an impulse voltage generator. The generator's operating principle is based on the basic single-stage circuit as shown in Figure 6-2, were the voltage is supplied through a variable HV transformer, connected in series to a diode for rectification. The supply voltage is slowly increased charging up the capacitor, *C1*, until the breakdown voltage for the spark gap, *d*, is reached. The spark gap acts like a switch between the supply voltage and the test object circuit. Resistor *R1*, *R2* and capacitance *C2* form the wave shaping elements [56]. *R2* discharges the capacitor (*C1*) controlling the tail time, *T2*, of the LI waveform whilst *R2* controls the front time, *T1*. *C2* is the discharging capacitor of the generator and is parallel to the load.

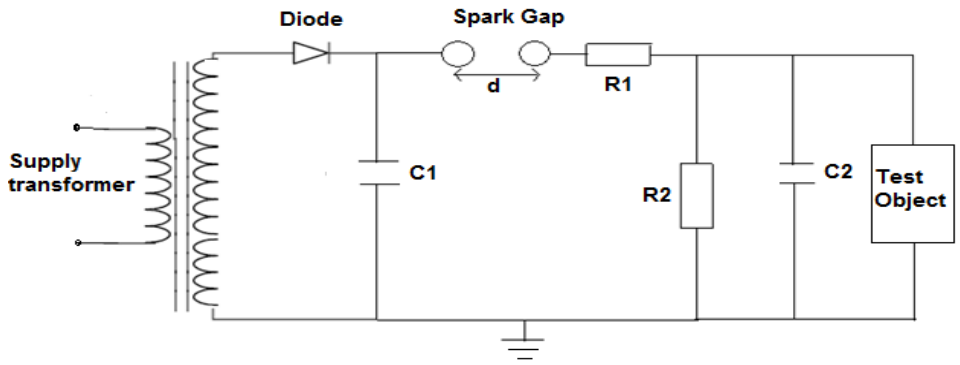

Figure 6-2: Single stage impulse generator circuit connected to a test object

To generate high voltage without increasing the physical dimensions of the capacitor, *C1*, a multistage LI generator is used. The following section discusses how the multistage Marx generator was used in this study.

6.3 Lightning impulse breakdown voltage tests of the pressboard test sample

A five stage Marx generator was used to generate a standard LI. The five stage circuit of the Marx generator is depicted in Figure 6-3. The capacitors *C1* to *C5* are charged in parallel through resistors, R1. Each capacitor is connected to the next capacitor in the stack through a spark gap. When the spark

gaps are set to fire at a desired voltage, the gaps break down in a cascade format thus charging and discharging the capacitors in series and developing an LI voltage across *C6*.

The polarity of the LI is changed by changing the polarity of the diode. The voltage across the test object is measured using a HV potential divider.

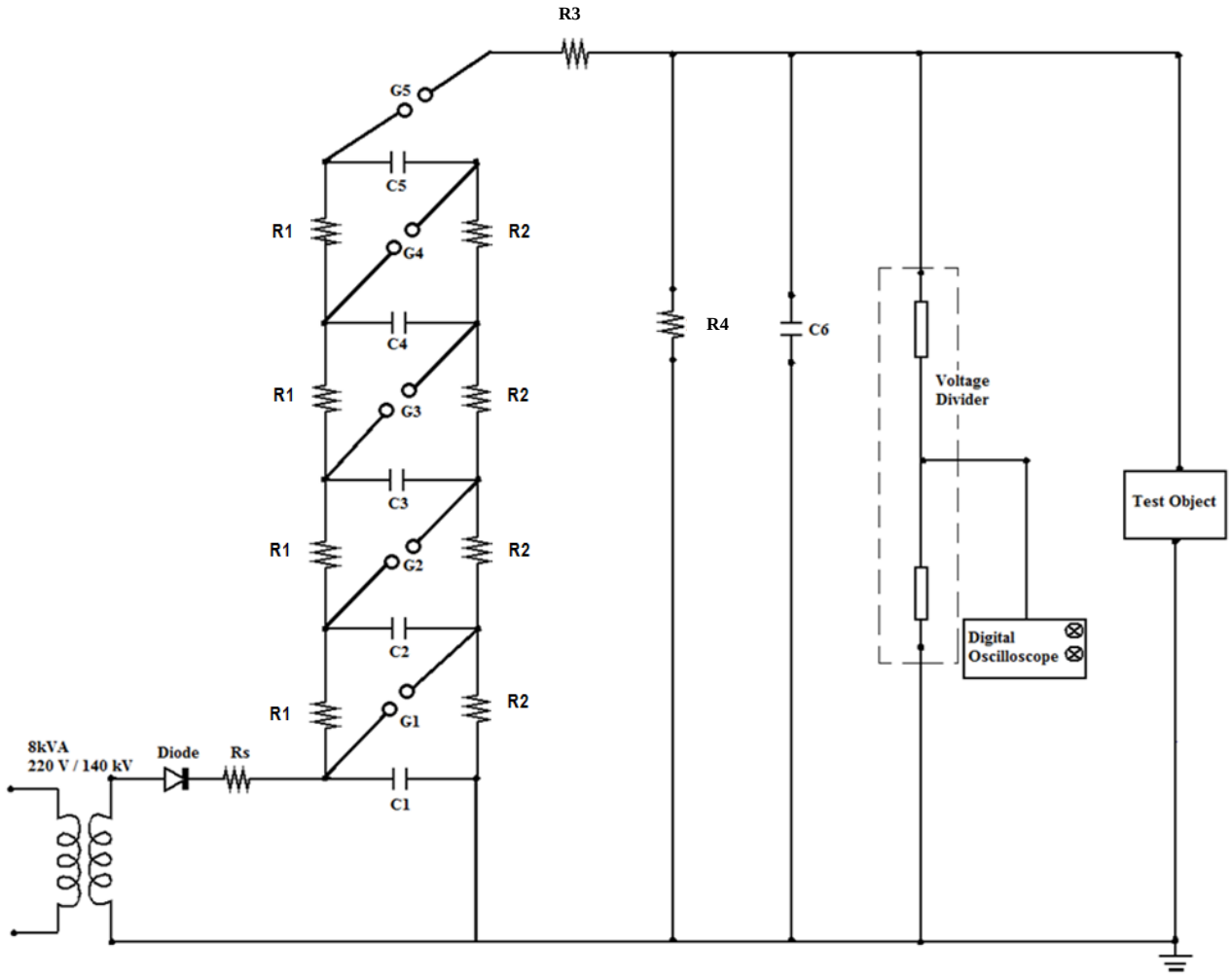

Figure 6-3: Five stage Marx LI voltage generator

6.3.1 The impulse voltage breakdown voltage test electrode

Specific electrode geometries are used for the impulse breakdown test in accordance with standards such as 60243-1[21]. These electrodes are commonly referred to as IEC electrodes. Figure 6-4 is a sketch of the IEC electrode used in this study.

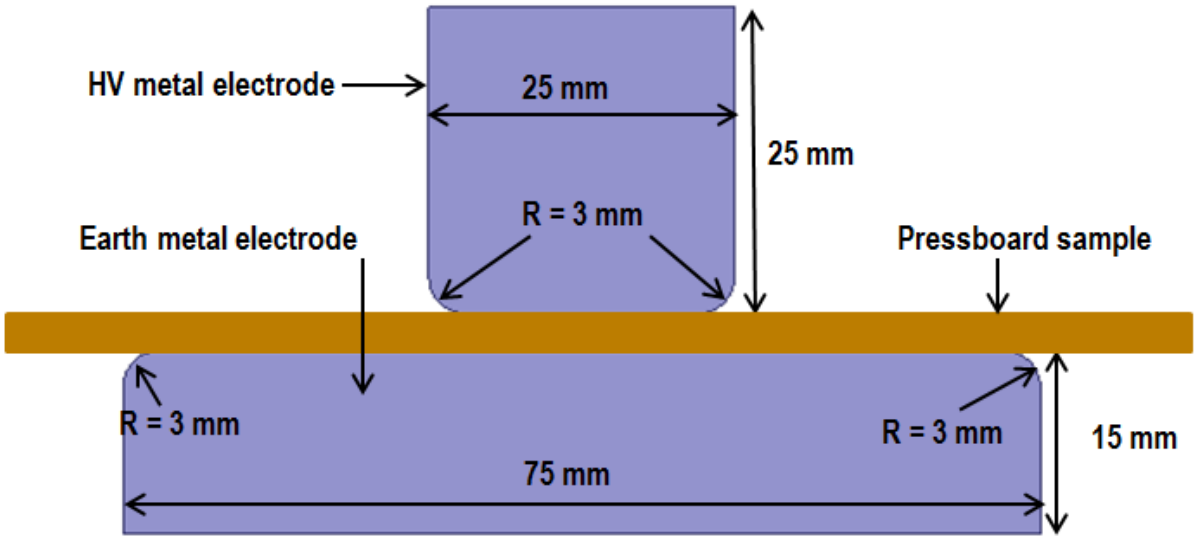

Figure 6-4: Schematic of IEC unequal electrodes

The HV electrode is 25 mm in diameter and the earth electrode is 75 mm in diameter. The electrodes were constructed such that the top HV electrode could be moved in a vertical direction to allow for test samples adjustment. The electrodes were supported by a structure of plastic screws and transparent Perspex material as shown in Figure 6-5. In Figure 6-6, the test sample in the Perspex tank immersed in oil is shown.

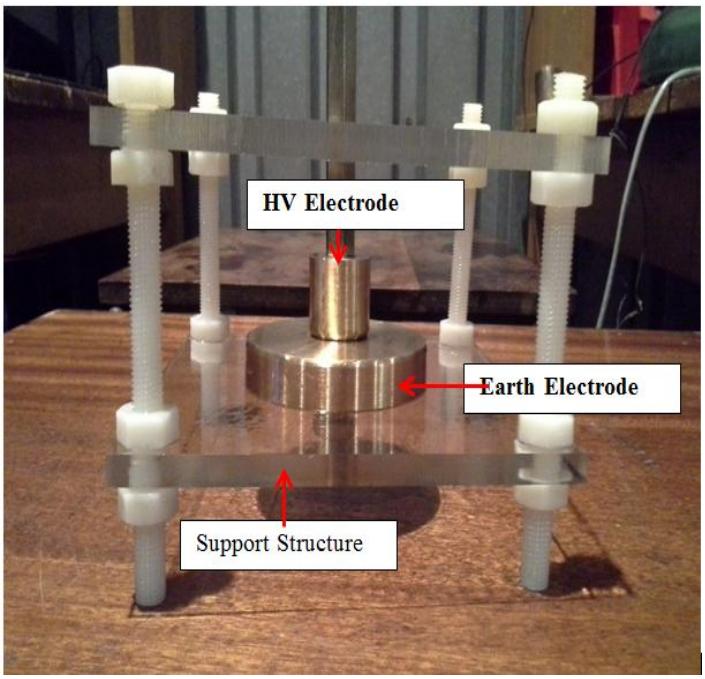

Figure 6-5: Electrode setup

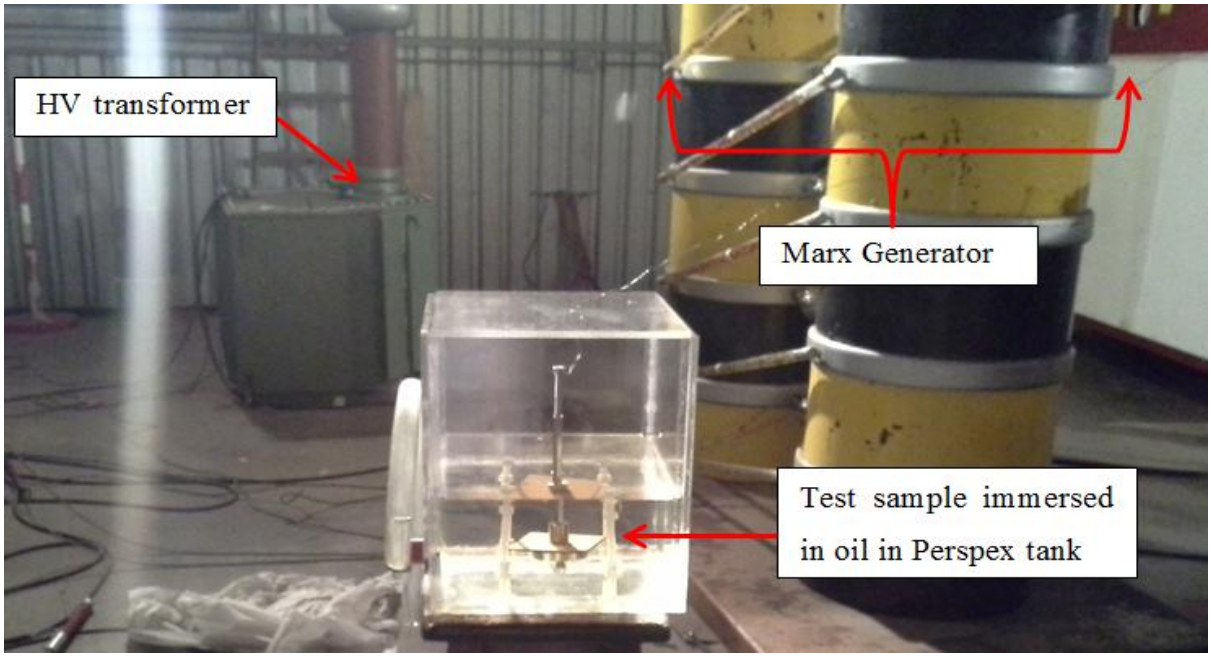

Figure 6-6: LI experiment setup

6.3.2 The impulse breakdown voltage test procedure

The LI experiments were conducted according to IEC 60243-1 [21] and IEC 60243-3 [22]. Due to the unequal sizes and different shapes of the electrodes, the polarity effect of the supply voltage is expected to have an effect on the breakdown voltage. Therefore, the experiment was performed for both negative and positive LI. For each polarity, the voltage was raised in steps of approximately 10 kV, with three impulses applied per voltage level. The step voltage raise of 10 kV is based on the guidelines outlined by IEC 60243-1, for starting impulse voltage between 100 kV and 200 kV [21]. The starting voltage is calculated in equation (6.2). One minute was allowed between each LI hit, to provide time for dissipation of the space charge created in the previous impulse event.

Calibration experiment was performed using two samples, one for the positive and the other for the negative impulse setup to determine the number of turns required on the Marx generator's spheres (electrodes) to reach an increment value of 10 kV. A digital oscilloscope was used to capture the applied LI to the test sample. Shown in Figure 6-6 and 6-7 are examples of the measured positive and negative LI waveforms during the experiment, respectively. Depicted in Appendix A.4 Figure A 4-1 are the details of the measured positive LI waveform with a front time of 1.29 µs and tail time of 53.9 µs, which are within the standard waveform tolerances as discussed in Section 6.2. Shown in Figure 6-9 and 6-10 are examples of the measured LI breakdown voltage for the positive and negative impulse waveforms during the experiment. In Figure 6-11 is an example of the discharge tracks

developed during LI breakdown voltage test. It is evident that the discharges start from the oil wedge developing into white marks leading to a carbon conduction path.

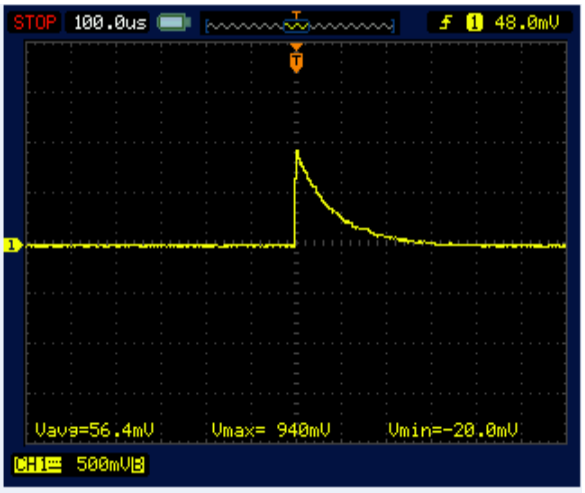

Figure 6-7: Positive LI waveform

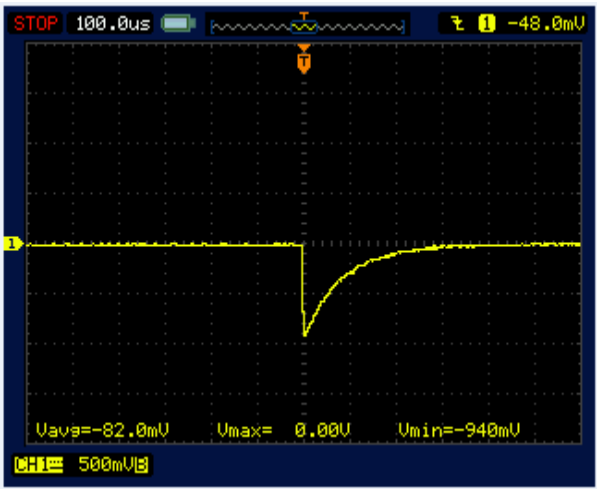

Figure 6-8: Negative LI waveform

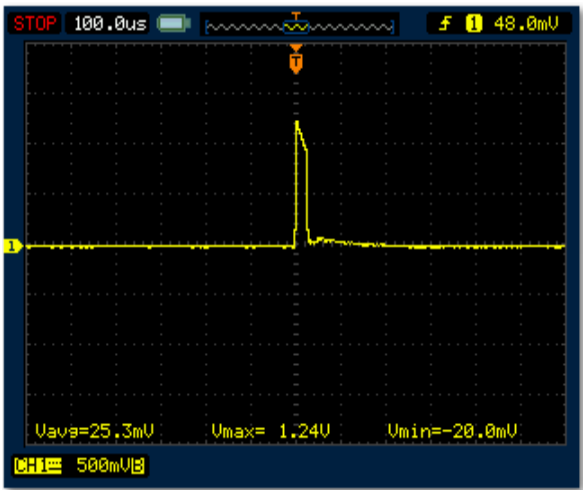

Figure 6-9: Positive LI breakdown waveform

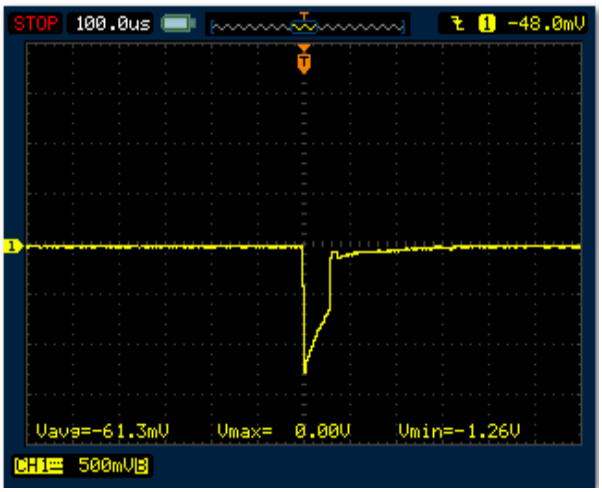

Figure 6-10: Negative LI waveform

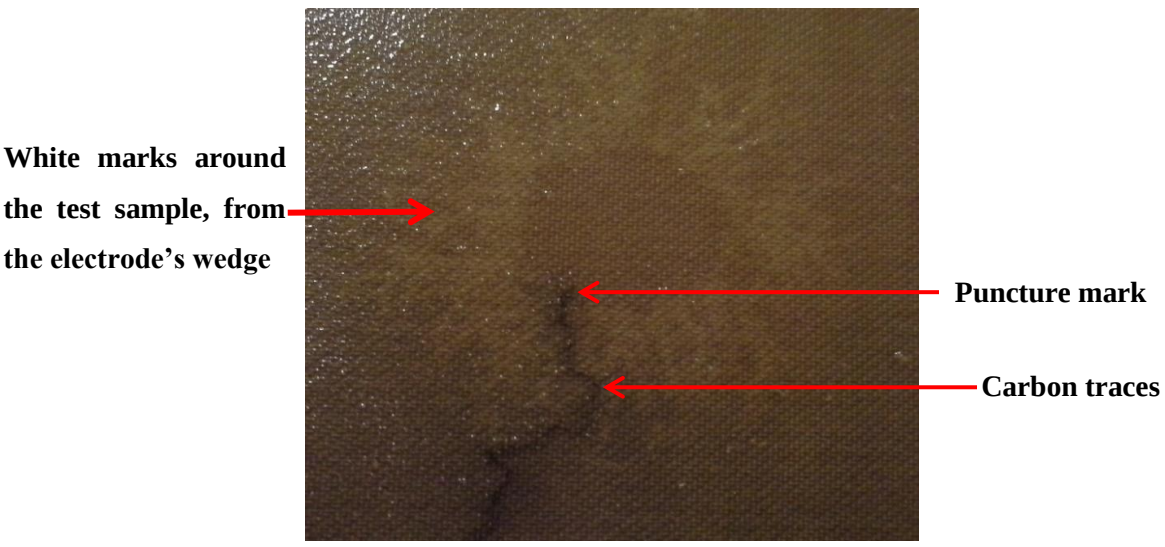

Figure 6-11: LI breakdown discharge tracks on the test sample

According to IEC 60243-3, the first applied LI voltage value must be 70% of the expected breakdown voltage of the test sample. In case of negative impulse, expected electrical field breakdown strength was determined by equation (6.1) [60].

$$E_b = \frac{94.6}{{d_t}^{0.22}} \text{ [60]} \quad (6.1)$$

Where: d_t is the thickness of the pressboard test sample. In this study all samples were 3 mm thick. The expected electrical field breakdown strength was calculated to be 74.3 kV/mm. Assuming uniform field distribution, the corresponding breakdown voltage is deduced as in equation (6.2).

$$V_b = E_b \times d = 74.3 \times 3 = 222.9\ kV \quad (6.2)$$

In ramped voltage method of LI dielectric breakdown tests, it is advised to consider 70% of the expected breakdown voltage as the starting voltage level. In this case, 156 kV was used for negative LI polarity and the 60% of V_b was assumed. And this worked out to be 134 kV. The difference in the negative and positive initial voltages is to take into account the polarity effect. The polarity effect phenomenon can be explained using a needle to plane electrode setup as depicted in Figure 6-12 and 6-13. These figures illustrate the difference in the accumulation of space charge and the shape they form in the gap between the charged tip electrodes and the grounded plane. The avalanche development starts near the needle electrode. In the case of negatively charged needle, the electrons move towards the ground plane, leaving behind the heavy and slow moving positive ions, building up a positive space charge near the needle tip. The positive ions extend towards the grounded plane, creating a high field region ahead of the avalanche, reducing the needed voltage required for flashover.

The positive space charge for positively charged electrodes is distributed such that the electric field is enhanced towards the ground plane. This reduces the required external applied voltage to cause breakdown in the same gap distance as that of negatively charged electrode [85] .

In the case of negatively charged needle, the negative space charge accumulate evenly near the ground plane, creating an electric field distribution that is less non-uniform compared to the positively charged electrode space charge distribution. Therefore, higher external voltage is needed to cause breakdown for negatively charged than positively charged needle.

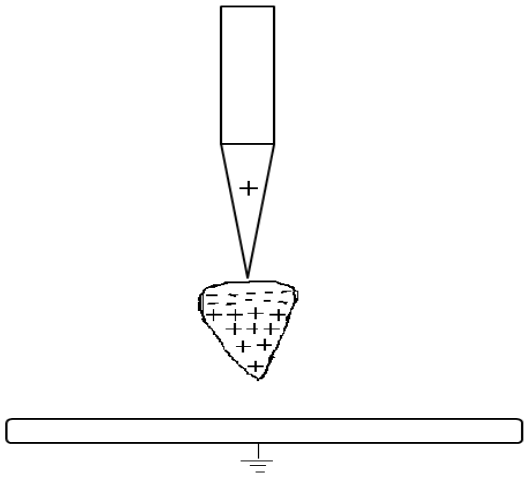

Figure 6-12: Positive polarity needle to plane electrodes

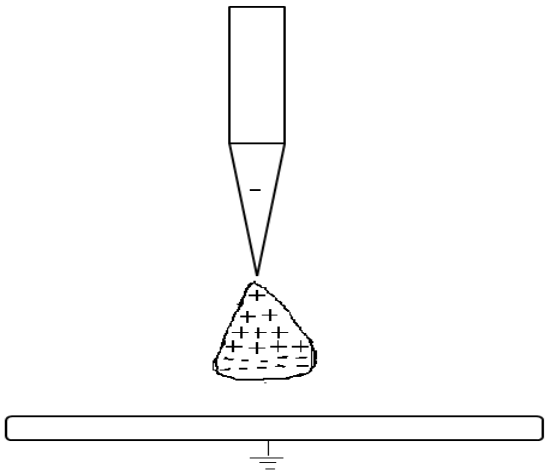

Figure 6-13: Positive polarity needle to plane electrodes

The following section presents the results of the positive and negative LI experiments.

6.4 The impulse breakdown voltage test results

The 12 test samples that were exposed to 3 hours surface discharge were divided into two sets of 6 test samples; one set for negative and the other for positive LI breakdown voltage test. The same was done for the other 12 test samples exposed to 7 hours surface discharge. A set of 12 test samples that were un-aged were also subjected to positive and negative LI breakdown voltage tests as a control tests. According to the multi-level method of breakdown voltage tests, IEC 60243-1 Clause 11, a minimum of 5 samples are required for the test to be valid.

The measured breakdown voltages for the positive and negative LI experiment are presented in Table 6-1 and Table 6-2. Note that the ranking is in ascending order of the breakdown voltage and not the sequence of testing. The ranking is used for further analysis in the next chapter.

Out of 12 un-aged samples, only 9 samples were considered in the results data tables. The other 3 samples were removed from the data as they prematurely failed without completing a set of three LI application test. A set of LI voltage application is defined as the voltage level that the test sample is able to withstand three subsequent LI strikes of the same magnitude without breakdown, in accordance to IEC 60243-3 [22]. The standard states that the test sample must complete three sets for the test to be valid, i.e. 9 LI strikes.

Table 6-1: Positive LI breakdown voltage results for un-aged and aged test sample

Sample number	**Un-aged LI breakdown voltage (kV)**	**3 hours aged LI breakdown voltage (kV)**	**7 hours aged LI breakdown voltage (kV)**
1	155	128	158
2	165	157	158
3	165	168	158
4	168	168	168
5	171	181	168
6	175	208	175
7	178	-	-
8	181	-	-
9	185	-	-
Average breakdown voltage (kV)	**171**	**168**	**164**

Table 6-2: Negative LI breakdown voltage results for un-aged and aged test sample

Sample number	**Un-aged LI breakdown voltage (kV)**	**3 hours aged LI breakdown voltage (kV)**	**7 hours aged LI breakdown voltage (kV)**
1	175	148	151
2	178	168	155
3	185	168	165
4	205	168	181
5	212	181	181
6	212	215	202
7	215	-	-
8	225	-	-
9	228	-	-
Average breakdown voltage (kV)	**204**	**175**	**173**

Presented in Figure 6-14 is a plot of the negative and positive LI average breakdown voltage versus time of surface ageing. An important conclusion is that exposure of pressboard material to surface discharge reduces the impulse voltage breakdown voltage of the pressboard. Furthermore it is evident from the figure that the negative LI breakdown voltages are higher than the positive LI voltage, as expected. The reduction of the average LI breakdown voltage between the un-aged and aged test samples with increase in time of exposure to surface discharge is more pronounced for negative LI than for positive LI.

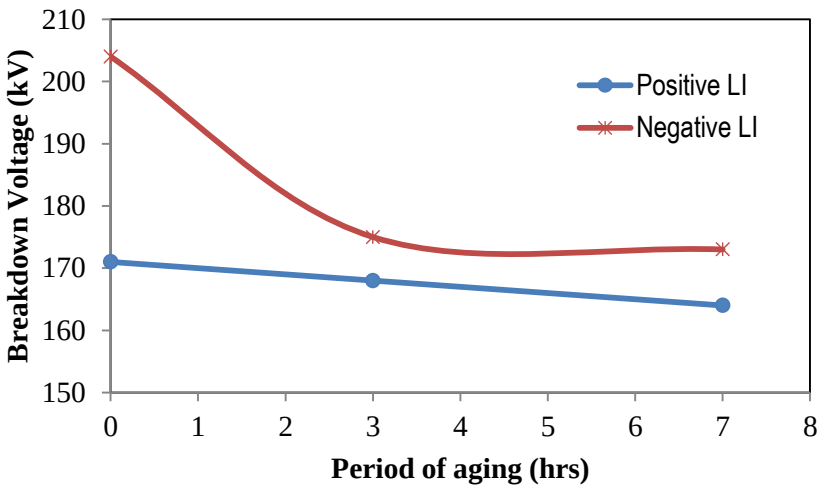

Figure 6-14: A plot of negative and positive LI breakdown voltage vs. the ageing period

The un-aged positive LI average breakdown voltage reduced by 1.8% and 4.2% for 3 hours and 7 hour aged test samples, respectively. The un-aged negative LI average breakdown voltage is reduced by 15.3% and 16.5% for 3 hours and 7 hours aged samples, respectively. The reduction of the breakdown voltage with ageing period seems to increase faster for positive LI than for negative LI as the percentage difference between 3 hours aged sample and 7 hours aged sample is 2.4% for positive LI and is 1.2% for negative LI. It can be concluded that once the pressboard sample is exposed to surface discharge, the reduction of the breakdown voltage with time is high in the initial stage of ageing and reduces relatively slowly with further exposure for the negative impulse. The opposite happens for positive LI.

Ding et al [11] reported that switching impulse breakdown strength reduces by 15% for pressboard that has been in service for more than 20 years. However, in another study by Ding et al reported that LI breakdown strength reduces by approximately 30% after 29 years of service [53]. This means that the test samples exposed to surface discharge in this study accelerated the ageing process by approximately half of the expected life of the transformer. This is deduced by comparing the negative LI breakdown voltage reduction percentage with the reduction of breakdown strength reported in [53].

6.5 Conclusion

Presented in this chapter are the results of the un-aged and aged pressboard LI breakdown voltage tests. The key findings are summarised as follows:

- Exposure of pressboard material to surface discharges reduces its LI voltage withstand level.

- The effect of surface discharges on the LI withstand voltage of pressboard is more prevalent in the initial period of surface discharge ageing process.
- Negative polarity LI breakdown voltage of surface discharge aged pressboard is higher than positive polarity LI breakdown voltage.

The following chapter discusses the Weibull statistical analysis results for the LI breakdown voltages presented in this chapter.

Chapter 7: Weibull statistical analysis of the LI breakdown voltages

7.1 Introduction

Chapter 6 presented the results for the LI breakdown voltages tests for un-aged, 3 hours and 7 hours aged pressboard test samples. In this chapter, the LI breakdown voltage results are further analysed using Weibull distribution function.

7.2 The theory of Weibull analysis

Weibull distribution function is one of the statistical distribution tools used to analyse the probability of wear-out of solid insulation material in its life cycle [23]. It is generally suited for analysing data with scattered values, like breakdown voltage values of liquid and solid insulation material. It is used to determine the statistical breakdown voltage of insulation system for defining the insulation strength of electrical equipment. In other applications, such us in mechanical engineering Weibull analysis is used to determine the wear-out of a mechanical machine, or in retail stores to manage the stock in the inventories (or to determine when to order new stock) etc.

Equation (7.1) and (7.2) give the two parameter Weibull distribution function and the cumulative function, respectively [23]. It should be noted that there is a three parameter Weibull distribution function, which will not be discussed in this document.

$$\mathrm{f(V_b)} = \frac{\beta}{\alpha}\left(\frac{V_b}{\alpha}\right)^{\beta-1} - exp\left(-\left(\frac{V_b}{\propto}\right)^{\beta}\right) \tag{7.1}$$

$$\mathrm{F(V_b)} = 1 - exp\left(-\left(\frac{V_b}{\propto}\right)^{\beta}\right) \tag{7.2}$$

Where:

$f(V_b)$ is the probability density function of the sample data

$F(V_b)$ is the cumulative distribution function of the sample data

V_b is the breakdown voltage of the test sample.

α is the scaling parameter of the Weibull function that gives the probability of failure of 63.2%

β is the shaping parameter of the Weibull function indicating whether the failure rate is increasing, constant or decreasing.

The cumulative function of Weibull function can be rewritten as a straight line in the form of y = mx + C, by taking the natural log twice in equation (7.2). This gives a straight line as:

$$\ln\left[-\ln\left(1-\mathrm{F}(\mathrm{V_b})\right)\right] = \beta \ln V_b - \beta \ln \alpha \tag{7.3}$$

Where the straight line parameters from equation (7.3) are as follows:

y is represented by $\ln\left[-\ln\left(1-\mathrm{F}(\mathrm{V_b})\right)\right]$

m is represented by β

x is represented by $\ln V_b$

C is represented by $\beta \ln \alpha$

Representation of Weibull cumulative function by a straight line allows for a linear regression to determine the relationship of the straight line parameters, by fitting the best straight-line to a set of sample data. The linear regression is used to determine the Weibull function parameter, β and α. The procedure for determining these parameters can be summarised as follows:

1. Record the breakdown voltage in a Microsoft Excel® sheet.
2. Rank the breakdown voltage data in ascending order.
3. Calculate the rank median using the Bernard's Approximation equal to ((*i – 0.3*)/ (*n+0.4*)), where *i* is the sample rank number in ascending order and *n* is the total number of tested samples. This approximation gives the proportion of the samples that will fail at the rank's breakdown voltage. For example, if the rank median is calculated to be 0.2 for sample rank number 1, with breakdown voltage of 175 kV, it means there is 20% chance that the samples will fail at 175 kV.
4. Calculate 1/ (1- median rank).
5. Calculate ln(ln(1/(1- median rank)) which represents the y data
6. Calculate $\ln(V_b)$ representing the x data
7. Perform linear regression using the build-in function, either in Microsoft Excel® or Matlab®.
8. Plot the predicted data set and the measured data versus x data
9. Interpret the results based on the Weibull parameters

The above steps were implemented in post-processing the LI breakdown voltages reported in Chapter 6. Matlab® code was written to perform the Weibull analysis. The code reads the data from a Microsoft Excel® sheet, step 1 to 6 were performed in Excel. Steps 7 to 9 were done in Matlab®. The summary of the input data samples as in the Excel spreadsheet are presented in Table A 5-1 to A 5-6 and the Matlab® code is in appendix A.4. The results from Matlab® were recorded into the Microsoft Excel® and are discussed in the following section.

7.3 Statistical analysis of the experimental results

Presented in this section are the statistical analysis results based on the two parameter Weibull distribution function. Listed in Table 7-1 are the Weibull parameters, α and β, including the lower and upper bound parameters for 95% confidence limits. Considering the shape parameter, β, in Table 7-1, the negative LI parameter is about 14 for un-aged, 8 for the 3 hour aged and 10 for 7 hours aged samples. The shape parameter, β, for positive LI parameter is about 22 for un-aged, 8 for the 3 hour aged and 26 for 7 hours aged samples. The calculated β values are greater than one, indicating an increasing failure rate with time of aging. It can be concluded from the shape parameter that the scattering of negative LI is less than that for the positive LI. This means that the breakdown voltage of the positive LI will happen in lower voltages than for negative LI. This confirms the results that were presented in the previous chapter, where it was noticed that positive LI breakdown happens at lower voltages than negative LI. This can be explained by the effect of polarity on the failure mechanism, which was explained in terms of ionisation process in the previous chapter. Furthermore, it can be concluded that surface discharge ageing in the positive LI is not the only influencing failure factor on the breakdown process, the polarity also plays a role.

The scaling parameter, α, results are as expected (the decreasing α values with aging time), high values are noted in Table 7-1 for negative LI than positive LI breakdown voltage. This is because the measured negative LI breakdown voltages were higher than positive LI (compare values in Table 6-1 and 6-2). The decrease of scaling parameter with the ageing period was expected. However, in the 3 hours aged positive LI there was a sudden increase in the scaling factor. This means that the breakdown voltage was too scattered for the positive LI and the lower and upper bound confidence limit confirms that as it has a wide range. Table A 5-3 shows the evidence of this scattering, the last two test samples for positive voltage breakdown are high compared to the other 4 test samples.

Figure 7-2 and 7-3 show the Weibull best fit versus the breakdown voltage for the un-aged, 3 hours aged and 7 hours aged negative and positive LI test samples. These plots show that the data of the LI breakdown voltage are best represented by a Weibull distribution function, as straight line fits were

achieved for all the data. The Weibull plot for the negative LI breakdown voltage data, in Figure 7-2, clearly indicates the decrease of the breakdown voltage for surface discharge aged test samples. The difference in the breakdown voltage between 3 hours and 7 hours ageing period is more significant for breakdown voltage probability above 35%. The Weibull plot for positive LI breakdown voltage, Figure 7-3, confirms what was observed with 3 hours aged test sample's scaling parameter, α, that during the experiment there were two test samples that had higher breakdown voltage than un-aged test samples. However, the 7 hours aged positive LI breakdown voltage is lower than the un-aged test samples.

Table 7-1: Weibull two parameter analysis results

Sample Study	**Alpha (α)**	**Beta (β)**	**Lower Bound Alpha (α)**	**Upper Bound Alpha (α)**	**Lower Bound Beta (β)**	**Lower Bound Beta (β)**
Un-aged Positive LI	175.6	22.4	169.2	182.2	19.0	26.8
Un-aged Negative LI	212.2	13.6	199.7	225.6	10.9	17.6
3 Hours aged Positive LI	178.8	7.7	156.8	204.1	6.6	9.2
3 Hours aged Negative LI	184.2	8.2	162.7	208.7	7.4	9.3
7 Hours Positive LI	167.4	26.0	161.0	174.2	21.7	31.6
7 Hours Negative LI	180.6	10.4	163.8	199.4	8.8	12.5

Figure 7-1 presents a plot for un-aged positive and negative LI breakdown voltage versus Weibull probability distribution. The upper bound of the positive LI overlaps the lower bound of negative LI. According to IEEE 930 [23], the confidence limits overlap between two test data at 10^{th} percentile is used to compare the data of two types of insulation. In the case of the Figure 7-1, the overlap happens below the probability of 20%. This means that there are some similarities in the failure mechanisms between the two LI polarities. Since this is a low percentage, the other failure mechanism can be the oil condition or space charge around the test sample. This will require more data to be tested to investigate this overlap further.

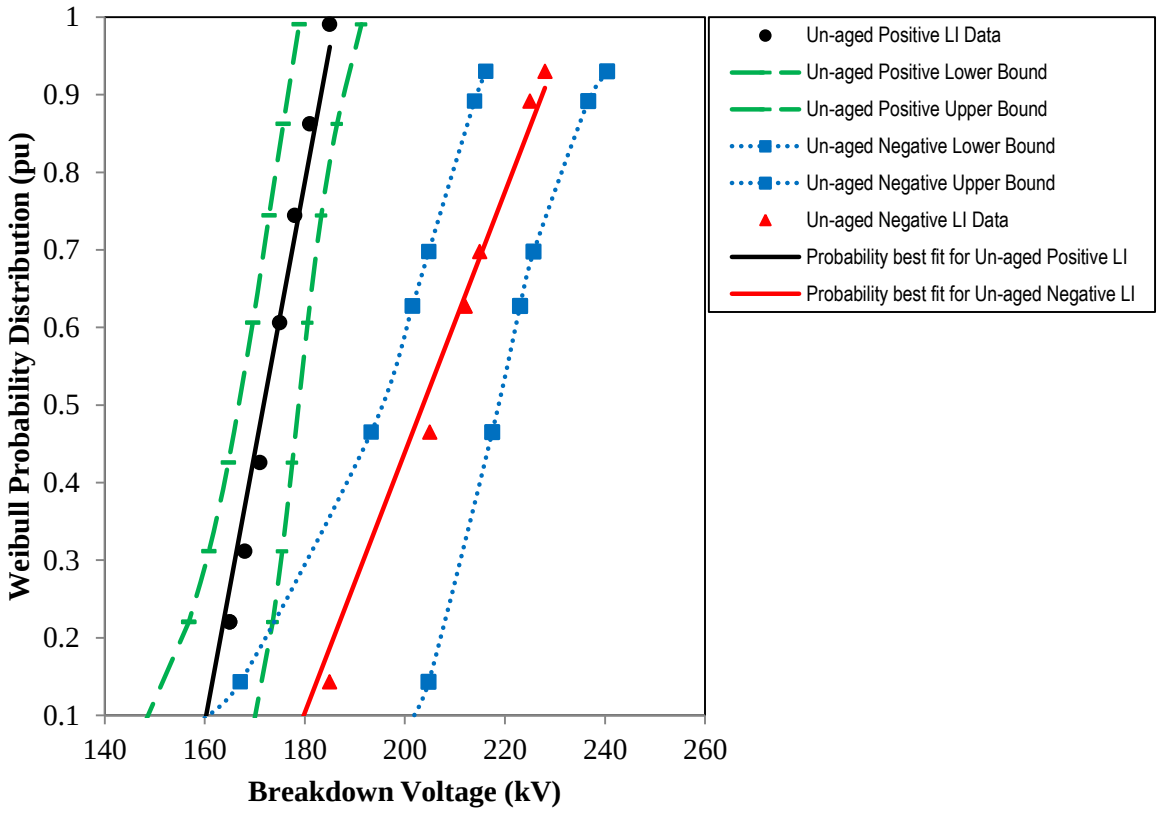

Figure 7-1: 95% confidence bound for un-aged negative and positive LI breakdown voltage

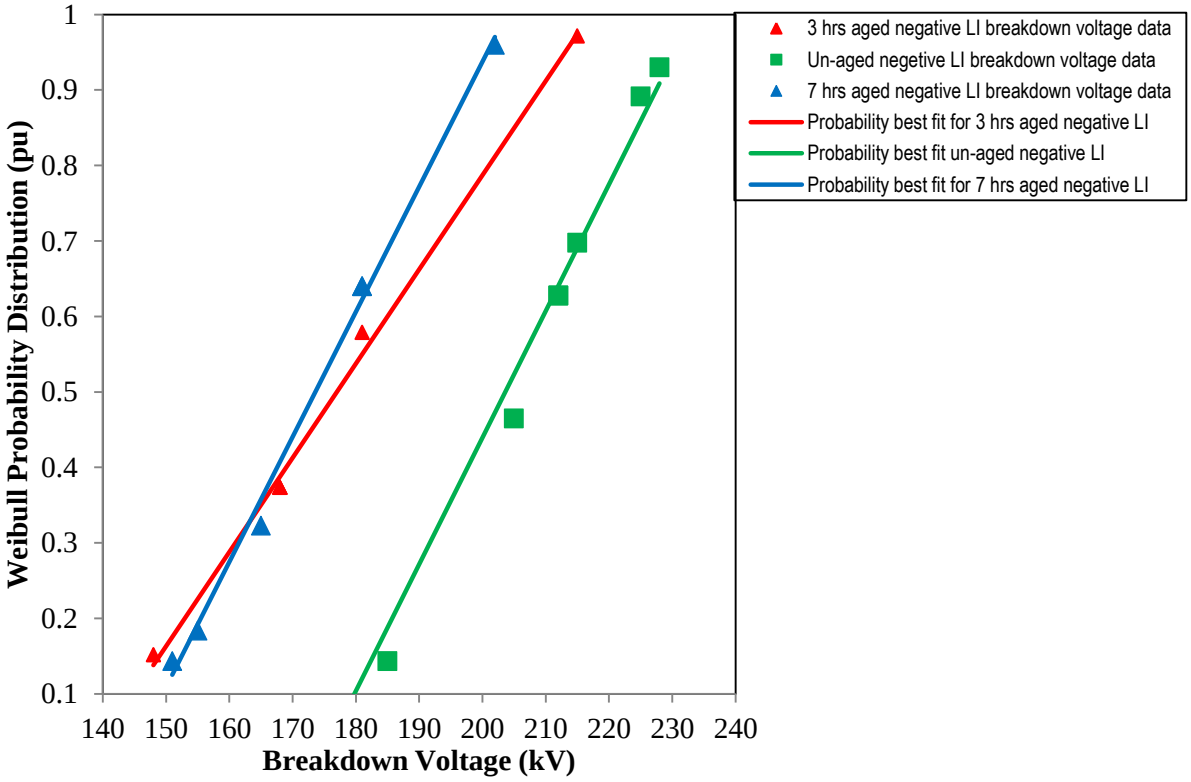

Figure 7-2: Weibull probability best fit for negative LI breakdown voltage

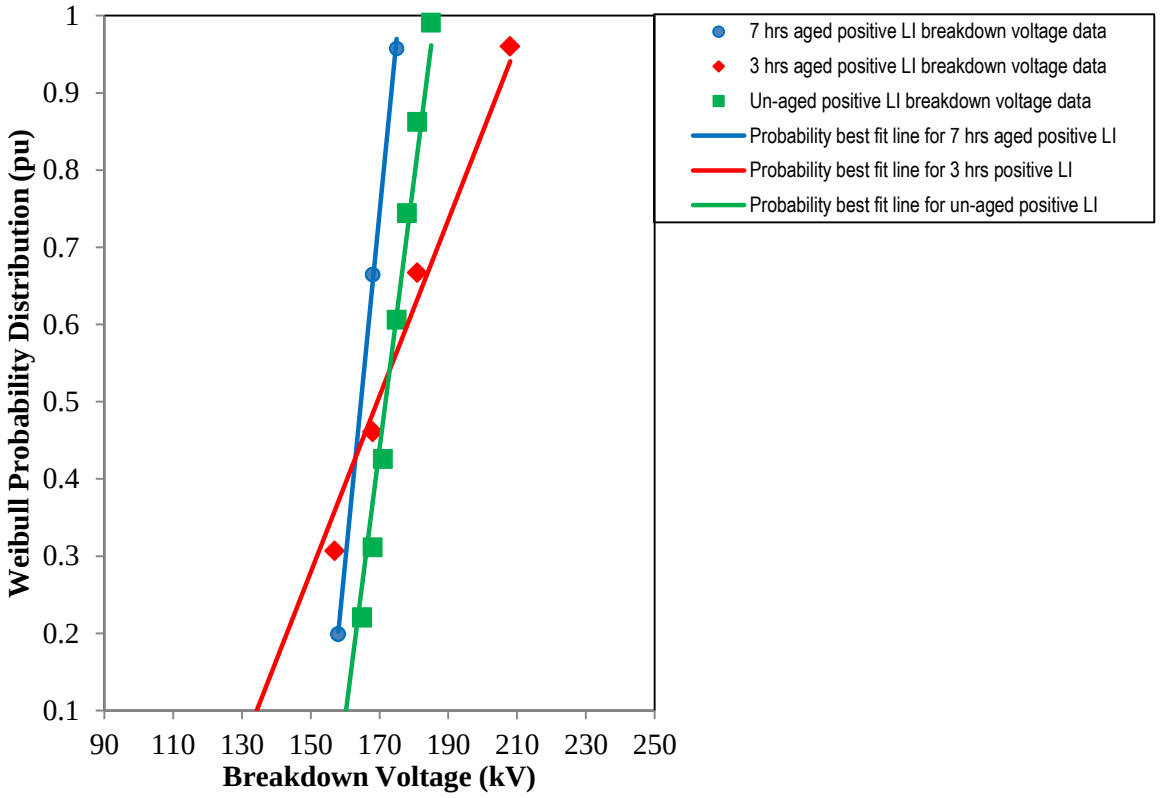

Figure 7-3: Weibull probability best fit for positive LI breakdown voltage

Table 7-2 lists the arithmetic mean, 50% and 63.2% Weibull probability breakdown voltages. Percentage difference between the un-aged sample and aged samples are represented in brackets in the Table 7-2. The percentage difference range is also listed in the table. The negative sign on the percentage numbers means that the breakdown voltage reduces with time of ageing by surface discharge. The scattering of 3 hours aged positive LI is evident at 63.2% Weibull probability breakdown voltage, showing an increase in the breakdown voltage. However, it shows a reduction for 50% Weibull probability breakdown voltage. As discussed in Chapter 6, the decrease in the breakdown voltage with the rate of ageing is slow for positive LI compared to negative LI Table A5-7 gives the statistical results data for Weibull distribution function, such as mean median mode, standard deviation, variance, skewness and kurtosis. This data are not used to discuss the LI results in this document. However, there are parts of the calculated data from the Matlab® code.

Table 7-2: Comparison of the arithmetic mean breakdown voltage to the 50% and 63% Weibull breakdown voltage probability

Sample Study	**Mean Breakdown Voltage**	**63.2% Breakdown Voltage**	**50% Breakdown Voltage**	**Percentage difference range (rounded)**
Surface Discharge Free Positive Impulse	171	175.6	172.7	-
Surface Discharge Free Negative Impulse	204	212.2	206.6	-
3 Hours Surface Discharge Exposed Positive Impulse	168 (-1.77%)	178.8 (+1.81%)	170.5 (-1.28%)	-2 % to -2%
3 Hours Surface Discharge Exposed Negative Impulse	175 (-15.3%)	184.2 (-14.1%)	176.2 (-15.9%)	-14% to -16%
7 Hours Surface Discharge Exposed Positive Impulse	164 (-4.2 %)	167.4 (-4.8%)	165.1 (-4.5%)	-4% to -5%
7 Hours Surface Discharge Exposed Negative Impulse	173 (-16.5 %)	180.6 (-16.1%)	174.4 (-16.9%)	-15% to -17%

7.4 Conclusion

Discussed in this chapter are the Weibull distribution analysis results for the LI breakdown voltage. Weibull distribution function fits well to the data samples. The shape parameter, β, is greater than one for all LI data sample thus proving that the failure mechanism is due to wear out, as was expected. The scaling parameter, α, lower and upper bound 95% conference limit revealed that the breakdown voltage reduces with the time of ageing. However, for aged positive LI samples, the rate of reduction was found to be slower compared to negative LI samples. The scaling parameter, α, showed a wide range for positive LI samples meaning that the breakdown voltage is scattered. This meant that there are other factors that are influencing the failure mechanisms besides surface discharge. Effect of polarity was another contributor in the scattering of the breakdown voltages for the positive LI samples.

Okabe et al [12] studied the effect of surface discharge on the LI withstand voltage on an oil immersed pressboard. Their study revealed that the LI withstand strength of pressboard starts to reduce when PD magnitude is between 10,000 pC and 20,000 pC or more. Their analysis showed that LI breakdown voltage reduced by 10% to 20% after the pressboard has been exposed to 20,000 pC, and reduces by about 30% for 50,000 pC [12].

Chapter 8: Conclusion and recommendation for future work

This dissertation presents the findings of an experimental study in investigating the effect of surface discharge on the LI breakdown voltage of oil-impregnated pressboard.

The key findings in this research can be summarised as follows:

- For a given needle tip radius (0.117 mm in this study), the optimal electrode gap distance of 45 mm and the voltage of 30 kV produced sustained surface discharge on pressboard for a reasonable long period without puncture or flashover.
- It was found that surface discharge on the pressboard material reduces the breakdown voltage of both positive and negative LI. The severity more pronounced on the negative LI. The reduction of breakdown voltage increases with increase of time of exposure of the pressboard to surface discharge.
- For positive lightning impulses, the breakdown voltage reduction was found to be 2 % for the 3 hour and 5 % for the 7 hour exposure to surface discharge.
- For negative lightning impulses, breakdown voltage the reduction was found to be 16 % for the 3 hour exposure and 17 % for the 7 hours exposure to surface discharge.

8.1 Further work

Possible future work on this research can be summarised as follows:

- Repeat the multiple test sample surface discharge ageing experiment with PD measurements, to gather more data for analysing the severity of the ageing.
- Breaking down the ageing time in steps of 1 hour, for statistical analysis to determine the lifecycle of the pressboard when it is exposed to surface discharge.
- Increase the number of test samples for LI breakdown voltage statistical analysis.

Appendices

A.1 Chemical structure of cellulose

In this appendix, details of the chemical structure of cellulose are presented in terms of its molecular chains. Depicted on Figure A 1-1 is five cellulose molecules linked by oxygen atom. It can also be observed form the figure the –OH, hydroxyl groups alongside the linked cellulose molecule chain that will form a bond with other parallel hydroxyl group from another cellulose molecule chain. Shown in Figure A1-2 is an example of a cellulose molecule chains linked in parallel forming crystalline.

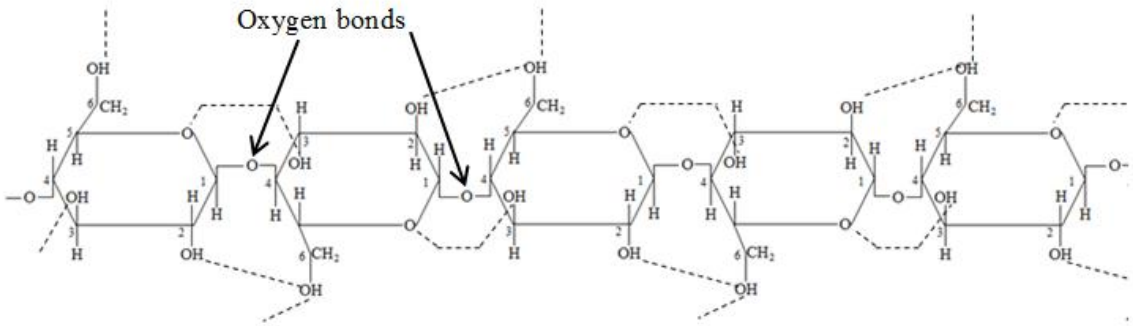

Figure A 1-1: The single chain of a cellulose molecule

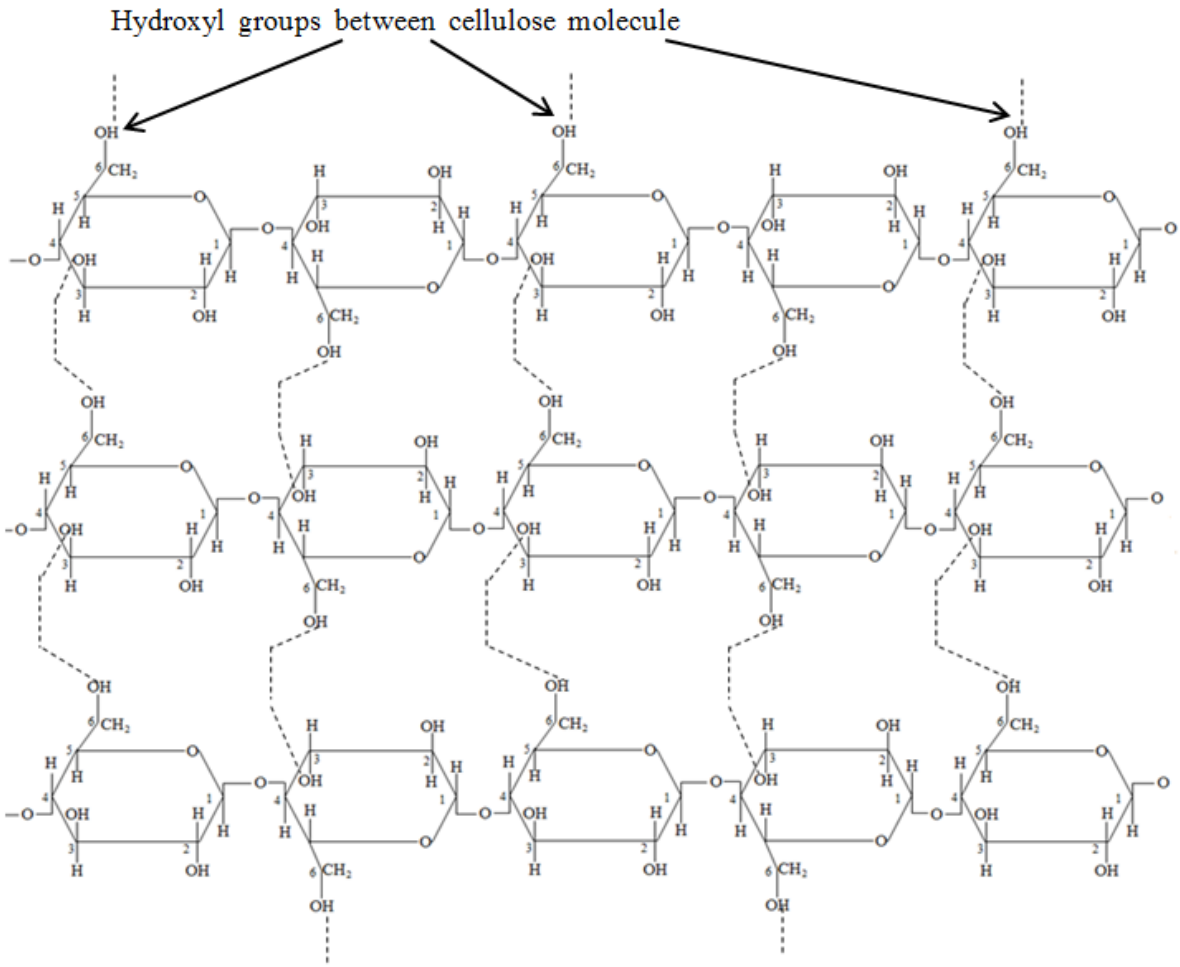

Figure A1-2: Hydrogen bond between neighboring chains to form a crystalline region

A.2 Experimental material and equipment

Table A 2-1: List of the experimental materials and equipment

Items	Dimensions or description	Quantity	Experiment ID
Pressboard test samples	(100 × 100 × 3) mm	54	All experiments
LI generator	Marx generator	1	Un-aged and aged test samples positive and negative LI breakdown voltage tests experiment
AC power supply	0 – 60 kV	1	Single and multiple test samples ageing experiment
ICMcompact PD measurement system	Single channel	1	Single test samples ageing experiment
Capacitive voltage divider	1000 :1 ratio	1	Multiple test samples ageing experiment
Needle HV electrode	0.53 mm diameter	13	Single and multiple test samples ageing experiment
Copper tubes for surface discharge electrodes	10 mm diameter 1.5 meter long	2	Single and multiple test samples ageing experiment
IEC earth electrode	15 mm height 75 mm diameter 3 mm radius	1	Un-aged and aged test samples positive and negative LI breakdown voltage tests experiment
IEC HV electrode	25 mm height 25 mm diameter 3 mm radius	1	Un-aged and aged test samples positive and negative LI breakdown voltage tests experiment
Oil tank for ageing rig	(738 × 485 × 335) mm	1	Multiple test samples ageing experiment
Perspex tank	(265 × 170 × 40) mm	1	Un-aged and aged positive and negative LI breakdown voltage tests and Single test samples ageing experiment
Fibre glass screw	M10	4	Un-aged and aged test samples positive and negative LI breakdown voltage tests experiment
Non - conduction screw	M10	4	Un-aged and aged test samples positive and negative LI breakdown voltage tests experiment
Transformer oil	100 litres	5 × 20 litres drums	All experiments

A.3 Electrode gap distance set up results

Presented in this appendix are the PD measurements results of the distance setup experiment which are discussed in Chapter 4.

Table A 3-1: Measured peak charge magnitude per distance per supplied voltage

Distance	55 mm	45 mm	35 mm	25 mm
Voltage (kV)	Peak Measured Charge (pC)			
5	1.7	0.6	1.6	0.7
10	1.6	0.7	1.7	0.6
15	1.8	0.7	1.6	0.7
20	30.0	0.6	1.6	2
23	30.0	2.0	1.8	2
26	60.0	1000.0	5.0	2
29	60.0	1000.0	5.0	2
33	300.0	2000.0	2000.0	-
36	300.0	1134.0	1800.0	-
39	300.0	765.7	147.0	-
40	2000.0	1400.0	200.0	-
43	4458.0	2000.0	200.0	-
46	6000.0	5648.0	5000.0	-
50	5495.0	5884.0	-	-

Table A 3-2: The PD measurement results for 55mm gap distance

Supply Voltage	PRPD pattern	PD pulse superimposed on the supply sine wave
20	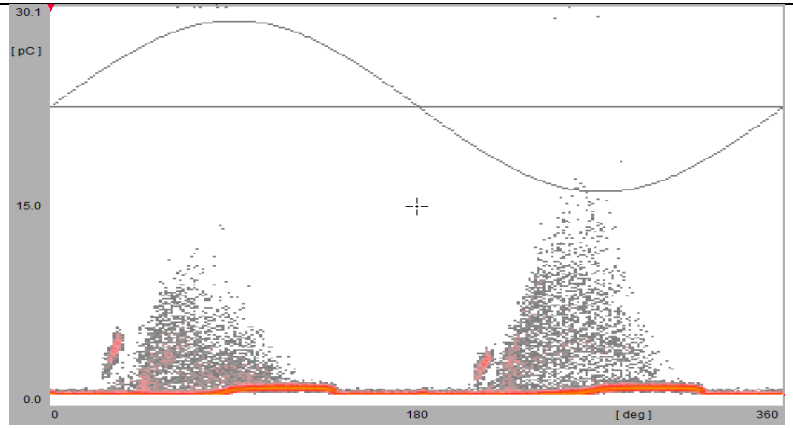	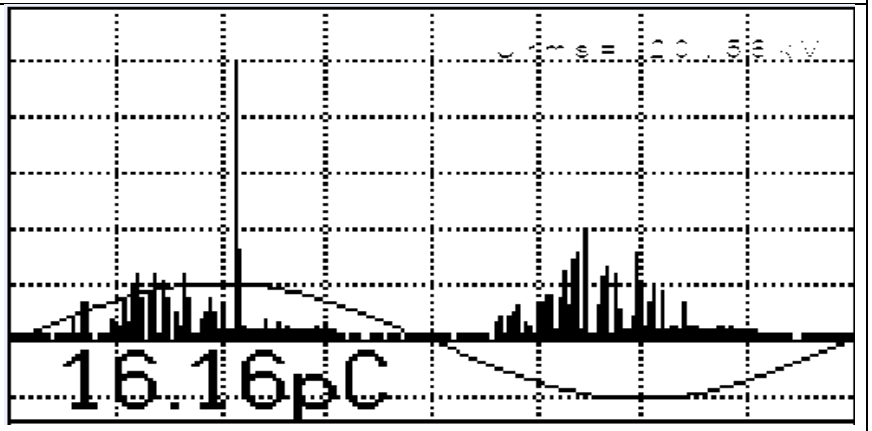
23	No Record	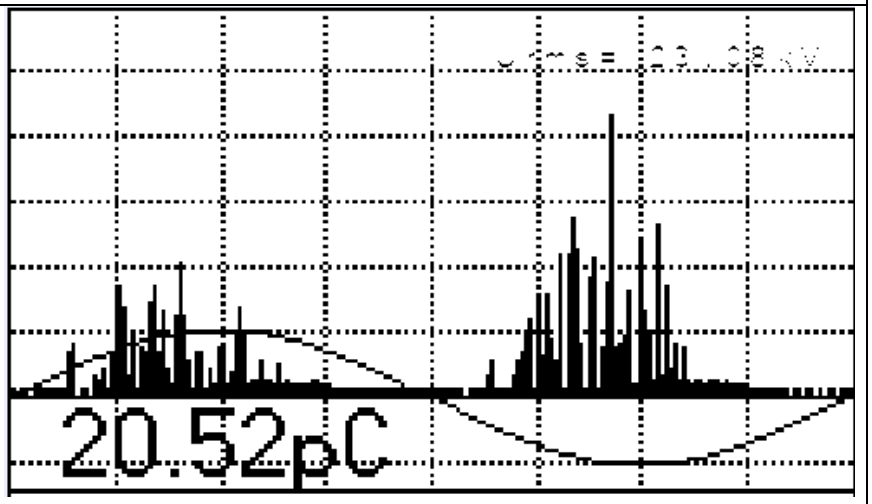

26	No Record	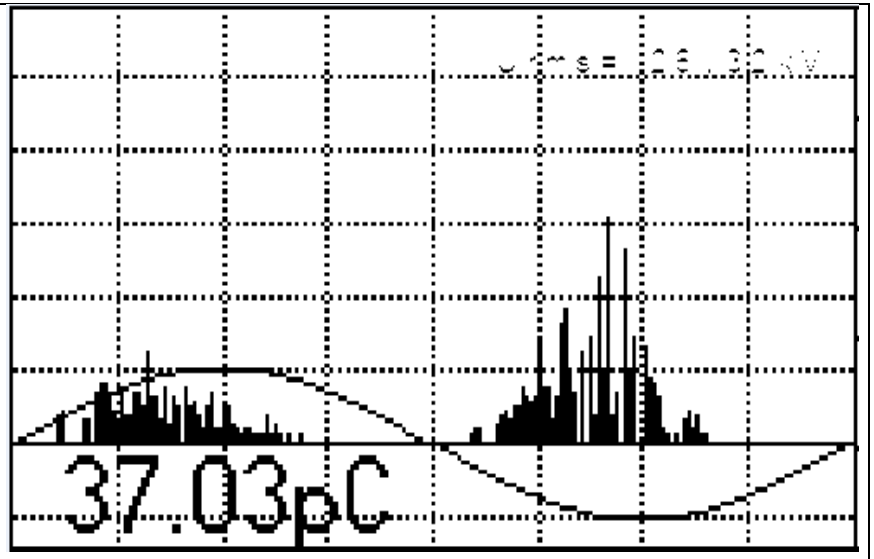
29	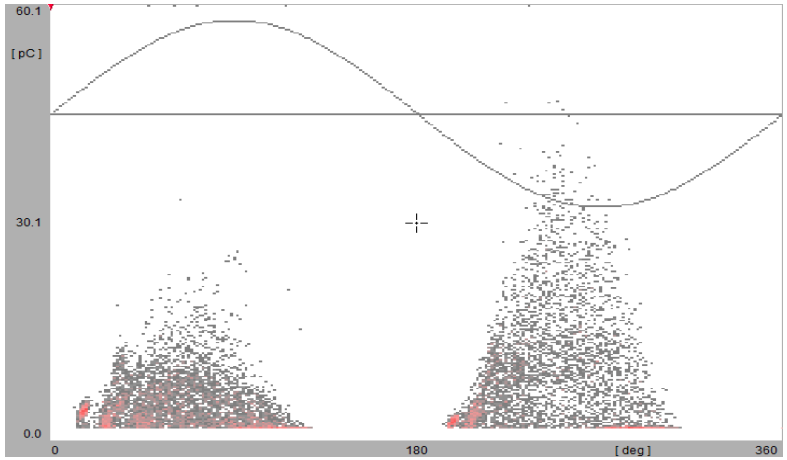	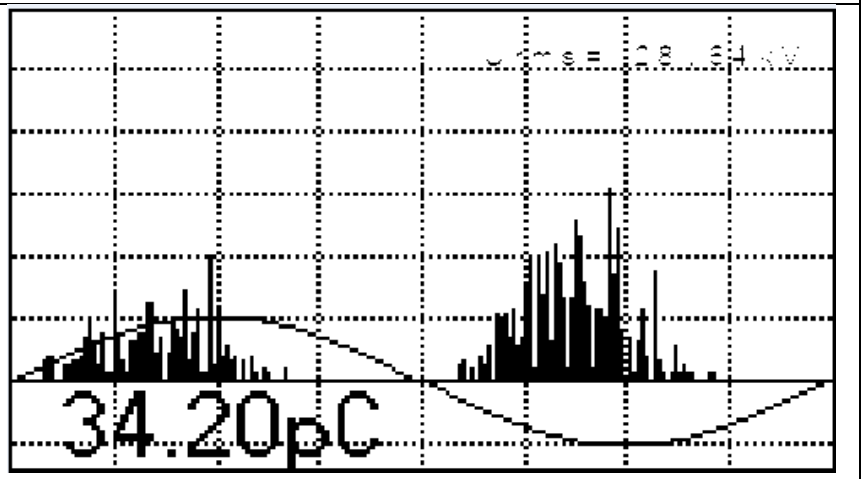

33	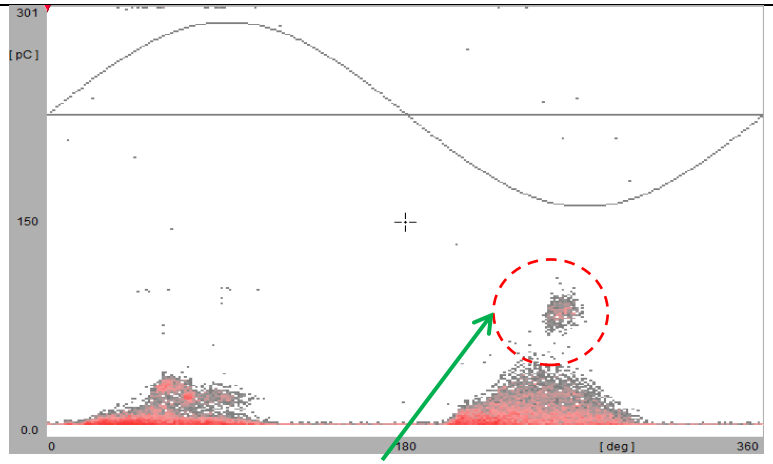 301 [pC] 150 0.0 0 180 [deg] 360	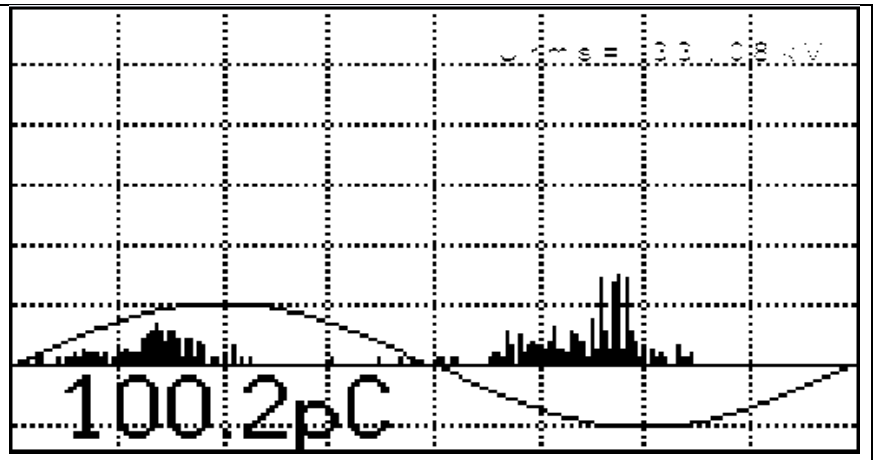 100.2pC
36	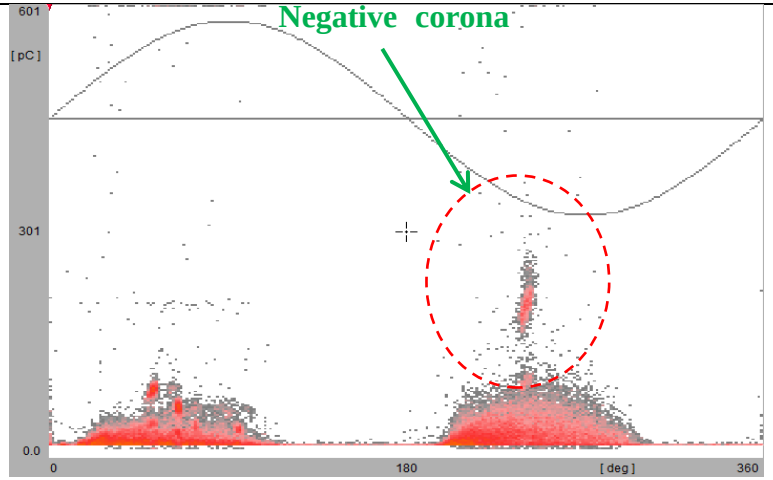 Negative corona 601 [pC] 301 0.0 0 180 [deg] 360	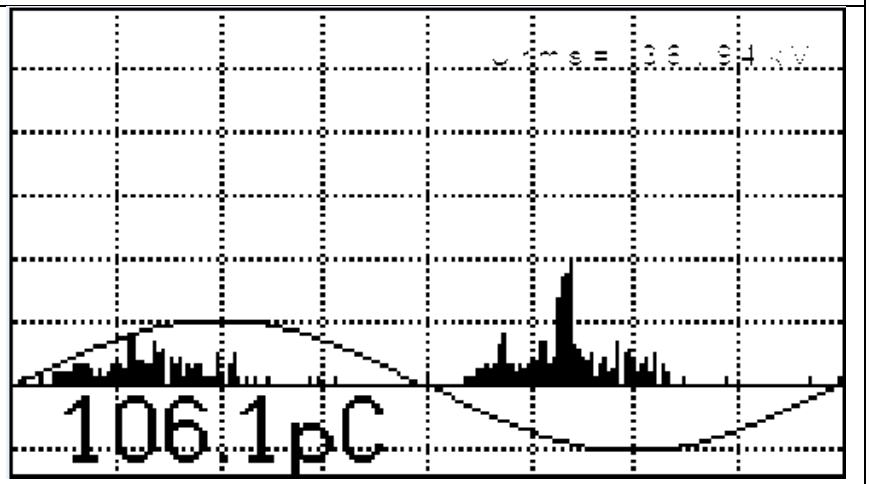 106.1pC

40	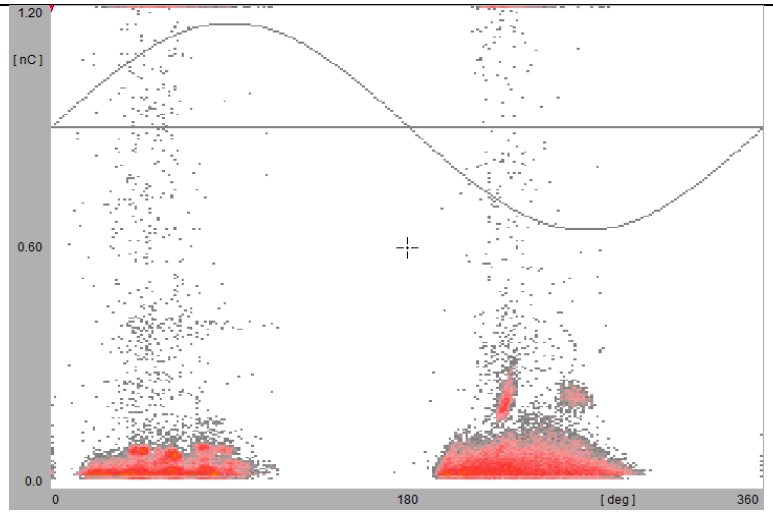 1.20 [nC] 0.60 0.0 0 180 [deg] 360	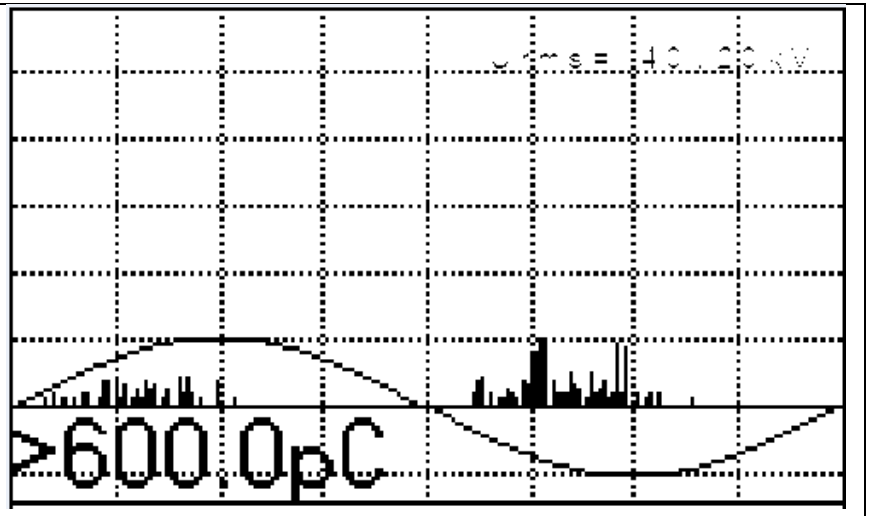 >600.0pC
43	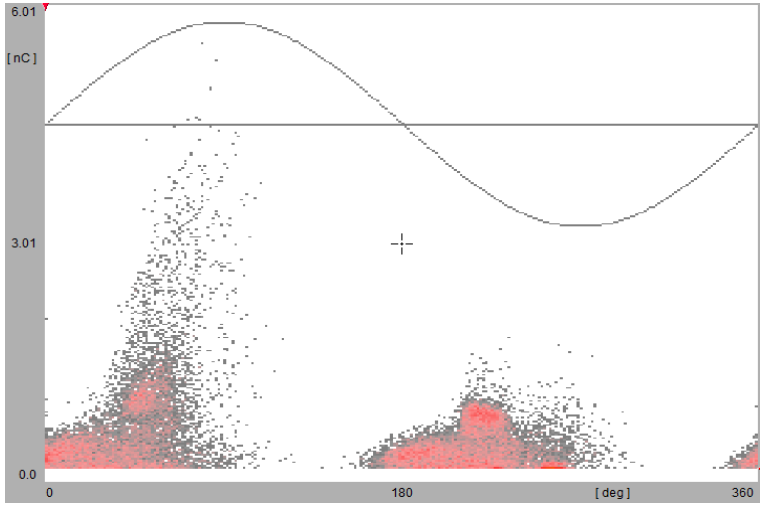 6.01 [nC] 3.01 0.0 0 180 [deg] 360	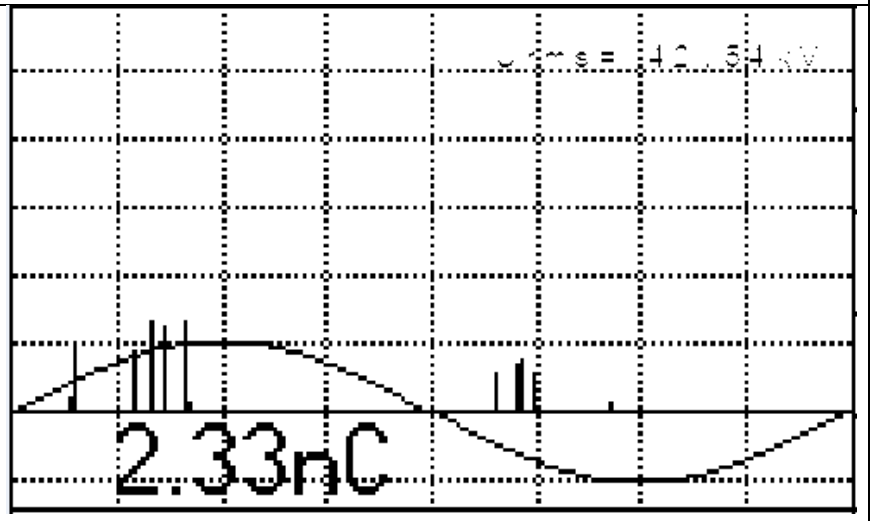 2.33nC

46	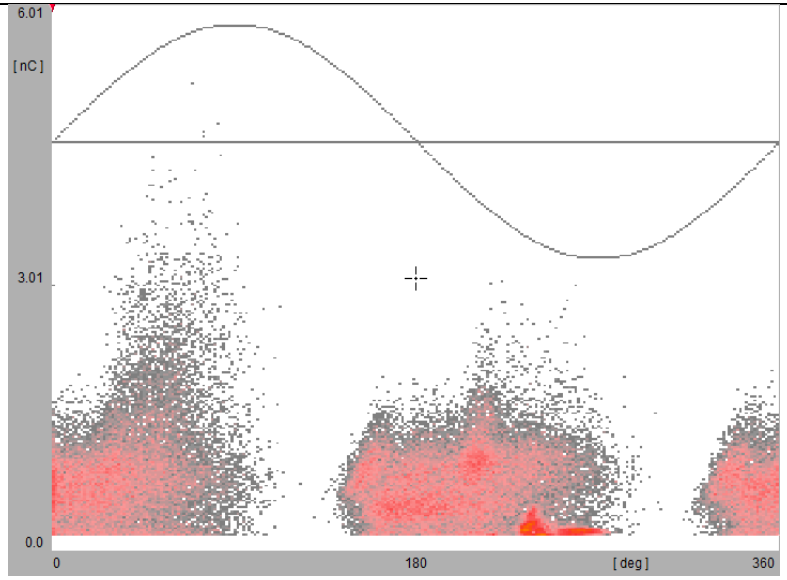	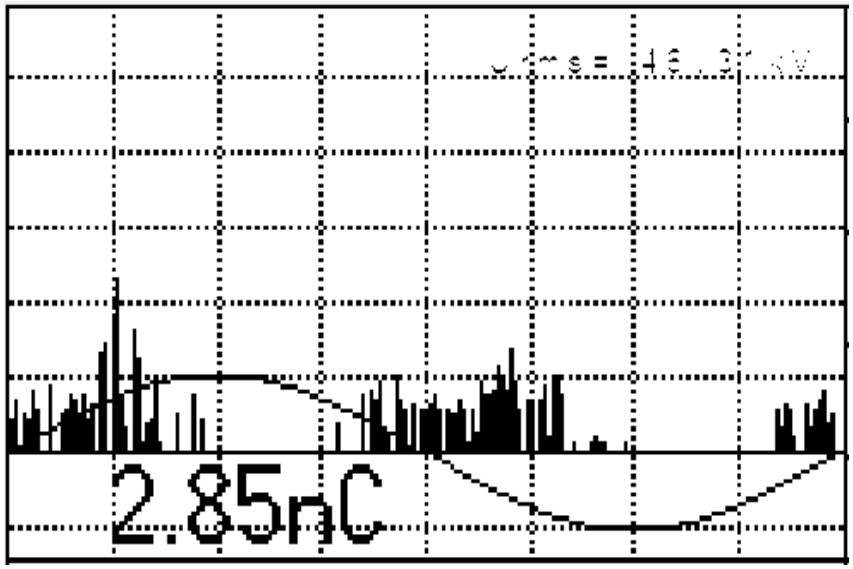
50	No Record	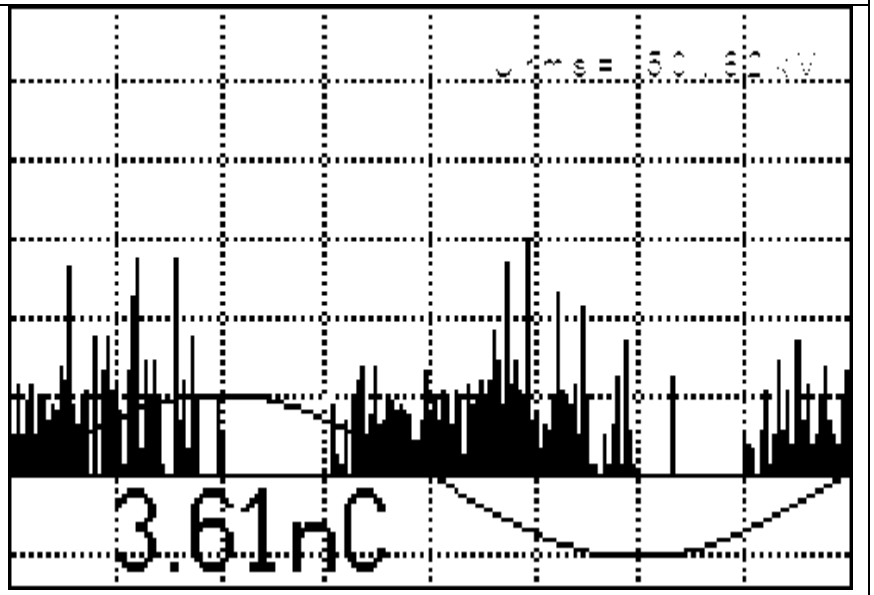

Table A 3-3: The PD measurement results for 45 mm gap distance

Supply Voltage	PRPD pattern	PD pulse superimposed on the supply sine wave
20	No Record	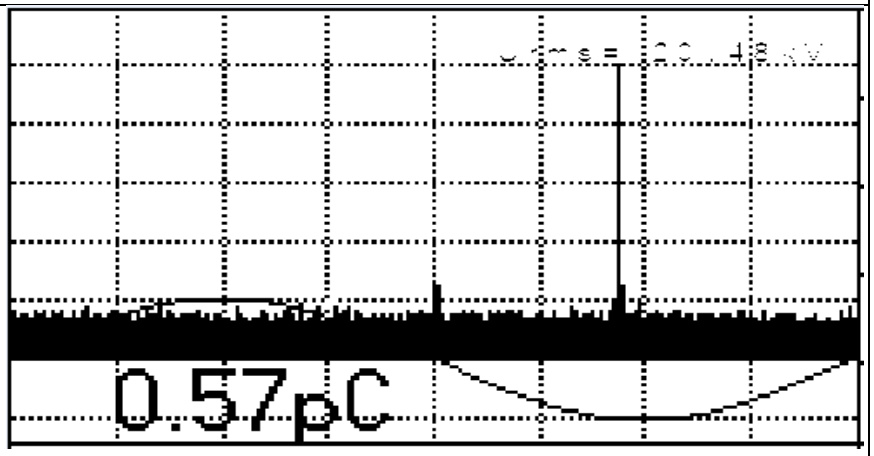
23	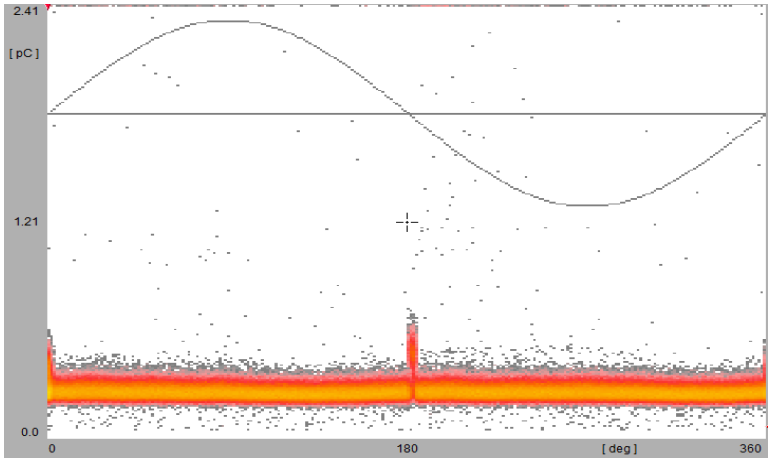	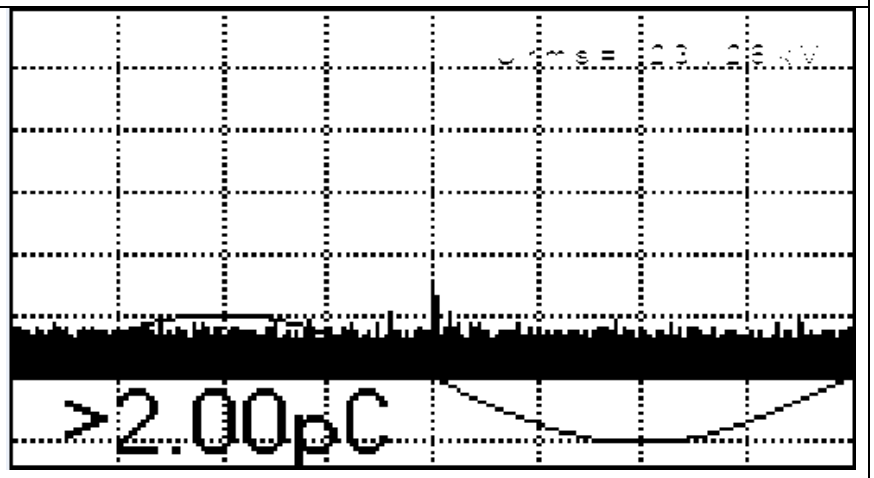
26	No Record	No Record

29	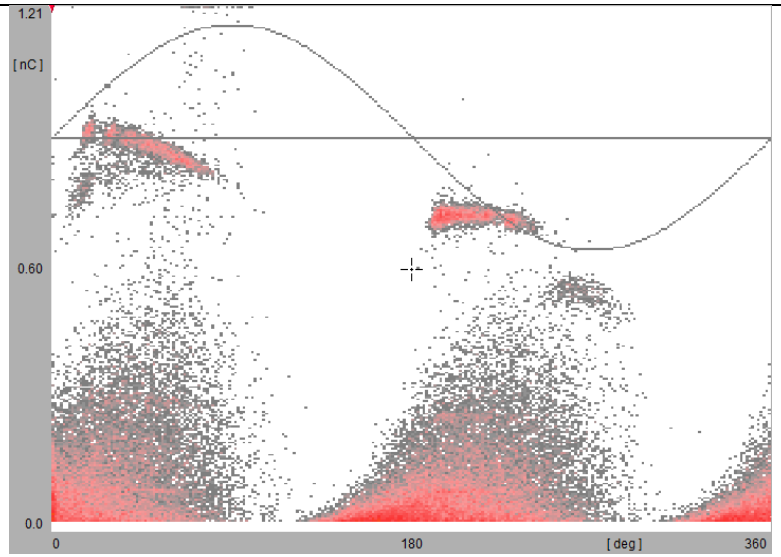 1.21 [nC] 0.60 0.0 0 180 [deg] 360	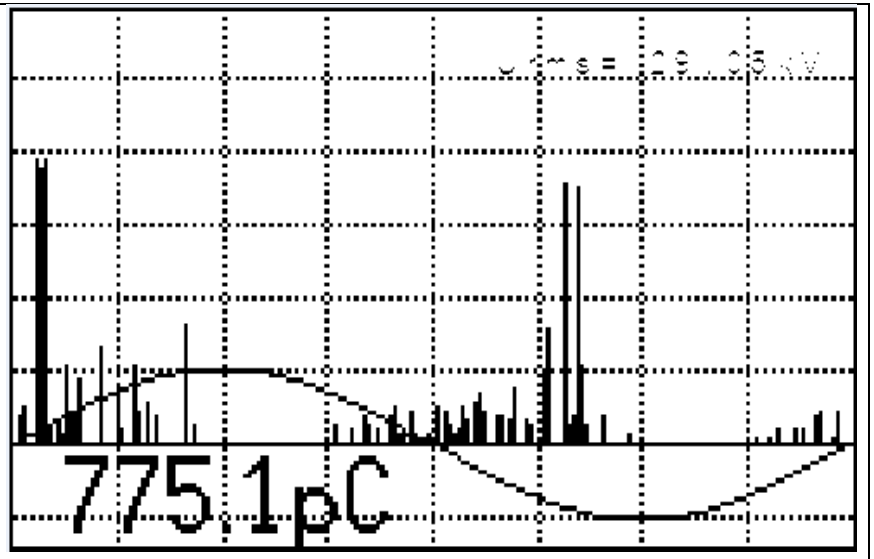 775.1pC
33	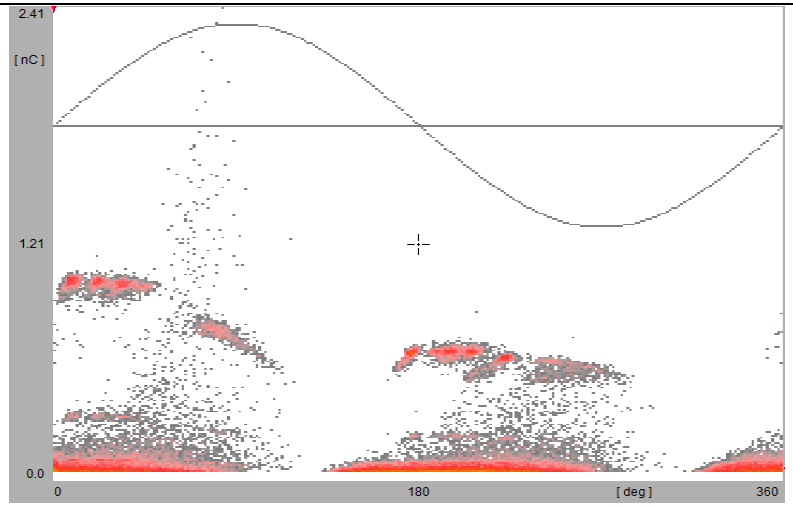 2.41 [nC] 1.21 0.0 0 180 [deg] 360	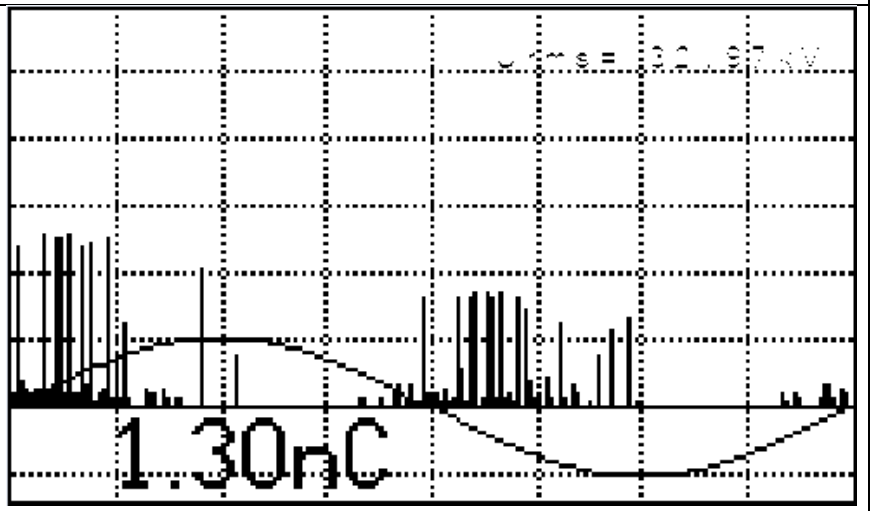 1.30nC

36	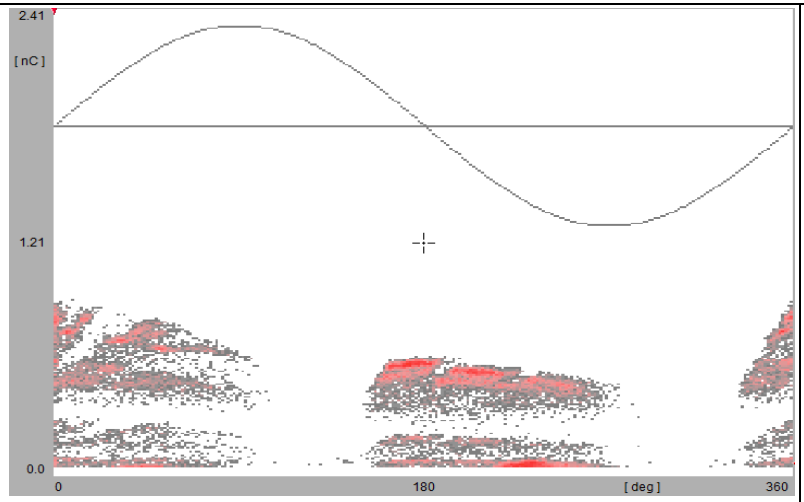 2.41 [nC] 1.21 0.0 0 180 [deg] 360	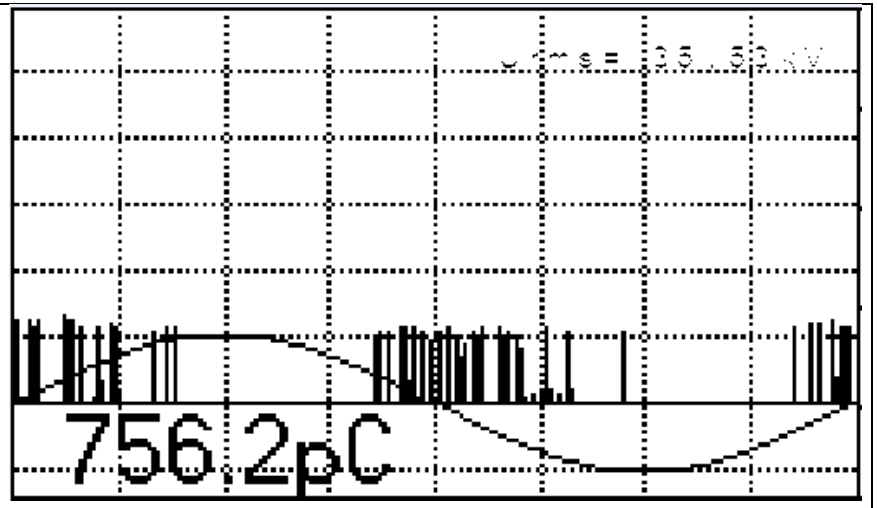 756.2pC
39	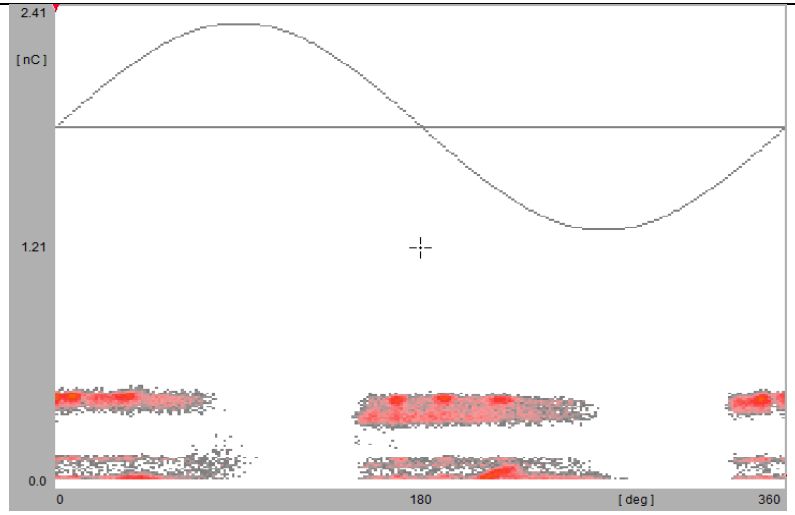 2.41 [nC] 1.21 0.0 0 180 [deg] 360	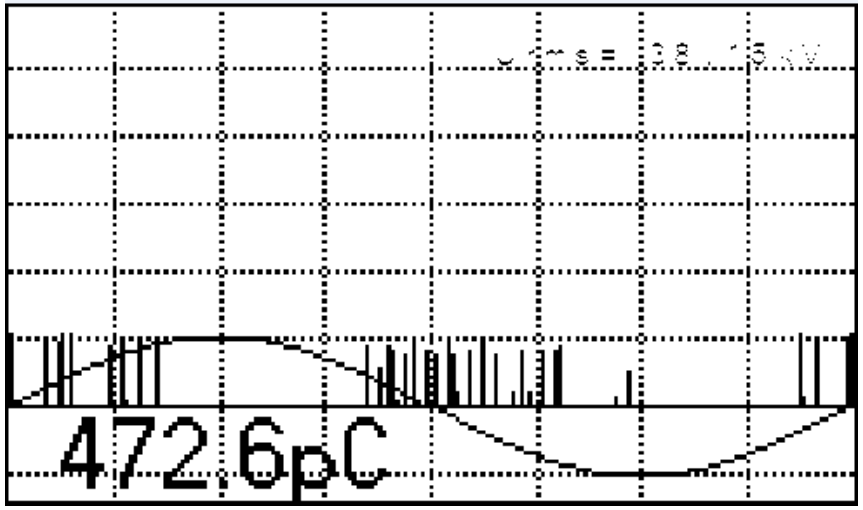 472.6pC

40	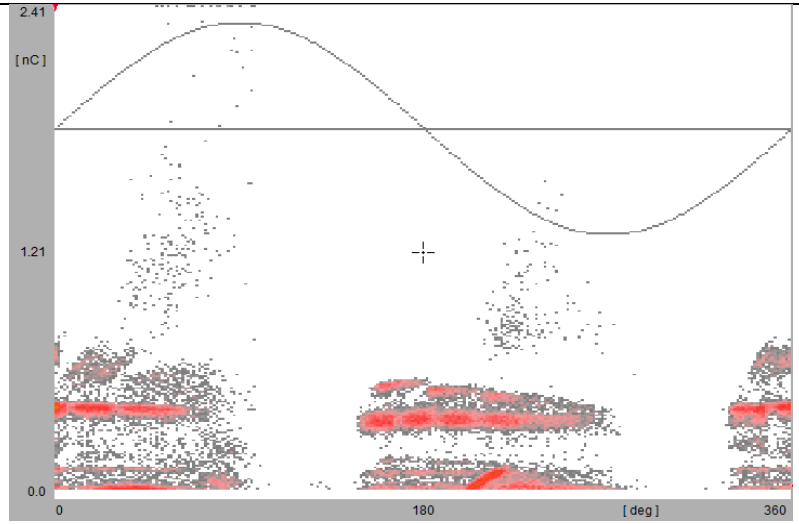	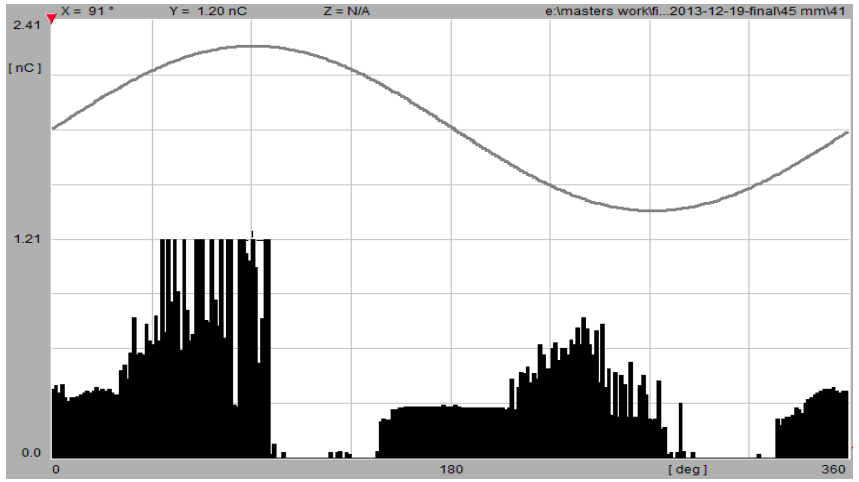
43	No Record	No Record
46	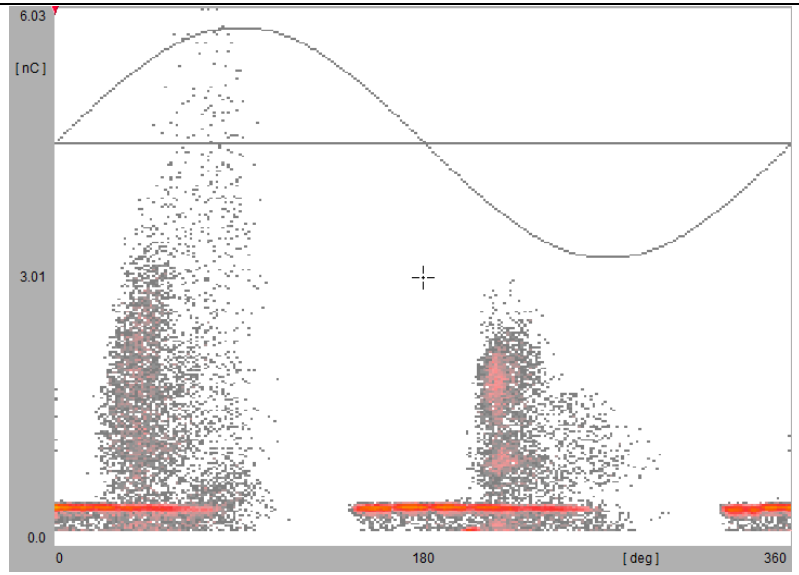	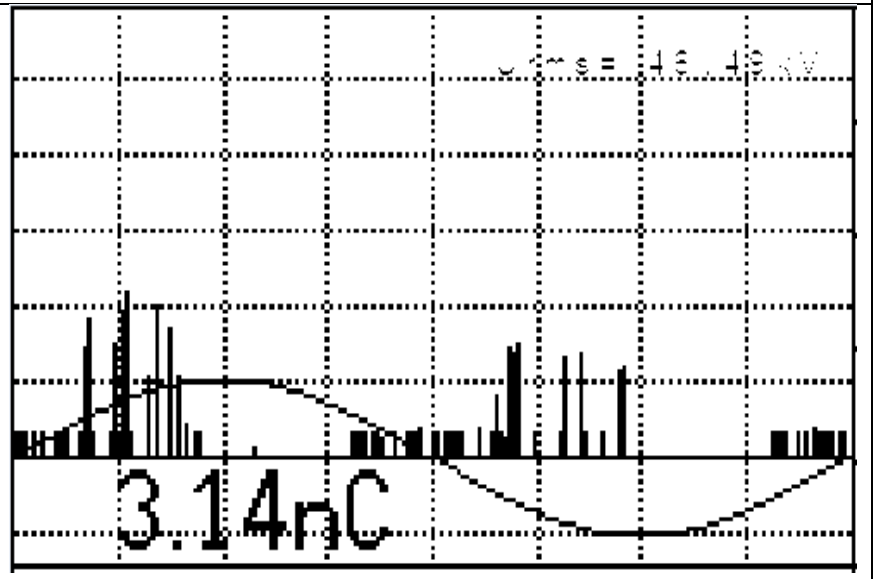

50	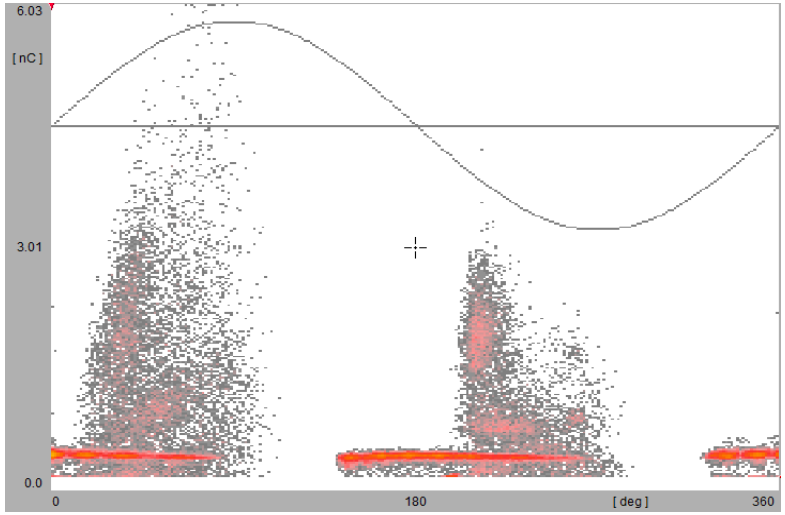	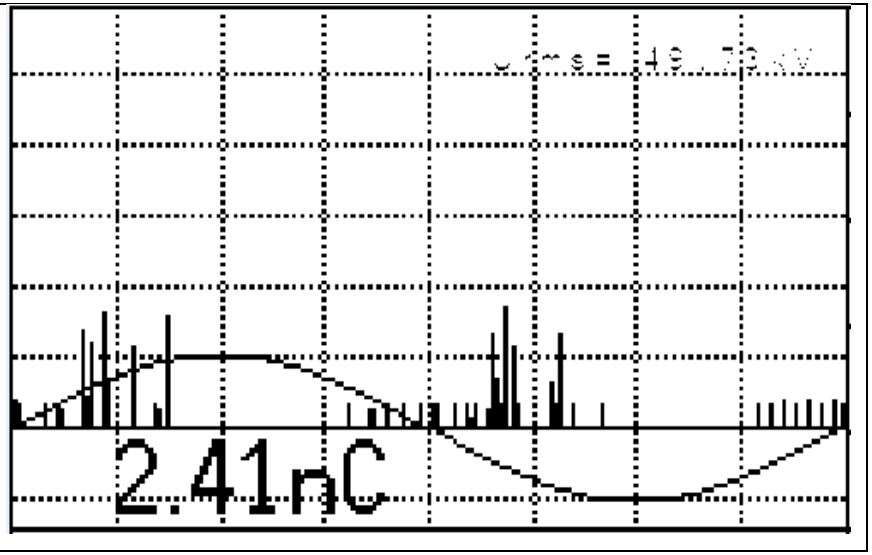

Table A 3-4: The PD measurement results for 35 mm gap distance

Supply Voltage	PRPD pattern	PD pulse superimposed on the supply sine wave
20	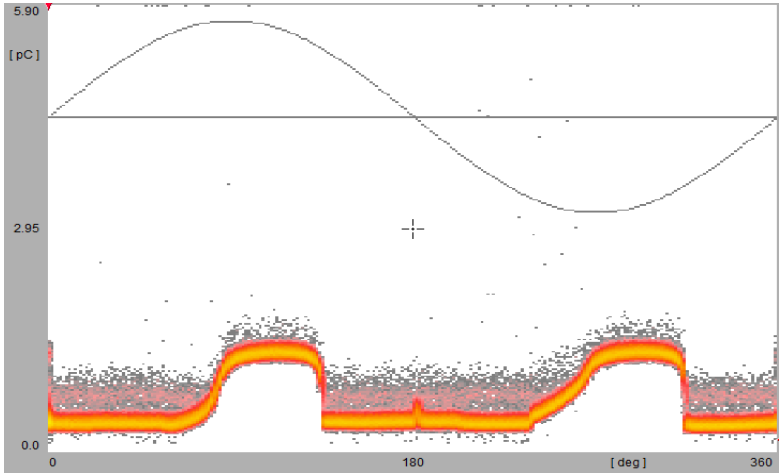	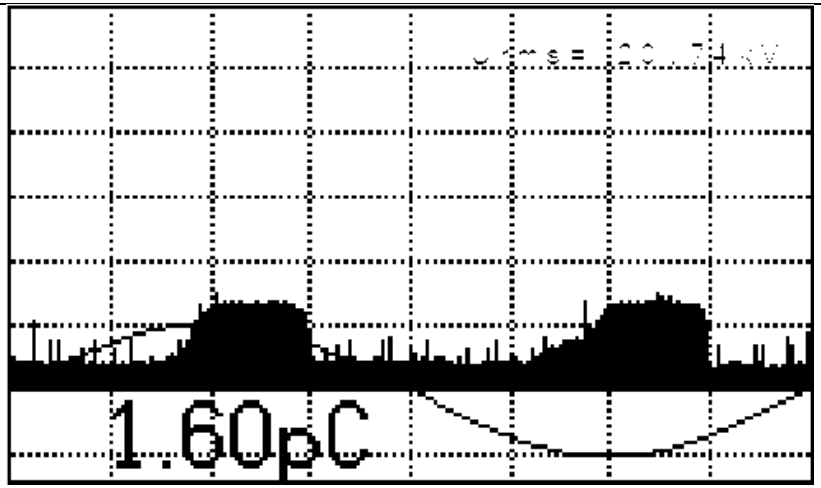
23	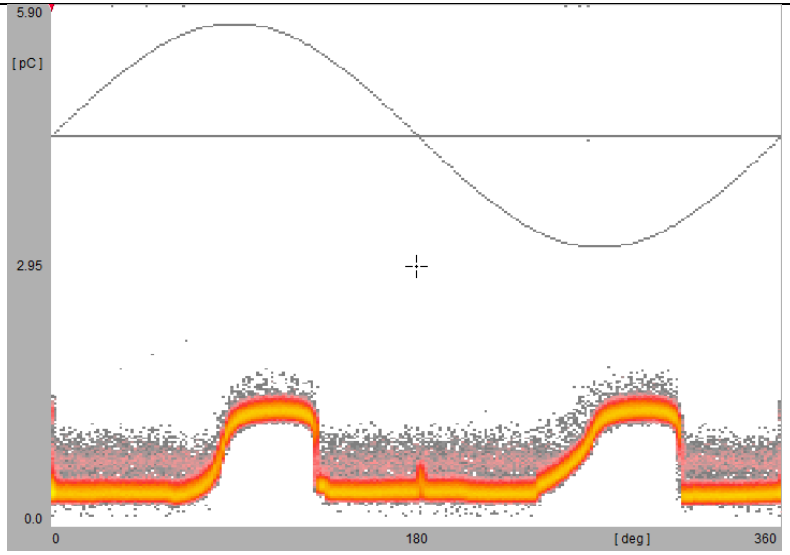	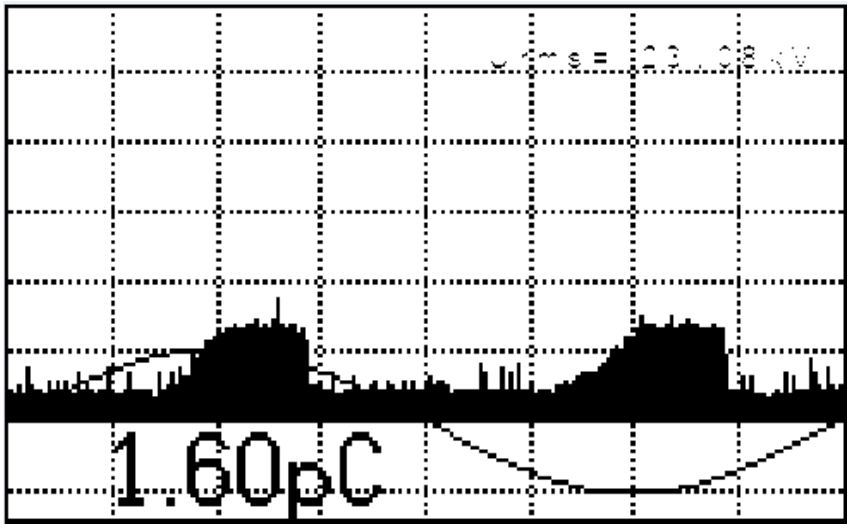

26	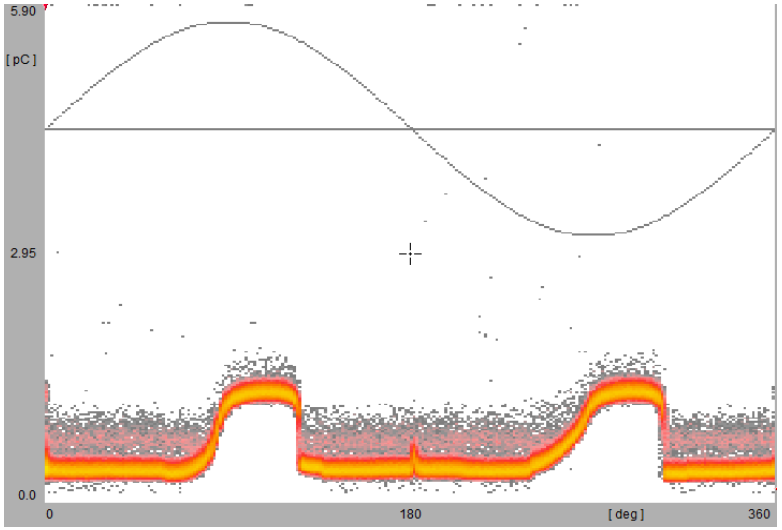 5.90 [pC] 2.95 0.0 0 180 [deg] 360	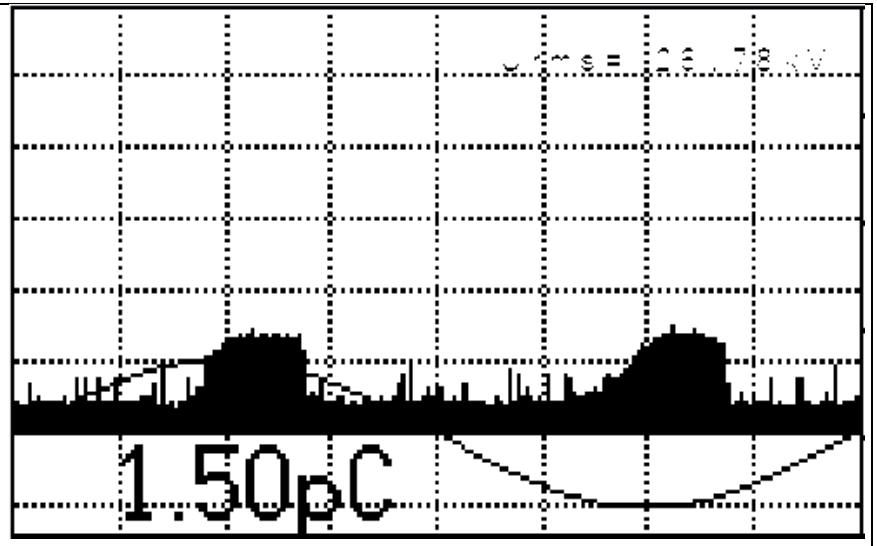 1.50pC
29	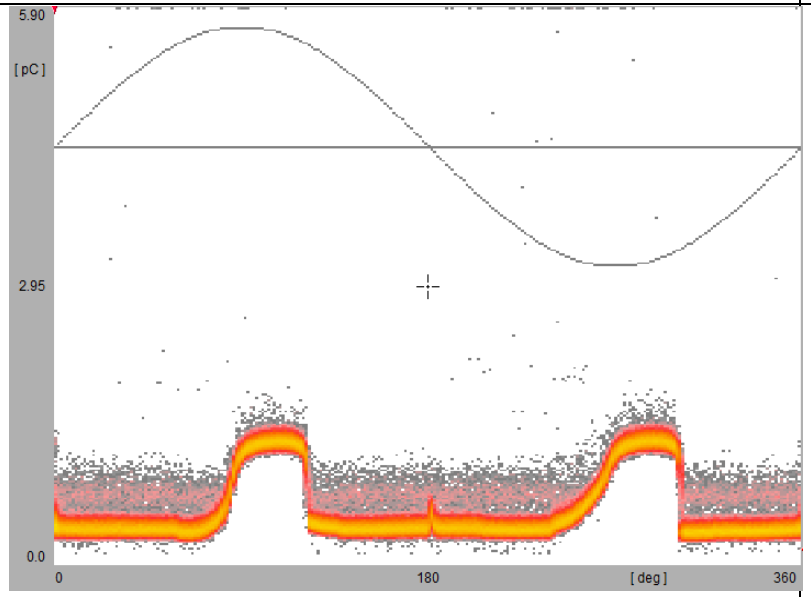 5.90 [pC] 2.95 0.0 0 180 [deg] 360	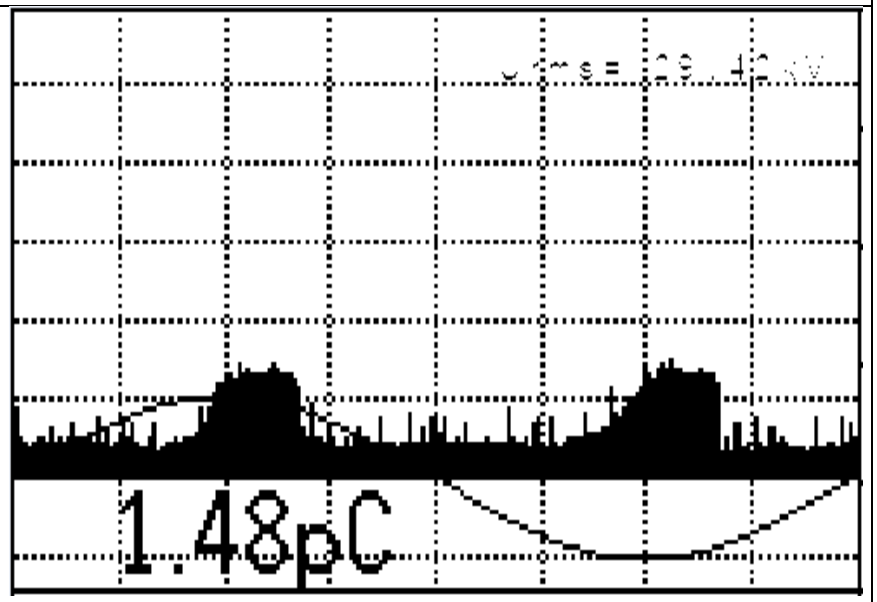 1.48pC

33	No records	No records
36	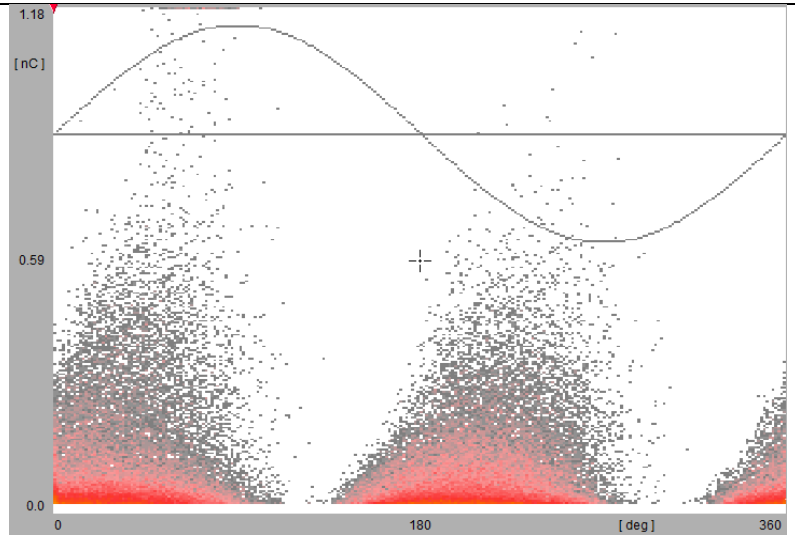	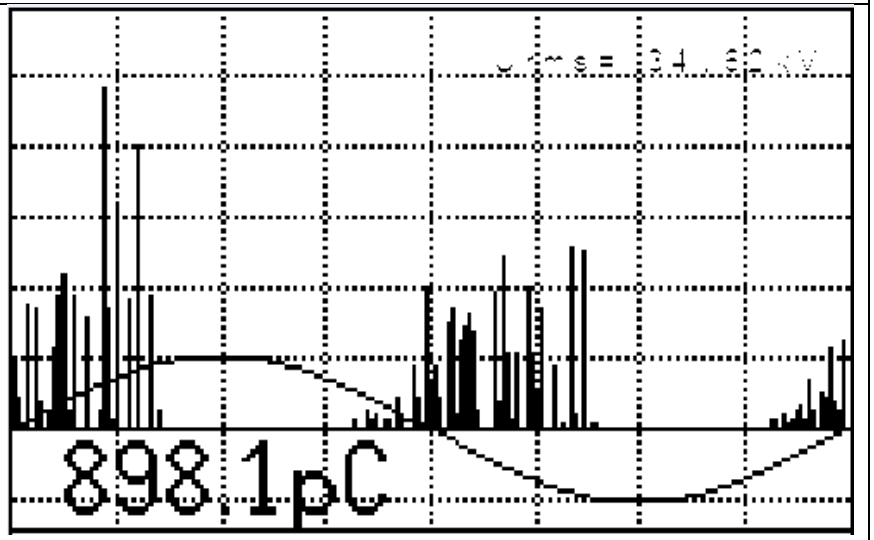
39	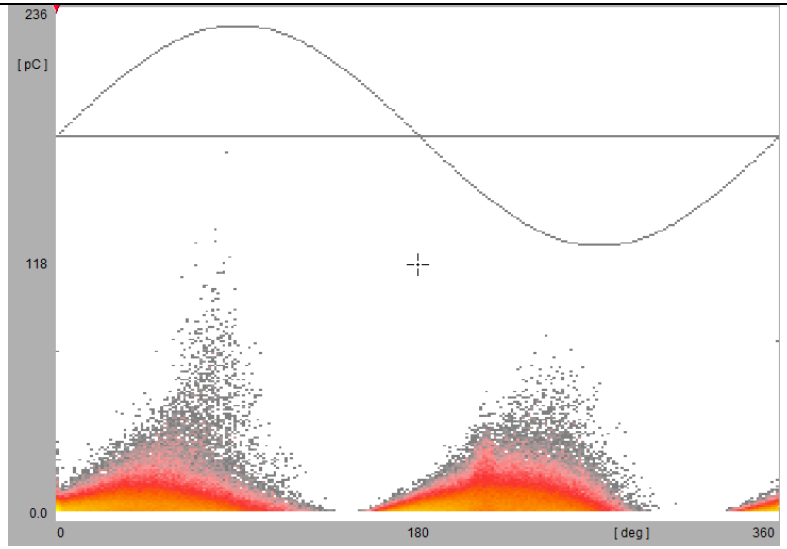	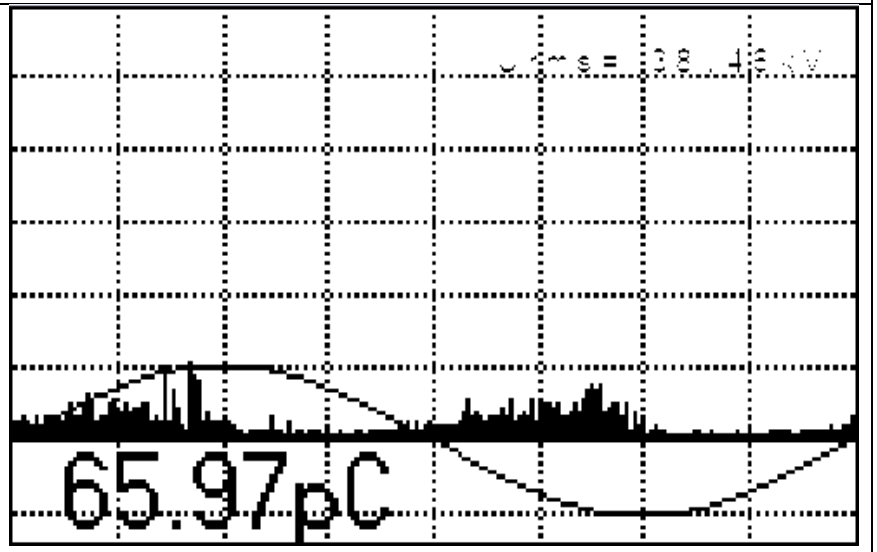

40	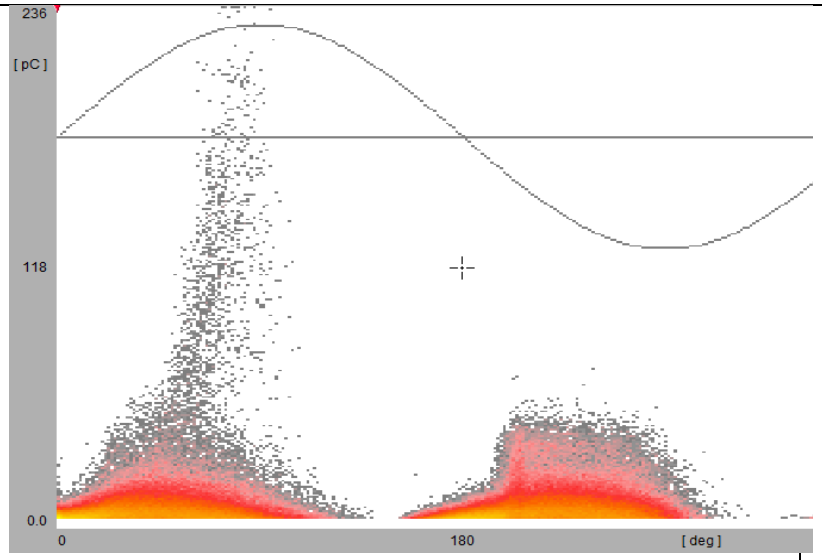 236 [pC] 118 0.0 0 180 [deg]	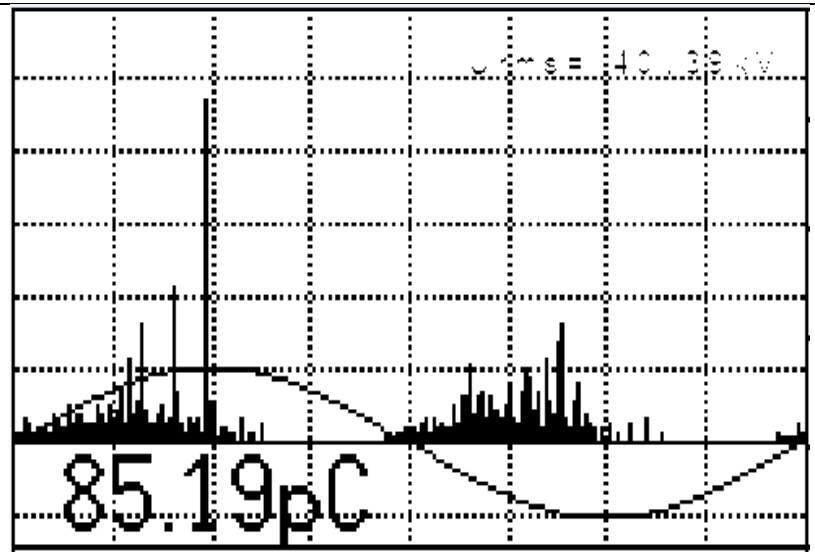 85.19pC
43	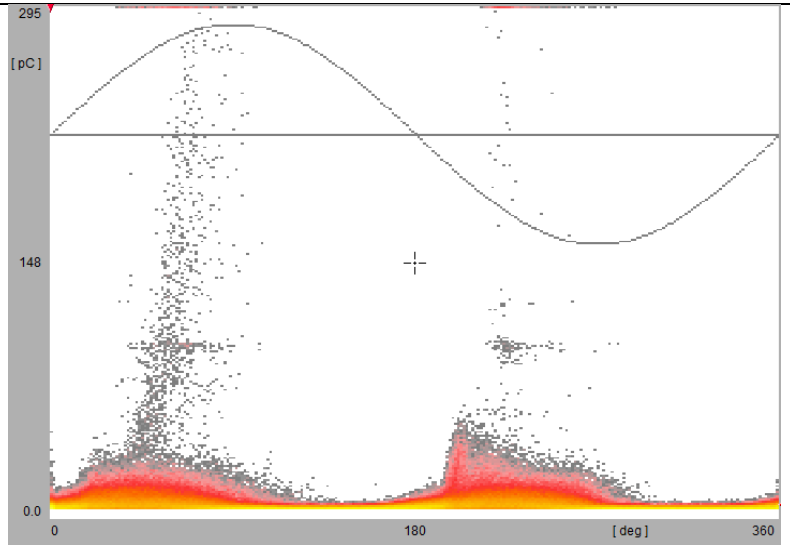 295 [pC] 148 0.0 0 180 [deg] 360	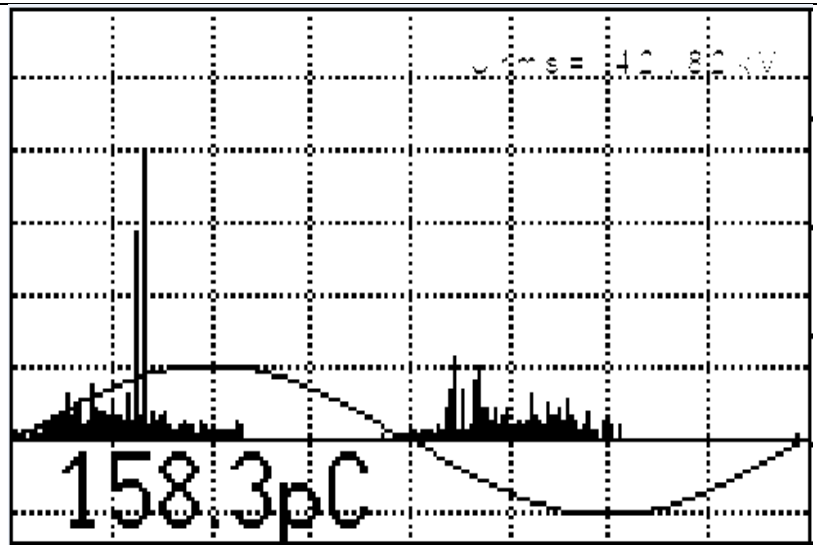 158.3pC

46	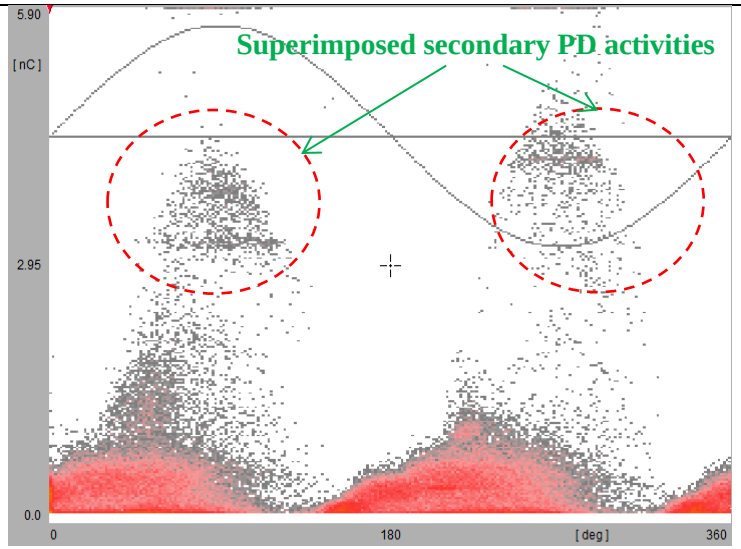 Superimposed secondary PD activities 5.90 [nC] 2.95 0.0 0 180 [deg] 360	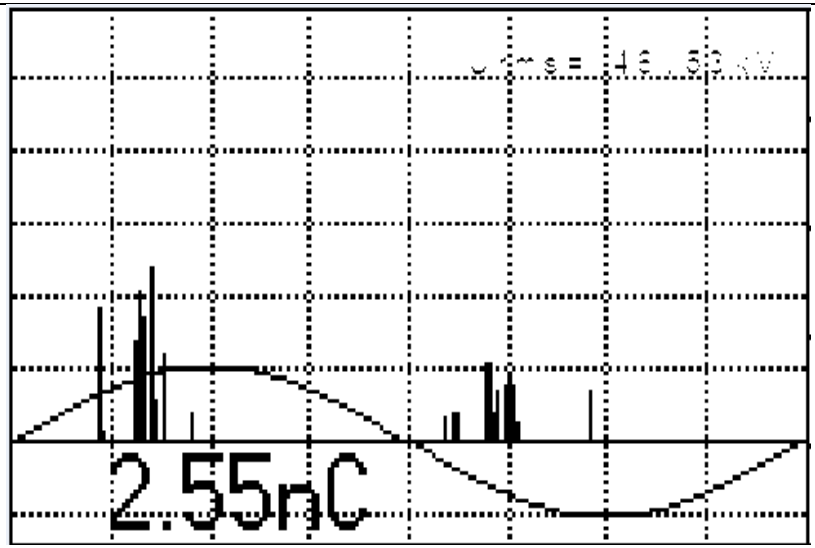 2.55nC

Table A 3-5: The PD measurement results for 25 mm gap distance

Supply Voltage	PRPD pattern	PD pulse superimposed on the supply sine wave
20	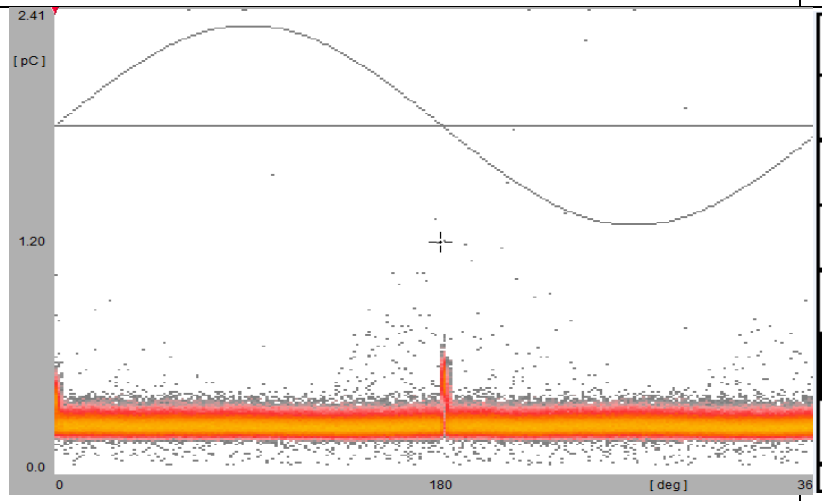	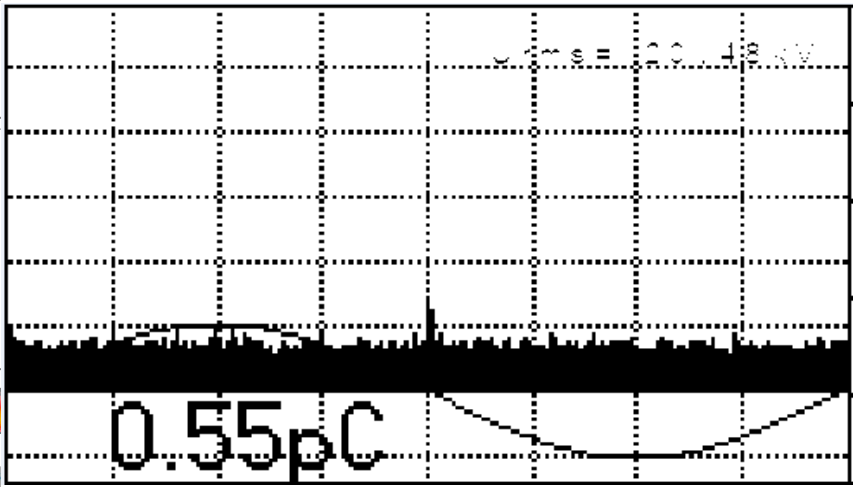
23	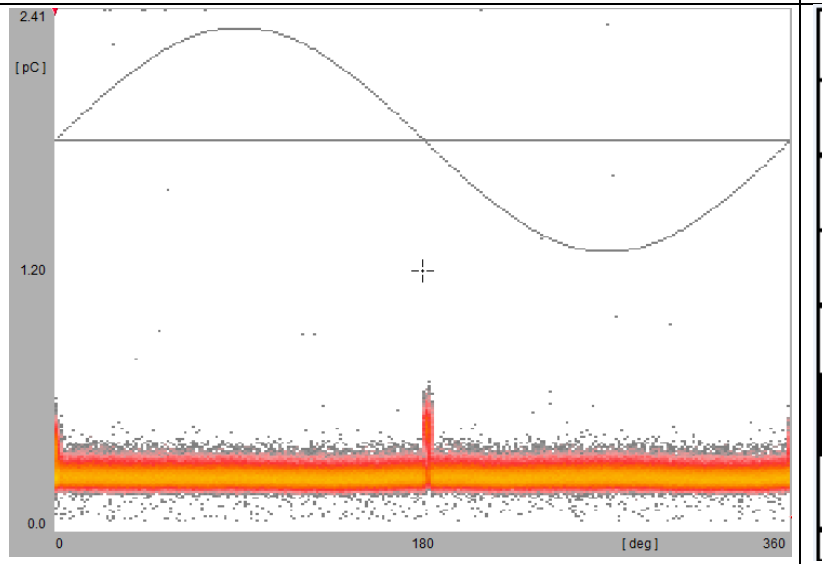	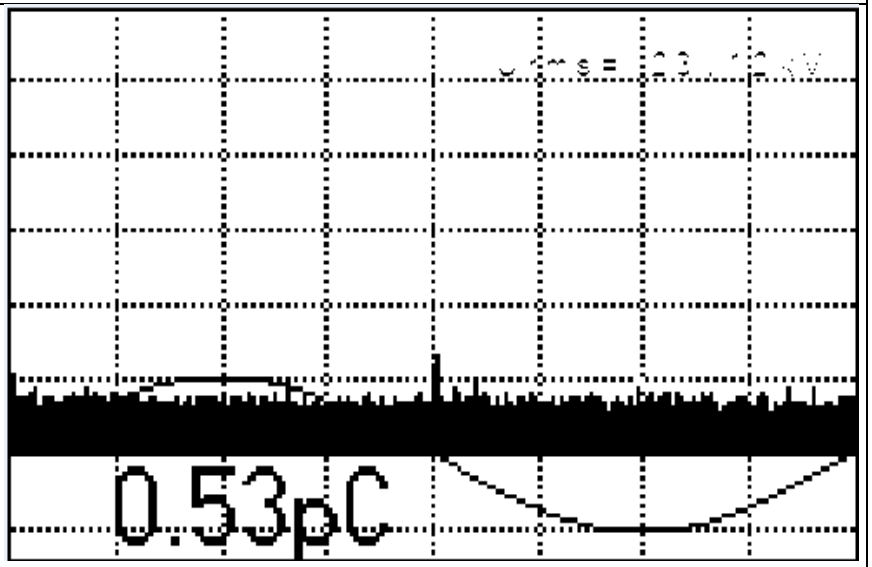

26	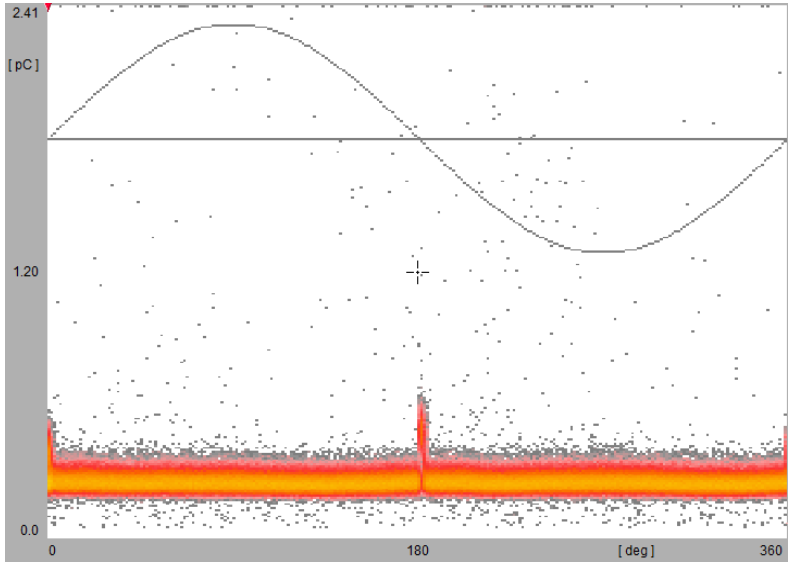 2.41 [pC] 1.20 0.0 0 180 [deg] 360	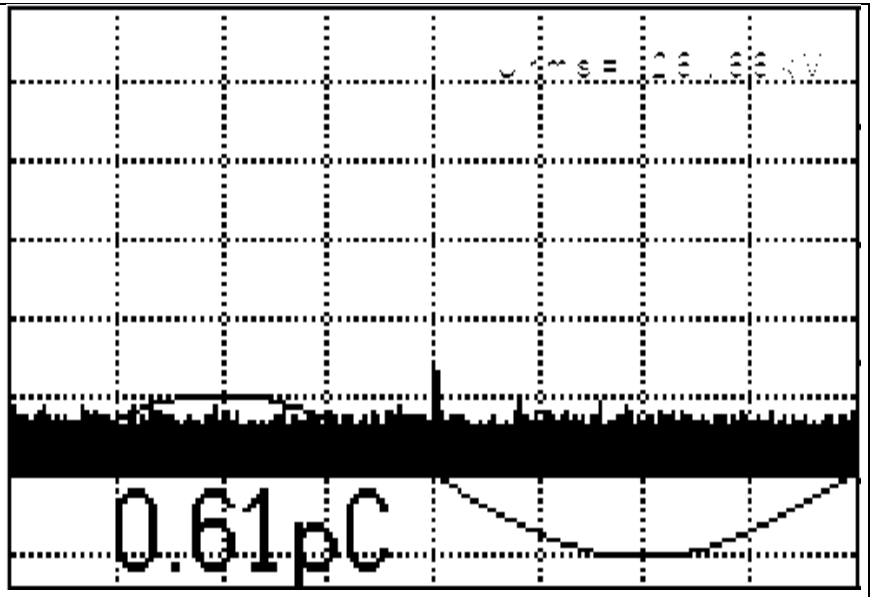 0.61pC
29	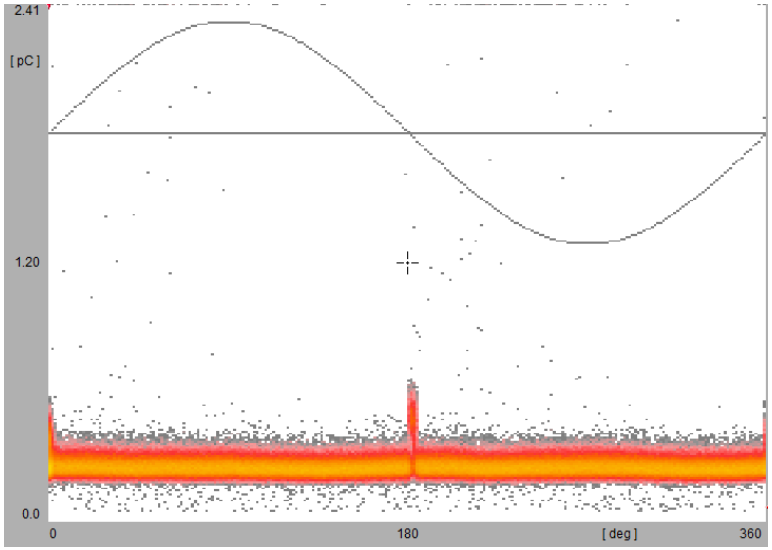 2.41 [pC] 1.20 0.0 0 180 [deg] 360	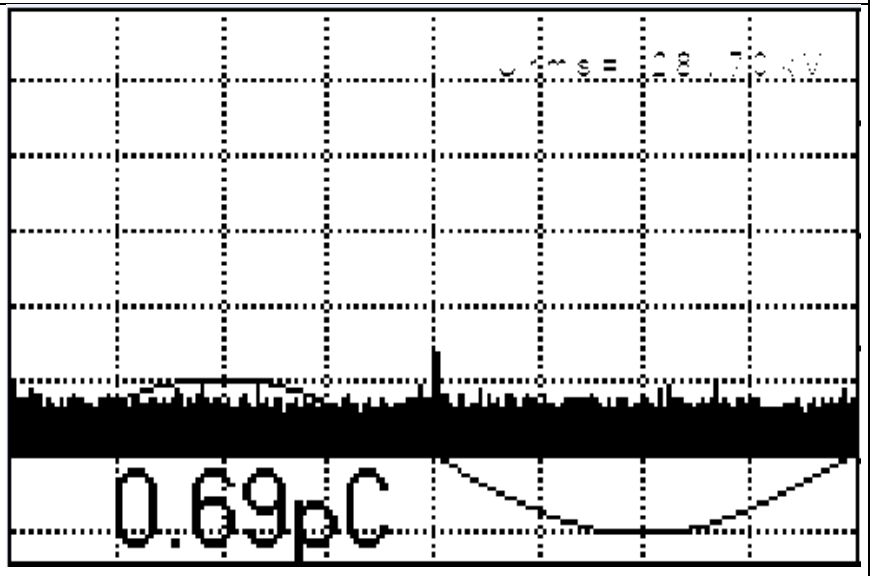 0.69pC

Table A 3-6: Gap distance setting experimental results summary

Distance (mm)	**PD inception voltage (kV)**	**Oil flashover voltage (kV)**	**Surface discharge breakdown voltage (kV)**
55	20	50	No Surface flashover observed
45	23	39	50
35	23	36	46
25	20	29	No Surface flashover observed

A.4 Lightning Impulse Waveform

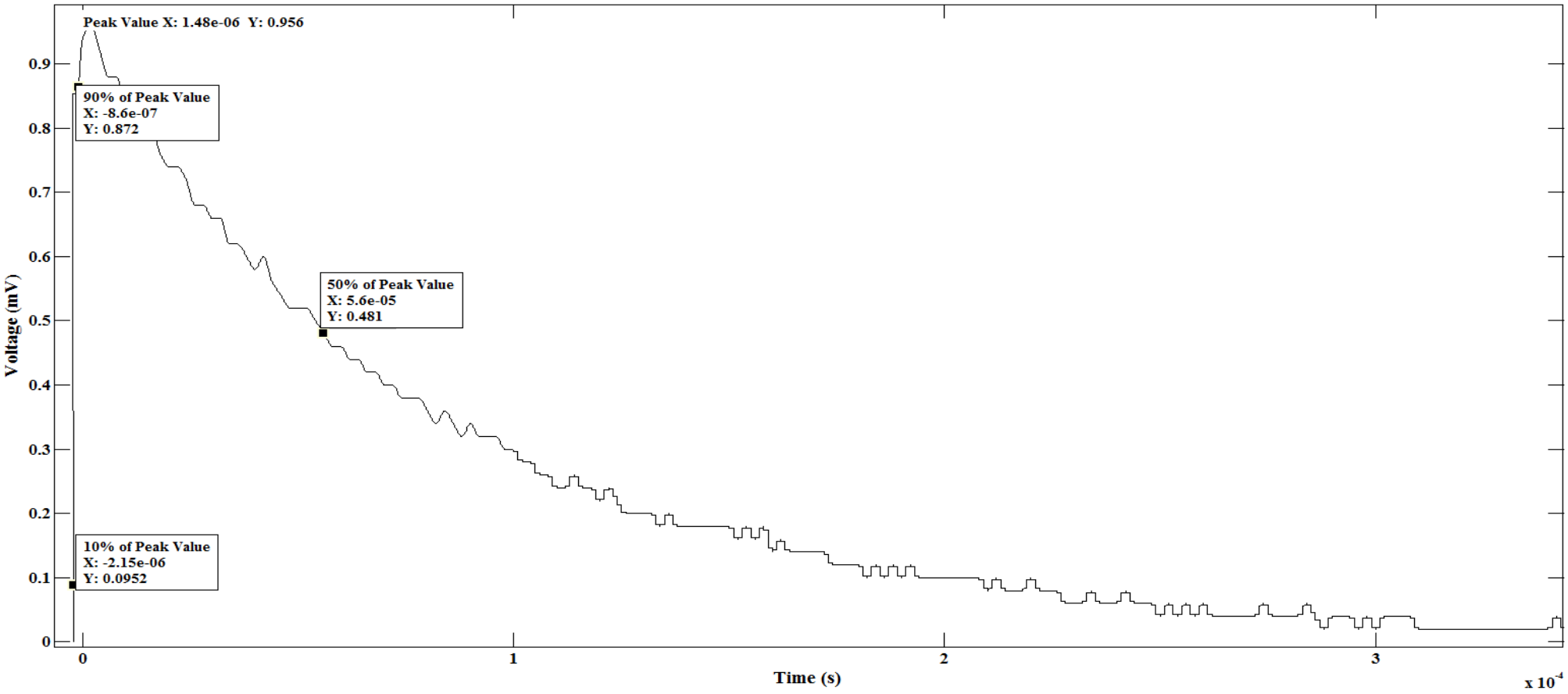

Figure A 4-1: Positive LI waveform used in the experiment

A.5 Post-processing of the breakdown voltage using Matlab®

```
%#########################################################################

function WeibullProbability (ExcelFileName)

%This function takes input data from an excel spread sheet. It uses the
%samples breakdown voltage data to perform the linear regression fit and
%calculates the Weibull statistical data. The calculated data are stored
%back into the excel spread sheet. The input ExcelFileName is passed as a
%string; 'C: \Users\mercy\Desktop\Masters MATLAB simulations\OverAll
%Weibull Calculation.xlsx'

%Read data breakdown data from excel sheet
PosNewBdVoltages = xlsread(ExcelFileName, 'Input Data', 'A3:A11');
%Read the Y and X values to perform linear regression
Y_PosNew = xlsread(ExcelFileName,'Input Data', 'E3:E11');
X_PosNew = xlsread(ExcelFileName,'Input Data', 'F3:F11');

[Alpha_PosNew,Beta_PosNew,LAlpha,UAlpha,LBeta,UBeta,Probability_FiftyPercen
t,Probability_SixtyThreePercent,CellArray,YCum,LowBound,UpperBound] = ...
linearRegression(X_PosNew,Y_PosNew,PosNewBdVoltages, 'for PD free Positive
LI' );

%Write the data in excel sheet
xlswrite(ExcelFileName,...
    [Alpha_PosNew,
Beta_PosNew,LAlpha,UAlpha,LBeta,UBeta,Probability_FiftyPercent,Probability_
SixtyThreePercent],'Output Data', 'B2:I2');

%Write the statistical parameters in excel sheet
xlswrite(ExcelFileName,CellArray,'Output Data', 'J2:P2');

%Write the cumulative probability in excel sheet
xlswrite(ExcelFileName,YCum,'Un-Aged Pos', 'B2:B10');

%Write the 95% lower bound data in excel sheet
xlswrite(ExcelFileName,LowBound,'Un-Aged Pos', 'C2:C10');

%Write the 95% lower bound data in excel sheet
xlswrite(ExcelFileName,UpperBound,'Un-Aged Pos', 'D2:D10');

%Write the 95% lower bound data in excel sheet
xlswrite(ExcelFileName,PosNewBdVoltages,'Un-Aged Pos', 'A2:A10');

%%

%Read data breakdown data from excel sheet
NegNewBdVoltages = xlsread(ExcelFileName, 'Input Data', 'A17:A25');
%Read the Y and X values to perform linear regression
Y_NegNew = xlsread(ExcelFileName,'Input Data', 'E17:E25');
X_NegNew = xlsread(ExcelFileName,'Input Data', 'F17:F25');

[Alpha_NegNew,
Beta_NegNew,LAlpha,UAlpha,LBeta,UBeta,Probability_FiftyPercent,Probability_
SixtyThreePercent,...
    CellArray,YCum,LowBound,UpperBound] = linearRegression
(X_NegNew,Y_NegNew,NegNewBdVoltages, 'for PD free Negetive LI');
```

```
%Write the data in excel sheet
xlswrite(ExcelFileName,...
    [Alpha_NegNew,
Beta_NegNew,LAlpha,UAlpha,LBeta,UBeta,Probability_FiftyPercent,Probability_
SixtyThreePercent],'Output Data', 'B3:I3');

%Write the statistical parameters in excel sheet
xlswrite(ExcelFileName,CellArray,'Output Data', 'J3:P3');

%Write the cumulative probability in excel sheet
xlswrite(ExcelFileName,YCum,'Un-Aged Neg', 'B2:B10');

%Write the 95% lower bound data in excel sheet
xlswrite(ExcelFileName,LowBound,'Un-Aged Neg', 'C2:C10');

%Write the 95% lower bound data in excel sheet
xlswrite(ExcelFileName,UpperBound,'Un-Aged Neg', 'D2:D10');

%Write the 95% lower bound data in excel sheet
xlswrite(ExcelFileName,PosNewBdVoltages,'Un-Aged Neg', 'A2:A10');

%%

%Read data breakdown data from excel sheet
ThreePosAgedBdVolt = xlsread(ExcelFileName, 'Input Data', 'A31:A36');
%Read the Y and X values to perform linear regression
Y_3HrAgedPos = xlsread(ExcelFileName,'Input Data', 'E31:E36');
X_3HrAgedPos = xlsread(ExcelFileName,'Input Data', 'F31:F36');

[Alpha_3HrAgedPos,
Beta_3HrAgedPos,LAlpha,UAlpha,LBeta,UBeta,Probability_FiftyPercent,Probabil
ity_SixtyThreePercent,...
    CellArray,YCum,LowBound,UpperBound] = linearRegression
(X_3HrAgedPos,Y_3HrAgedPos,ThreePosAgedBdVolt, 'for 3Hr PD Exposed Positive
LI');

%Write the data in excel sheet
xlswrite(ExcelFileName,...
   [Alpha_3HrAgedPos,
Beta_3HrAgedPos,LAlpha,UAlpha,LBeta,UBeta,Probability_FiftyPercent,Probabil
ity_SixtyThreePercent],'Output Data', 'B4:I4');

%Write the statistical parameters in excel sheet
xlswrite(ExcelFileName,CellArray,'Output Data', 'J4:P4');

%Write the cumulative probability in excel sheet
xlswrite(ExcelFileName,YCum,'Aged Pos 3hrs', 'B2:B7');

%Write the 95% lower bound data in excel sheet
xlswrite(ExcelFileName,LowBound,'Aged Pos 3hrs', 'C2:C7');

%Write the 95% lower bound data in excel sheet
xlswrite(ExcelFileName,UpperBound,'Aged Pos 3hrs', 'D2:D7');

%Write the 95% lower bound data in excel sheet
xlswrite(ExcelFileName,PosNewBdVoltages,'Aged Pos 3hrs', 'A2:A7');
```

```
%%

%Read data breakdown data from excel sheet
ThreeNegAgedBdVolt = xlsread(ExcelFileName, 'Input Data', 'A42:A47');
%Read the Y and X values to perform linear regression
Y_3HrAgedNeg = xlsread(ExcelFileName, 'E42:E47');
X_3HrAgedNeg = xlsread(ExcelFileName, 'F42:F47');

[Alpha_3HrAgedNeg,
Beta_3HrAgedNeg,LAlpha,UAlpha,LBeta,UBeta,Probability_FiftyPercent,Probabil
ity_SixtyThreePercent,...
    CellArray,YCum,LowBound,UpperBound] =
linearRegression(X_3HrAgedNeg,Y_3HrAgedNeg,ThreeNegAgedBdVolt, 'for 3Hr PD
Exposed Negetive LI');

%Write the data in excel sheet
xlswrite(ExcelFileName,...
   [Alpha_3HrAgedNeg,
Beta_3HrAgedNeg,LAlpha,UAlpha,LBeta,UBeta,Probability_FiftyPercent,Probabil
ity_SixtyThreePercent],'Output Data', 'B5:I5');

%Write the statistical parameters in excel sheet
xlswrite(ExcelFileName,CellArray,'Output Data', 'J5:P5');

%Write the cumulative probability in excel sheet
xlswrite(ExcelFileName,YCum,'Aged Neg 3hrs', 'B2:B7');

%Write the 95% lower bound data in excel sheet
xlswrite(ExcelFileName,LowBound,'Aged Neg 3hrs','C2:C7');

%Write the 95% lower bound data in excel sheet
xlswrite(ExcelFileName,UpperBound,'Aged Neg 3hrs','D2:D7');

%Write the 95% lower bound data in excel sheet
xlswrite(ExcelFileName,PosNewBdVoltages,'Aged Neg 3hrs','A2:A7');

%%

%Read data breakdown data from excel sheet
SevenPosAgedBdVolt = xlsread(ExcelFileName, 'Input Data', 'A53:A58');
%Read the Y and X values to perform linear regression
Y_7HrAgedPos = xlsread(ExcelFileName,'Input Data', 'E53:E58');
X_7HrAgedPos = xlsread(ExcelFileName,'Input Data', 'F53:F58');

[Alpha_7HrAgedPos,
Beta_7HrAgedPos,LAlpha,UAlpha,LBeta,UBeta,Probability_FiftyPercent,Probabil
ity_SixtyThreePercent,...
    CellArray,YCum,LowBound,UpperBound] = linearRegression
(X_7HrAgedPos,Y_7HrAgedPos,SevenPosAgedBdVolt, 'for 7Hr PD Exposed Positive
LI');

%Write the data in excel sheet
xlswrite(ExcelFileName,...
   [Alpha_7HrAgedPos,
Beta_7HrAgedPos,LAlpha,UAlpha,LBeta,UBeta,Probability_FiftyPercent,Probabil
ity_SixtyThreePercent],'Output Data', 'B6:I6');

%Write the statistical parameters in excel sheet
xlswrite(ExcelFileName,CellArray,'Output Data', 'J6:P6');
```

```
%Write the cumulative probability in excel sheet
xlswrite(ExcelFileName,YCum,'Aged Pos 7hrs', 'B2:B7');

%Write the 95% lower bound data in excel sheet
xlswrite(ExcelFileName,LowBound,'Aged Pos 7hrs','C2:C7');

%Write the 95% lower bound data in excel sheet
xlswrite(ExcelFileName,UpperBound,'Aged Pos 7hrs','D2:D7');

%Write the 95% lower bound data in excel sheet
xlswrite(ExcelFileName,PosNewBdVoltages,'Aged Pos 7hrs','A2:A7');

%%

%Read data breakdown data from excel sheet
SevenNegAgedBdVolt = xlsread(ExcelFileName, 'Input Data', 'A64:A69');
%Read the Y and X values to perform linear regression
Y_7HrAgedNeg = xlsread(ExcelFileName,'Input Data', 'E64:E69');
X_7HrAgedNeg = xlsread(ExcelFileName,'Input Data', 'F64:F69');

[Alpha_7HrAgedNeg,
Beta_7HrAgedNeg,LAlpha,UAlpha,LBeta,UBeta,Probability_FiftyPercent,Probabil
ity_SixtyThreePercent,...
    CellArray,YCum,LowBound,UpperBound] =
linearRegression(X_7HrAgedNeg,Y_7HrAgedNeg,SevenNegAgedBdVolt, 'for 7Hr PD
Exposed Negetive LI');

%Write the data in excel sheet
xlswrite(ExcelFileName,...
   [Alpha_7HrAgedNeg,
Beta_7HrAgedNeg,LAlpha,UAlpha,LBeta,UBeta,Probability_FiftyPercent,Probabil
ity_SixtyThreePercent],'Output Data', 'B7:I7');

%Write the statistical parameters in excel sheet
xlswrite(ExcelFileName,CellArray,'Output Data', 'J7:P7');

%Write the cumulative probability in excel sheet
xlswrite(ExcelFileName,YCum,'Aged Neg 7hrs', 'B2:B7');

%Write the 95% lower bound data in excel sheet
xlswrite(ExcelFileName,LowBound,'Aged Neg 7hrs','C2:C7');

%Write the 95% lower bound data in excel sheet
xlswrite(ExcelFileName,UpperBound,'Aged Neg 7hrs','D2:D7');

%Write the 95% lower bound data in excel sheet
xlswrite(ExcelFileName,PosNewBdVoltages,'Aged Neg 7hrs','A2:A7');

end

function [Alpha,
Beta,LAlpha,UAlpha,LBeta,UBeta,Probability_FiftyPercent,Probability_SixtyTh
reePercent,CellArray,YCum,LowBound,UpperBound]...
    = linearRegression (X,Y,SampleData,FigureTitle)

%apply linear regression on the data to calculate the two parameter of the
%straightline
```

```
Model = LinearModel.fit(X,Y);

%calculate the predicted linear y values using the two straight line
%parameters

[PredictedY] = predict(Model,X);

%Plot the predicted straight line on the same figure as the actual
%calculated y values of the Breakdown data

h = plot (X,PredictedY);
hold all
plot(X,Y,'*');


title(['Weibull Distribution Best Fit ' FigureTitle]);
xlabel('ln[Breakdown Voltages (kV)]');
ylabel('ln[-ln(1-median rank)]');

saveas(h,FigureTitle,'fig');

close all hidden
%Calculate the alpha and beta values, by getting the model coefficients
SampleDataParameters = wblfit(SampleData);

%Assign the parameters
Alpha = SampleDataParameters (1);
Beta = SampleDataParameters (2);

%Calculate the cumulative distribution function
YCum = wblcdf (SampleData,Alpha,Beta);

%Weibull log-likelihood
[~,pcov] = wbllike([Alpha,Beta],SampleData);

%calculating the x-data for the cdf for the lower and upper bound
[~,LowBound,UpperBound] = wblinv(YCum,Alpha,Beta,pcov);

%Sortun the lower and the Upper bound x-data
LowBound = sort(LowBound);
UpperBound = sort(UpperBound);
%Calculate the upper and lower parameters
LowBoundPara = wblfit(LowBound);
LAlpha = LowBoundPara (1);
LBeta = LowBoundPara (2);
UpperBoundPara = wblfit(UpperBound);
UAlpha = UpperBoundPara (1);
UBeta = UpperBoundPara (2);

%ploting the Sample data
Fig = plot (SampleData,YCum,'*');
hold all

%fit a trend line on the sample data
FitSample = fit(SampleData,YCum,'poly1');
%Plot the trendline
plot(FitSample,SampleData,YCum);
hold all
```

```
%Plot the lower and upper bound
plot (LowBound,YCum,'--',UpperBound,YCum,':');

title(['Weibull Cumulative Probability Distribution' FigureTitle]);
xlabel('Breakdown Voltages (kV)');
ylabel('Cumulative Probability(%)');
 saveas(Fig,[FigureTitle 'CumulativeFig'],'fig');
close all hidden

%Reliability Calculation
Probability_FiftyPercent = reliabilityCalculator(0.5,Beta,Alpha);
Probability_SixtyThreePercent = reliabilityCalculator(0.368,Beta,Alpha);

%calculating statistical data
[CellArray] =  StatisticalData(Beta,Alpha,SampleData);

end
function[CellArray] =  StatisticalData(Beta,Alpha,SampleData)

%%
%Calculate the statistical data
pd = wblpdf(SampleData,Alpha,Beta);
%Mean
[Mean,~] = wblstat(Alpha,Beta);

%Variance
[~,Variance] = wblstat(Alpha,Beta);

%Median
Median = Alpha*((log(2))^(1/Beta));

%Mode
Mode = Alpha*(1-(1/Beta))^(1/Beta);

%STD Deviation
STD_Deviation = sqrt(Variance);

%Skewness
Skew = skewness(pd);

%Kurtosis
kurtoses = kurtosis(pd);
% kurtoses = kurtosis(SampleData);
CellArray = {Mean,Median, Mode, STD_Deviation,Variance,Skew, kurtoses};

end

function [CycleValue] = reliabilityCalculator(probabilityValue,Beta,Alpha)
%passes in this function, the probability value in per units and the two
%straight line parameters. The output is the value at that probability
%percentage.
CycleValue = Alpha* (-log(probabilityValue))^(1/Beta);

end
%##########################################################################
```

Table A 5-1: Un-aged positive LI breakdown voltage statistical input data

Breakdown Voltage	**Rank**	**Median Ranks**	**1/(1-median rank)**	**ln(ln(1/(1-median rank))**	**ln(Breakdown Voltage)**
155	1	0.074468085	1.08045977	-2.558940818	5.043425117
165	2	0.180851064	1.220779221	-1.611994375	5.105945474
165	3	0.287234043	1.402985075	-1.082929422	5.105945474
168	4	0.393617021	1.649122807	-0.69266027	5.123963979
171	5	0.5	2	-0.366512921	5.141663557
175	6	0.606382979	2.540540541	-0.070018179	5.164785974
178	7	0.712765957	3.481481481	0.221107814	5.18178355
181	8	0.819148936	5.529411765	0.536540994	5.198497031
185	9	0.925531915	13.42857143	0.954505028	5.220355825

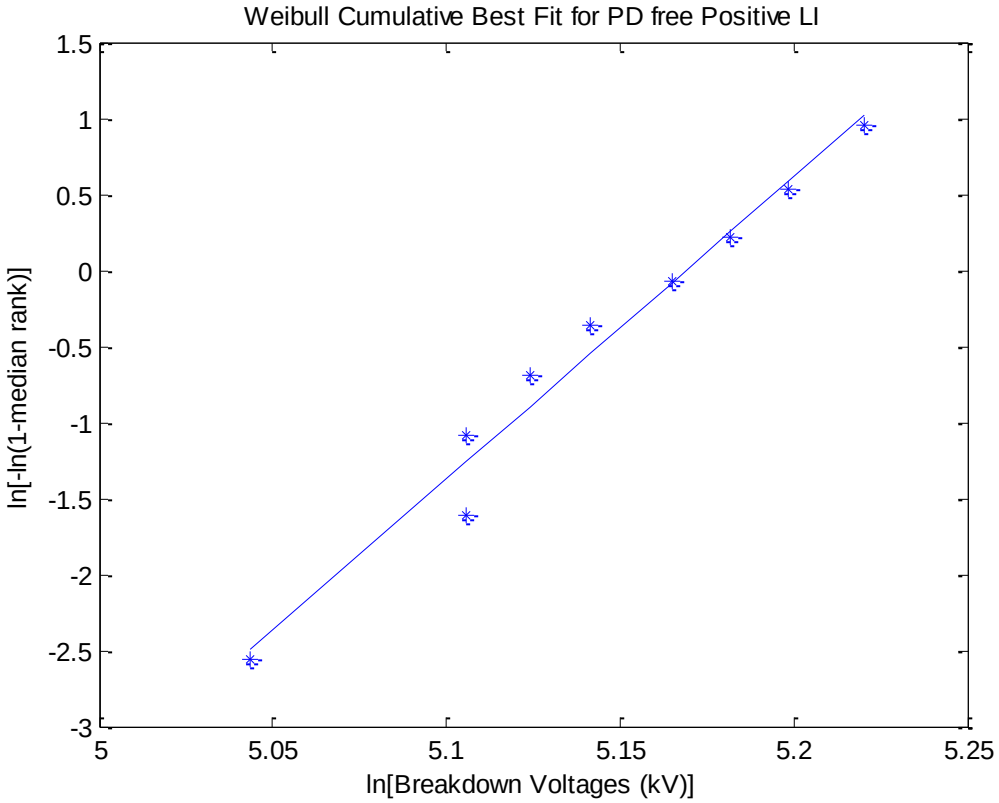

Table A 5-2: Un-aged negative LI breakdown voltage statistical input data

Breakdown Voltage	**Rank**	**Median Ranks**	**1/(1-median rank)**	**ln(ln(1/(1-median rank))**	**ln(Breakdown Voltage)**
175	1	0.074468085	1.08045977	-2.558940818	5.164785974
178	2	0.180851064	1.220779221	-1.611994375	5.18178355
185	3	0.287234043	1.402985075	-1.082929422	5.220355825
205	4	0.393617021	1.649122807	-0.69266027	5.323009979
212	5	0.5	2	-0.366512921	5.356586275
212	6	0.606382979	2.540540541	-0.070018179	5.356586275
215	7	0.712765957	3.481481481	0.221107814	5.370638028
225	8	0.819148936	5.529411765	0.536540994	5.416100402
228	9	0.925531915	13.42857143	0.954505028	5.429345629

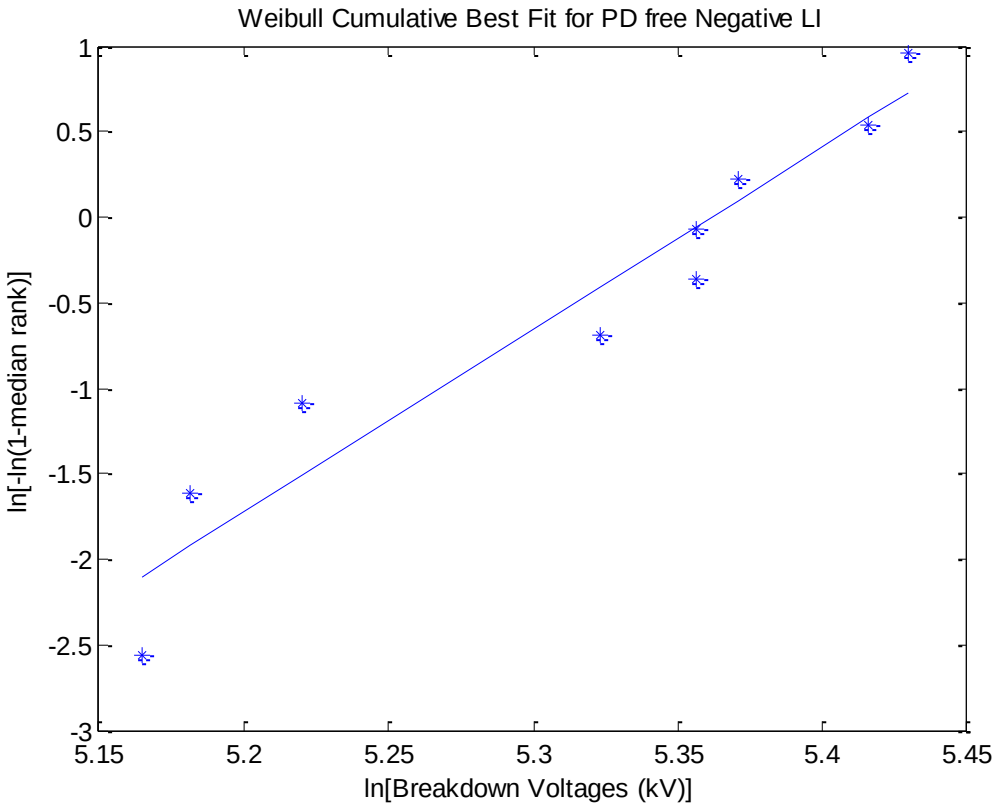

Table A 5-3: 3 hours aged positive LI breakdown voltage statistical input data

Breakdown voltage	**Rank**	**Median Ranks**	**1/(1-median rank)**	**ln(ln(1/(1-median rank))**	**ln(Breakdown Voltage)**
128	1	0.109375	1.122807018	-2.155616006	4.852030264
157	2	0.265625	1.361702128	-1.175270415	5.056245805
168	3	0.421875	1.72972973	-0.601543551	5.123963979
168	4	0.578125	2.37037037	-0.147287035	5.123963979
181	5	0.734375	3.764705882	0.281917795	5.198497031
208	6	0.890625	9.142857143	0.794336831	5.33753808

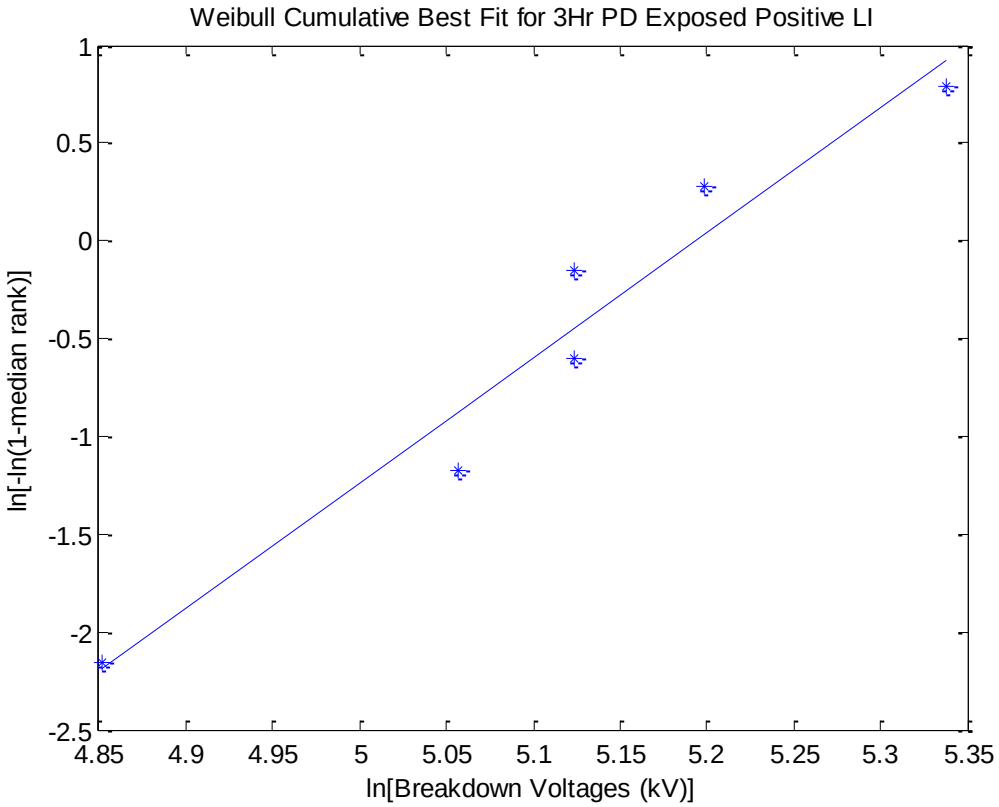

Table A 5-4: 3 hours aged negative LI breakdown voltage statistical input data

Breakdown voltage	**Rank**	**Median Ranks**	**1/(1-median rank)**	**ln(ln(1/(1-median rank))**	**ln(Breakdown Voltage)**
148	1	0.109375	1.122807018	-2.155616006	4.997212274
168	2	0.265625	1.361702128	-1.175270415	5.123963979
168	3	0.421875	1.72972973	-0.601543551	5.123963979
168	4	0.578125	2.37037037	-0.147287035	5.123963979
181	5	0.734375	3.764705882	0.281917795	5.198497031
215	6	0.890625	9.142857143	0.794336831	5.370638028

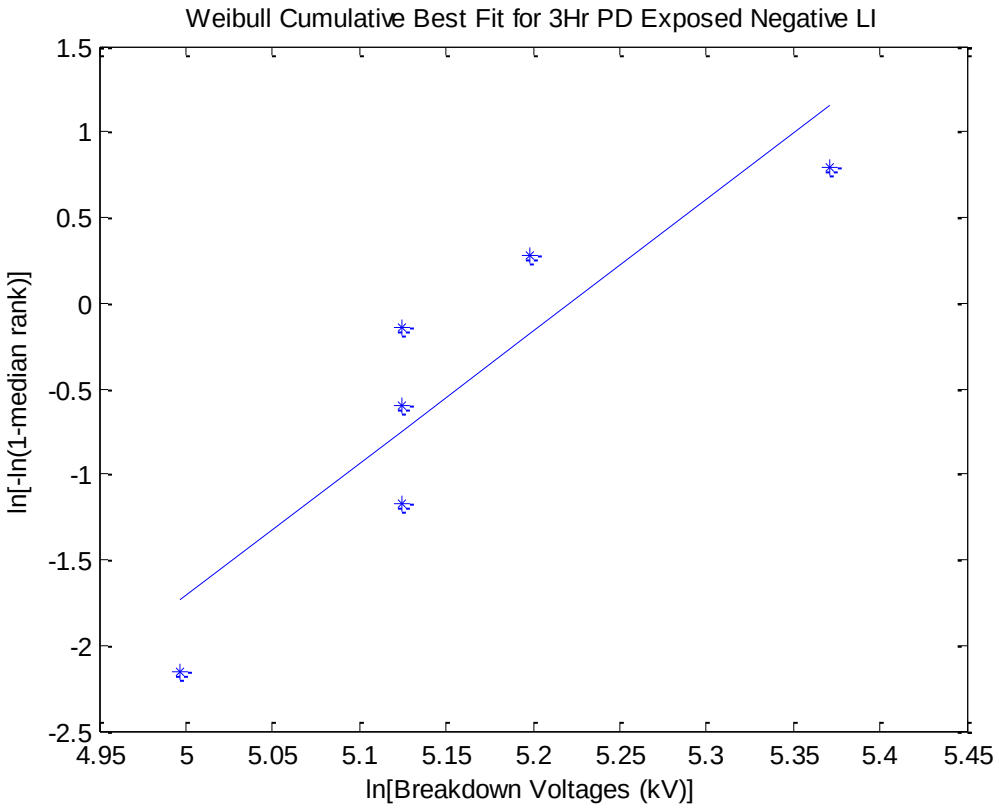

Table A 5-5: 7 hours aged positive LI breakdown voltage statistical input data

Breakdown voltage	**Rank**	**Median Ranks**	**1/(1-median rank)**	**ln(ln(1/(1-median rank))**	**ln(Breakdown Voltage)**
158	1	0.109375	1.122807018	-2.155616006	5.062595033
158	2	0.265625	1.361702128	-1.175270415	5.062595033
158	3	0.421875	1.72972973	-0.601543551	5.062595033
168	4	0.578125	2.37037037	-0.147287035	5.123963979
168	5	0.734375	3.764705882	0.281917795	5.123963979
175	6	0.890625	9.142857143	0.794336831	5.164785974

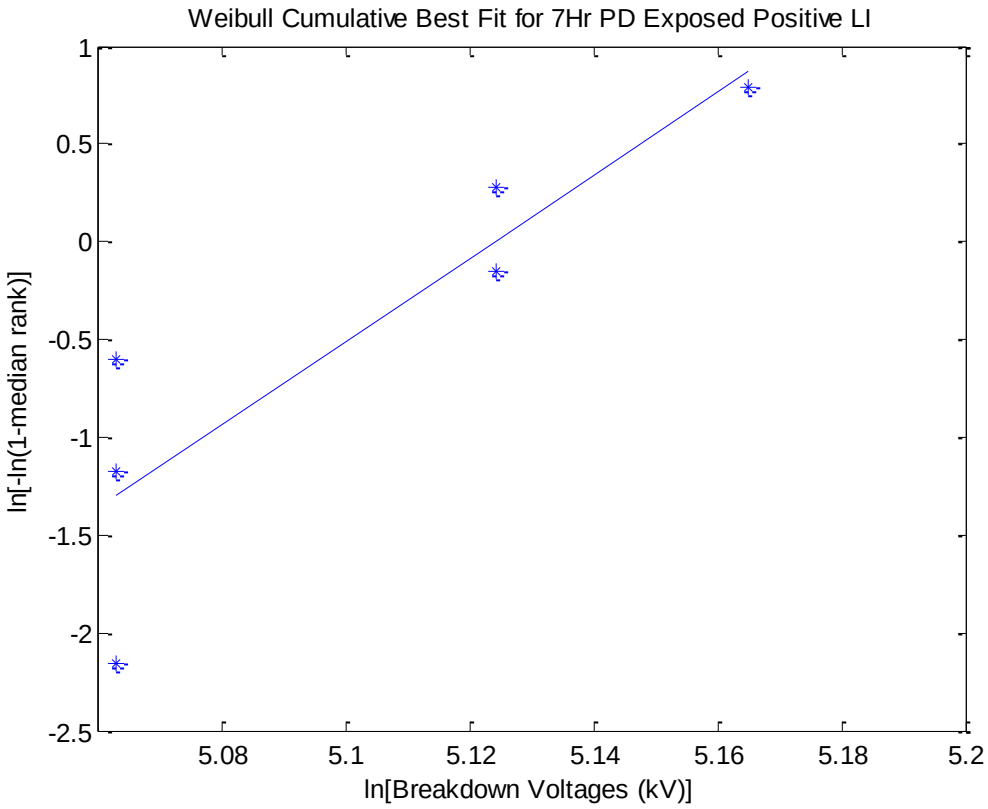

Table A 5-6: 7 hours aged negative LI breakdown voltage statistical input data

Breakdown Voltage	**Rank**	**Median Ranks**	**1/(1-median rank)**	**ln(ln(1/(1-median rank))**	**ln(Breakdown Voltage)**
151	1	0.109375	1.122807018	-2.155616006	5.017279837
155	2	0.265625	1.361702128	-1.175270415	5.043425117
165	3	0.421875	1.72972973	-0.601543551	5.105945474
181	4	0.578125	2.37037037	-0.147287035	5.198497031
181	5	0.734375	3.764705882	0.281917795	5.198497031
202	6	0.890625	9.142857143	0.794336831	5.308267697

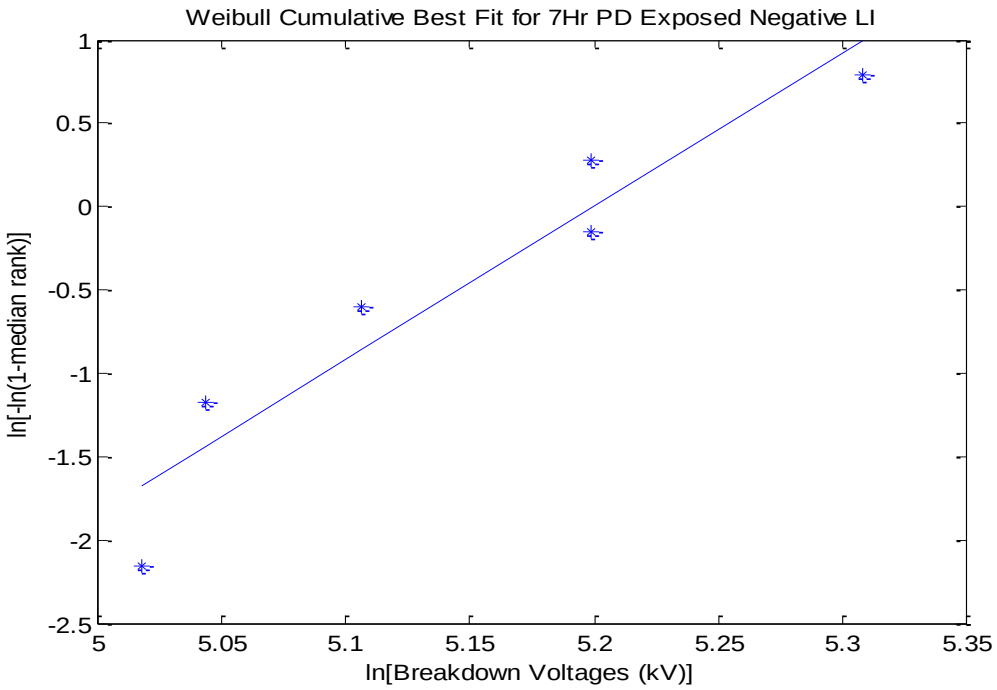

Table A 5-7: Statistical Weibull additional data

Sample Study	**Mean**	**Median**	**Mode**	**STD Dev.**	**Variance**	**Skegness**	**Kurtosis**
Surface Discharge Free Positive Impulse	171.4	172.7	175.2	9.5	90.5	-0.4	2.1
Surface Discharge Free Negative Impulse	204.3	206.6	211.0	18.3	335.8	-0.1	1.3
3 Hours Surface Discharge Exposed Positive Impulse	168.1	170.5	175.6	25.8	663.2	-0.6	1.5
3 Hours Surface Discharge Exposed Negative Impulse	173.7	176.2	181.4	25.1	629.8	-0.8	2.0
7 Hours Surface Discharge Exposed Positive Impulse	163.9	165.1	167.2	7.9	62.2	0.5	1.6
7 Hours Surface Discharge Exposed Negative Impulse	172.1	174.4	178.9	19.9	396.7	0.0	1.4

References

[1] T.A. Prevost and T. V. Oommen, "Cellulose insulation in oil-filled power transformers: part ii-maintaining insulation integrity and life", *IEEE Electrical Insulation Magazine*, Vol. 22. No 2, pp. 4 - 14, 2006.

[2] V. Sokolov, J. Aubin, V. Davydov, H. P. Gasser, P. Griffin, M. Koch, L. Lundgaard, O. Roizman, M. Scala, S. Tenbohlen and B. Vanin, "Moisture equilibrium and moisture migration within transformer insulation systems", *CIGRE WG A2.30*, June 2008.

[3] H.P. Moser and V. Dahinden, *Transformerboard II*, Scientia Electrica, Second edition, 1999.

[4] H. P. Gasser, B. Heinrich and C. Krause, "Condition assessment of the cellulosic insulation power transformers taken out of service", *XIVth International Symposium on High Voltage Engineering*, Tsinghua University, Beijing, China, 25-29 August 2005.

[5] R. Braunlich, M. Hassig, J. Fuhr and T. Aschwanden, "Assessment of insulation condition of large transformers by on-site electrical diagnostic methods", *IEEE international symposium on electrical insulation*, pp. 368-372, 2000.

[6] A. S. Kumar, R.P Gupta and A. Venkatasami, "Online partial discharge detection and location techniques for condition monitoring of power transformers: A review", *IEEE International Conference on Condition Monitoring and Diagnosis*, pp. 927 - 931, 2008.

[7] J. Fuhr, "Procedure for identification and location of dangerous PD sources in power transformers", *IEEE Transactions on Dielectric and Electrical Insulation*, Vol. 12. No. 5, pp. 1005 – 1014, 2005.

[8] J. Xu, W. Wang, C. Li, X. Wang, B. Zhou, Y. Li and T. Wang, "Experimental research on the evolution of creepage discharge in aged pressboard*", IEEE Annual Report Conference on Electrical Insulation and Dielectric Phenomena,* pp. 484 -488, 2011.

[9] H. Zainuddin, P.L. Lewin and P.M. Mitchinson, "Characteristics of leakage current during surface discharge at the oil-pressboard interface", *IEEE Annual Report Conference on Electrical Insulation and Dielectric Phenomena*, pp. 483-486, 2012.

[10] W. Wang, J. Xue, , Y. Cheng, B. Zhou, j. Xu, and C. Li, "Diagnosis of severity degree for oil/pressboard insulation surface", *IEEE Annual Report Conference on Electrical Insulation and Dielectric Phenomena*, pp. 472 – 475, 2011.

[11] H. Z. Ding, Z. D. Wang and P. Jarman, "Ageing and moisture effects on the AC electrical strength of transformerboard", *IEEE Conference on Solid Dielectrics*, pp. 106 - 109, 2007.

[12] S. Okabe, G. Ueta, H. Wada and H. Okubo, "Partial discharge-induced degradation characteristics of insulating structure constituting oil-immersed power transformers", *IEEE Dielectrics and Electrical Insulation*, Vol. 17, No. 5, pp. 1649 – 1656, 2010.

[13] P.M. Mitchincon, P.L. Lewin and B.D. Strawbridge, "Tracking and surface discharge at the oil-pressboard interface", *IEEE Electrical Insulation Magazine,* Vol. 26, No. 2, pp. 34-41, 2010.

[14] A.K. Lokhanin, G.Y. Shneider, V.V. Sokolov, V.M. Chornologotsky and T.I. Morozova, "Internal insulation failure mechanisms of HV equipment under service conditions", *CIGRE Session,* Paris, 15-201, 2002.

[15] H.P. Gasser, Ch. Krause and T. Prevost, "Water absorption of cellulosic insulating materials used in power transformers", *IEEE International Conference on Solid Dielectrics*, pp. 289-293, 2007.

[16] M. Wang, A.J. Vandermaar and K.D. Srivastava, "Review of condition assessment of power transformers in service", *IEEE Electrical Insulation Magazine,* Vol. 18, No. 6, pp. 12-25, 2002.

[17] M.S.A. Minhas, J.P. Reynders and P.J. de Klerk, "Failure in power transformers and appropriate monitoring techniques", *IEEE Eleventh International Symposium on High Voltage Engineering, ,* Vol. 1, No. 467, pp. 94-97, 1999.

[18] *Cellulosic paper for electrical purposes, Part 2: Methods of testing*, IEC 60554 – 2, Second edition, November 2001.

[19] *High voltage test techniques – Partial discharge measurements*, SANS IEC 60270, First Edition, SABS, 2000.

[20] *High-voltage test techniques, Part 1: General definitions and test requirements*, IEC 60060-1, Second edition, November 1989.

[21] *Electrical; strength of insulating materials – Test method, Part 1: Tests at power frequency*, IEC 60243-1, Second edition. January 1998.

[22] *Electric strength of insulating materials- Test methods, Part 3: Additional requirements for 1.2/50 µs impulse tests*, IEC 60243-3, Second edition, July 2001.

[23] *Guide for the statistical analysis of electrical insulation breakdown data*, IEEE 930™, First Edition, July 2007.

[24] S. Jeszensky, "History of transformers*", IEEE Power Engineering Reviews*, Vol. 16, No 12, pp.9-12, 1996.

[25] T.A. Prevost and T. V. Oommen, "Cellulose insulation in oil-filled power transformers: Part I - History and development*", IEEE Electrical Insulation Magazine*, Vol. 22, No. 1, pp. 28-35, 2006.

[26] F. J. Vogel, "Insulation tests of transformers as influenced by time and frequency", *Midwinter Transactions, Convention of the AIEE*, Philadelphia, pp. 348 – 355, February 1924.

[27] H.P. Moser, *Transformerboard*, Scientia Electrica, 1979.

[28] R. Arora and W. Mosch, *High voltage and electrical insulation engineering*, John Wiley & Sons, Inc., IEEE Press, 2011, Chapter 6 and 7.

[29] H. W. Beaty, D. G. Fink, *Standard handbook for – Electrical engineering*, McGraw-Hill, Fiftieth edition, 2007, Chapter 4.

[30] M. Tshivhilinge, B. van Jaarsveld, L. Ramphele and R. Szewczyk, "Impact of selected insulation materials on electric field stress distribution in high voltage transformer windings", *Advance Research Workshop on Transformers*, Baiona – Spain, 28 - 30 October 2013.

[31] R. Girgis, M. Bernesjö and G.K. Frimpong, "Detailed performance of a 50 MVA transformer filled with a natural ester fluid versus mineral oil", *CIGRE Technical Programme*, A2-107, 2010.

[32] G. J. Pukel, R. Schwarz, F. Baumann, H.M. Muhr, R. Eberhardt, B. Wieser and D. Chu, "Power transformers with environmentally friendly and low flammability ester liquids", *CIGRE Technical Programme*, A2-201, 2012.

[33] R. Frotscher, J. Harthun, C. Perrier, D. Vukovic, M. Jovalekic and M. Schafer, "Behaviour of ester liquids under dielectric and thermal stress- from laboratory testing to practical use", *CIGRE Technical Programme*, D1-105, 2012.

[34] J. Duart and L. C. Bates, "Use of high temperature insulation with alternative fluids", *75th Annual International Double Client Conference*, ©Doble Engineering Company, 2008.

[35] J. Hajek, J. Kranenborg, P. Sundqvist, R. Kranenborg, T. Skytt, B. Samuelsson, R. Asano Jr, G. K. Frimpong, and R. Girgis, "Considerations for design, manufacturing and retro-filled of power transformers with high fire point, biodegradable ester fluids", *CIGRE Technical Programme*, A2-203, 2012.

[36] M. Lashbrook and M. Kuhn, "The use of ester transformer fluids for increased fire safety and reduced cost", *CIGRE Technical Programme*, A2 - 210, 2012.

[37] D. Kweon, K. Koo and J. Woo, "Hot spot temperature for 154 kV transformer filled with mineral oil and natural ester fluid", *IEEE Transactions on Dielectric and Electrical Insulation*, Vol. 19, No.3, pp. 1013 – 1020, 2012.

[38] G. J. Pukel, F. Baumann, R. Schwarz, F. Schatzl and A. Gerstl, "Environmentally friendly insulating liquids – A challenge for power transformers", *6th Southern Africa Regional Conference, CIGRE*, Paper P510, 2009.

[39] *Power transformers – Part 14: Liquid-immersed power transformers using high-temperature insulation materials*, IEC 60076-14, First edition, September 2013.

[40] Z.D. Wang, Q. Liu, X. Wang, X. Pi, P. Jarman, G. Wilson, P. Dyer, F. Perrot, C. Perrier, D. Walker, M. Lashbrook and J. Noakhes, " Ester insulating liquids for power transformers", *CIGRE Technical Programme*, A2-209, 2012.

[41] P. Jarman, G. Wilson, M. Lashbrook, P. Dyer, J. Noakhes, F. Perrot, D. Walker, Q. Liu, X. Wang, X. Yi and Z.D. Wang, "Electrical performance of ester insulating liquids for power transformers", *CIGRE SC A2 & D1 Joint Colloquium*, 2011.

[42] D. Martin, Z. D. Wang, P. Dyer, A. W. Darwin and I.R. James, "A comparative study of the dielectric strength of ester impregnated cellulose for use in large power transformer", *IEEE International Conference on Solid Dielectrics*, pp. 294 - 297, 2007.

[43] Y. Bertrand, "Development of a low viscosity insulation fluid based on vegetable oil", *IEEE International Symposium on Electrical Insulation*, pp. 413 – 418, 2012.

[44] "Experiences in service with new insulating liquids", *CIGRE Working Group A2 - 35*, October 2010.

[45] F. Bachinger and P. Hamberger, "Steady state and transient thermal behaviour of transformers filled with various insulating liquids", *CIGRE Technical Programme*, 12, 2007.

[46] J. Walker, A. Valot, Z.D. Wang, X. Yi and Q. Liu, "M/DBT, New alternative dielectric liquid for transformer", *CIGRE Technical Programme*, D1-107, 2012.

[47] R. Arora and W. Mosch, "High voltage and electrical insulation engineering", John Wiley & Sons, INC, IEEE Press, 2011.

[48] K. J. Kots, P. M. Treichel and J. R. Townsend, "Chemistry and chemical reactivity", Thomson Brooks/Cole, 2009, Seventh edition, Chapter 10.

[49] W Muller, WILEC Transformer Division, "Thermally upgraded paper in oil filled transformers", *EE publishers (Pty) Ltd*, 5th February 2007.

[50] *Pressboard and presspaper for electrical purposes – Part 2: Methods of tests*, IEC 60641-2, Second edition, June 2004.

[51] J. Dai, Z. D. Wang and P. Jarman, "Moisture and ageing effect on the creepage discharge characteristics at the oil/transformer-board interface under divergent field", *IEEE Annual Report Conference on Electrical Insulation Dielectric Phenomena*, pp. 662 – 665, 2008.

[52] S. V. Kulkarni and S. A. Khalparde, *Transformer Engineering: design and practice*, Marcel Dekker, Inc, 2004, Chapter 8.

[53] H. Z. Ding, Z. D. Wang and P. Jarman, "Effect of ageing on the impulse breakdown strength of oil-impregnated pressboard used in power transformers *", IEEE International Conference on Electrical Insulation and Dielectric Phenomena*, pp. 497 - 500, 2006.

[54] ABB, *Transformer Handbook*, Third edition, 2007.

[55] T.V. Oommen and T.L. Andrady, "Graft polymerization and other methods to reduce the Hygroscopic of cellulose insulation", *IEEE International Symposium on Electrical Insulation*, Vol. 2, pp. 538-541, 1996.

[56] E. Kuffel, W. S. Zaengl and J. Kuffel, *High voltage engineering: Fundamentals*, Butterworth-Heinemann, Second edition, 2005.

[57] C. L. Wadhwa, *High Voltage Engineering*, Third Edition, New Age International, 2010.

[58] V. M. Montsinger, "Effect of time and frequency on insulation test of transformers", *AIEE Journal*, Vol. 43, No. 2, pp. 145 – 155, 1924.

[59] F. J. Vogel, "Insulation tests of transformers as influenced by time and frequency", *AIEE Transactions*, Vol. XLIII, pp. 348 – 355, 1924.

[60] R. M. Del Vecchio, B. Poulin, P. T. Feghali, D. M. Shah and R. Ahuja, *Transformer Design Principles with Applications to Core-Form Power Transformers*, Second edition, CRC Press, 2010, Chapter 13.

[61] C. Nyamupangedengu and I. R. Jandrell, "Partial discharge spectral response to variations in the supply voltage frequency", *IEEE Transactions on Dielectrics and Electrical Insulation*, Vol. 19, No 2, pp. 521 – 532, 2012.

[62] M. Nagel and T. Leibfried, "Investigation on the frequency, high voltage insulation properties of mineral transformer – oil", *IEEE Conference on Electrical Insulation and Dielectric Phenomena*, pp. 226 – 228, 2006.

[63] W. G. Ariastina and T.R. Blackburn, " Characteristics of partial discharge in oil impregnated insulation using different test voltage frequencies", *IEEE Proceedings of the 6th International Conference on Properties and Applications of Dielectric Materials*, Vol. 1, pp. 487 – 492, 2000.

[64] D. K. Cheng, *Field and wave electromagnetics,* Addison-Wesley Publishing Company, Inc, Second edition, 1992.

[65] W. Seitlinger, *Dielectric design fundamentals*, VA Tech Transformer Academy, January 2005.

[66] M. Hemmer, R. Badent and T. Leibfried, "Electrical Properties of Vegetable Oil-Impregnated Paper Insulation", *IEEE Annual Report Conference on Electrical Insulation and Dielectric Phenomena*, pp. 60 – 63, 2003.

[67] T. A. Prevost, "Dielectric properties of natural esters and their influence on transformer insulation system design and performance - An update", *IEEE Power and Energy Society General Meeting*, pp. 1-7, 2009.

[68] P.M. Mitchincon, P.L. Lewin, G. Chen and P.N. Jarman, "A new approach to the study of surface discharge on the oil-pressboard interface", *IEEE International Conference on Dielectric Liquids*, pp. 1-4, 2008.

[69] Gunnar Berg and Lars E. Lundgaard, "Discharges in combined transformer oil/paper insulation", *IEEE 13th International Conference on Dielectric Liquids*, pp. 144-147, 1999.

[70] C. Dervos, P. D. Bourkas, E. A. Kayafas and I.A. Stathopulos, "Enhanced partial discharge temperature increase in the combined system of solid-liquid dielectric", *IEEE Transactions on Electrical Insulation*, Vol. 25, No. 3, pp. 469 – 474, 1990.

[71] J. Li, W. SI, X. Yao and Y. Li, "Partial discharge characteristics over differently aged oil/pressboard interfaces", *IEEE Transactions on Dielectrics and Electrical Insulation*, Vol. 16, No. 6, pp. 1640 – 1647, 2009.

[72] V. Dahinden, K. Schultz and A. Kuchler, "Function of solid insulation in transformers", *TRANSFORM 98*, Germany, pp. 41-54, April 1998.

[73] *Power transformers, Part 7: Loading guide for oil-immersed power transformers*, 60076-7, First edition, December 2005.

[74] X. Yi, Z. D. Wang, F. Perrot and M. Lashbrook, "Surface treeing on pressboard barriers in synthetic and natural ester liquids under AC stress", *IEEE International Conference on Dielectric Liquids*, pp. 1 – 4, 2011.

[75] K. Raja and R. S. Nema, "Comparative statistical ageing studies on an oil-pressboard insulation mode", *IEEE Proceedings of the 5th International Conference on Properties and Applications of Dielectric Materials*, Vol. 1, pp. 259 – 262, 1997.

[76] *Power transformers – Part 3: Insulation levels, dielectric tests and external clearances in air*, IEC 60076 – 3, Second edition, March 2000.

[77] M. G. Niasar, *Partial Discharge Signatures of Defects in Insulation Systems Consisting of Oil and Oil Impregnated Paper*, Licentiate Thesis, KTH School of Electrical Engineering, Stockholm, Sweden, 2012.

[78] E. Lemke, S. Berlijn, E. Gulski, M. Muhr, E. Pultrum, T. Strehl, W. Hauschild, J. Rickmann and G. Rizzi, "Guide for electrical partial discharge measurements in compliance to IEC 60270", *Technical Brochure WG D1.33, ELECTRA*, No. 241, pp. 61 – 67, December 2008.

[79] Y. Cheng, E. Gockenbach, C. Eichler and C. Li, "The partial discharge phenomena on the surface of oil impregnated paper with parallel electric field", *IEEE Annual Report Conference on Electrical Insulation and Dielectric Phenomena*, pp. 1 – 4, 2010.

[80] H. Zainuddin, P.L. Lewin and P.M. Mitchison, "Partial discharge characteristics of surface tracking on oil-impregnated pressboard under AC voltages", *IEEE International Conference on Solid Dielectrics*, pp. 1016 – 1019, 2013.

[81] C. Nyamupangedengu, R. Kochetov, P.H.F Morshuis and J.J. Smit, "A study of electrical tree partial discharges in nanocomposite-epoxy", *IEEE Annual Report Conference on Electrical Insulation and Dielectric Phenomena*, pp. 906 – 911, 2012.

[82] POWEROIL TO 1020 TO datasheet, http://www.engen.co.za/downloads/products_and_services/lubricants/engen_lubricants/industrial/transformer_oils/POWEROIL%20TO%201020%20(60%20UX).pdf, last accessed 31 March 2014.

[83] *Fluids for electrotechnical applications – Unused mineral insulating oils for transformers and switchgear*, IEC 60296, Third edition, November 2003.

[84] *Insulating liquids – Determination of the breakdown voltage at power frequency – Test method*, IEC 60156, Second edition, July 1995.

[85] J. P. Holtshausen and W.L. Vosloo, *High voltage engineering – Practice and theory*, Stellenbosch University, 2009, Chapter 3.

[86] C. Nyamupangedengu, *PD-type-dependent spectral bandwidth in solid polymer dielectric*, Thesis, University of the Witwatersrand, Johannesburg, 2011.